CHAPTER (5)

CAPILLARY PRESSURE

CHAPTER (5)

CAPILLARY PRESSURE

5.1 Introduction

Capillary pressure concept is used by geologists, petrophysicists and petroleum engineers to evaluate reservoir rock quality, pay versus non pay, expected reservoir fluid saturations, seal capacity i.e., height of hydrocarbon column a seal can hold before it leaks, depth of the reservoir fluid contact, thickness of transition zone and to approximate recovery efficiency. Evaluating capillary pressure of potential hydrocarbon reservoir and seal rocks is important because capillarity controls the static distribution of fluids in reservoir prior to the production and the remaining hydrocarbons after primary recovery.

5.2 Capillary pressure

Washburn (1921) first suggested the use of mercury injection as a laboratory method to determine the capillary pressure, i.e. the pore aperture size distribution in porous rocks. The Washburn equation can be expressed as:

$$P_c = 2\,\gamma \cos\theta / r \qquad (5.1)$$

Where:

P_c = capillary pressure, dynes/cm^2.

γ = interfacial tension of the air/mercury system, 485 dynes/cm.

θ = air/mercury/solid contact angle, 140°.

r = radius of pore aperture for cylindrical pore, microns.

Capillary pressure is defined as the difference in pressure existing between two immiscible phases, measured at the interface between the two phases. In other words, capillary pressure is the amount of extra pressure required to

force the non-wetting phase to displace the wetting phase in the capillary, (Vavra et al, 1992). Capillary pressure can be calculated as:

$$P_c = (\rho w - \rho nw)\, gh \qquad (5.2)$$

Where:

P_c = capillary pressure, psi.

ρ_w = the specific gravities of wetting fluid, gm/cc.

ρ_{nw} = the specific gravities of nonwetting fluid, gm/cc.

g = the gravitational constant, m/sec^2

h = height above free water level, ft.

5.3 Determination of capillary pressure

There are several methods to determine the capillary pressure of a given rock type. Each method has its advantages and disadvantages. Determination of capillary pressure by mercury injection technique (Purcell, 1949, Burdine et al., 1950, Brown, 1951, Wardlaw and Taylor, 1976 and El Sayed, 1981), was chosen because it is the best known method to determine the pore-throat size distribution which is the main target of the capillary pressure in the present study (Schowalter 1979, Yuan et al., 1989, Vavra et al., 1992 and El Sayed 1997). Purcell (1949), developed the system used to perform mercury injection testes on the selected samples. The system consists of a mercury pump and a pressure control system. A sample chamber is mounted vertically above the pump and is connected to the cylinder by small diameter steel tubing. The pressure control system is used to provide the desired injection pressure up to 2000 psia. Prior to performing the test, a pressure-volume correction curve is derived.

5.3.1 Capillary pressure by high pressure mercury injection

In the present study, the determination of capillary pressure was performed utilizing `Micromeritics` mercury injection apparatus. A clean and dry sample was loaded into a glass penetrometer consisting of a sample chamber

attached to a cylindrical coaxial capacitor capillary stem. The sample and penetrometer assembly were loaded into the mercury injection apparatus. The assembly was initially filled with mercury under a vacuum. Mercury is forced into the sample at low pressure, about 0.7 psia which is maintained until stabilized condition is achieved. The process is repeated through a range of pressures up to a maximum pressure of 30000 psia. The volume of mercury injected at each pressure was determined by the change in capacitance in the capillary stem. The pressure is then plotted against the mercury saturation. Irreducible water saturation (percent of unsaturated pore volume), was estimated as the percentage of pore spaces volume not filled with mercury. For hydrocarbon/water systems, the displacement of the wetting phase (water) by nonwetting phase (oil) will occur. In air/mercury system, the wetting phase is a partial vacuum, and the nonwetting phase is mercury. Pore-size distribution data were calculated from the mercury injection tests results. For these calculations, standard values for an air-mercury system were used (140° for the contact angle and 485 dynes per centimeter for the interfacial tension). The capillary pressure has determined for (47) samples collected from BED-1 field (BED1-11 well) and (63) samples collected from GPTSW field (TSW-7, 8, 13, 15 and 21 wells). The forty seven (47) samples in BED1-11 well represent the lower part of the Bahariya Formation. In GPTSW wells, the sixty three (63) samples divided as follows: 38 samples represent the upper part of the Bahariya Formation, 11 samples represent Abu Roash `F` Member (all TSW-8 well samples) and 14 samples represent Abu Roash `G` Member. Each well will be treated separately for every measured petrophysical parameter and then the samples of Abu Roash `G` Member in TSW-21 well will be treated separately. In addition, all the studied samples of the upper part of the Bahariya Formation collected from TSW-wells will be treated separately too. All the tables of this chapter have been compiled

and displayed in the appendices of the respective chapter. For displaying the reservoir anisotropy in the present chapter, we have traced the different groups (that result from the porosity-permeability relations in the previous chapter) in each studied unit (formation/member) through the capillary pressure test and its derived parameters where we found out that each group has its own petrophysical characteristics and marked with a definite line in the capillary pressure-water saturation relation (Figs. 5.1-5.8) as follows:

1-Group (A): it comprises the samples of tight flow properties; this group has been marked with a green line.

2-Group (B): it comprises the samples of intermediate flow properties; this group has been marked with a red line.

3-Group (C): it comprises the samples of high flow properties; this group has been marked with a blue line.

In this chapter we will concentrate mainly on the results of the formation or the member.

Figure (5.1) displays the capillary pressure curves of the studied samples of the lower part of the Bahariya Formation obtained from BED1-11 well. Groups (A), (B) and (C) are represented petrographically by plate (5.1), (Figs. A, B and C respectively).

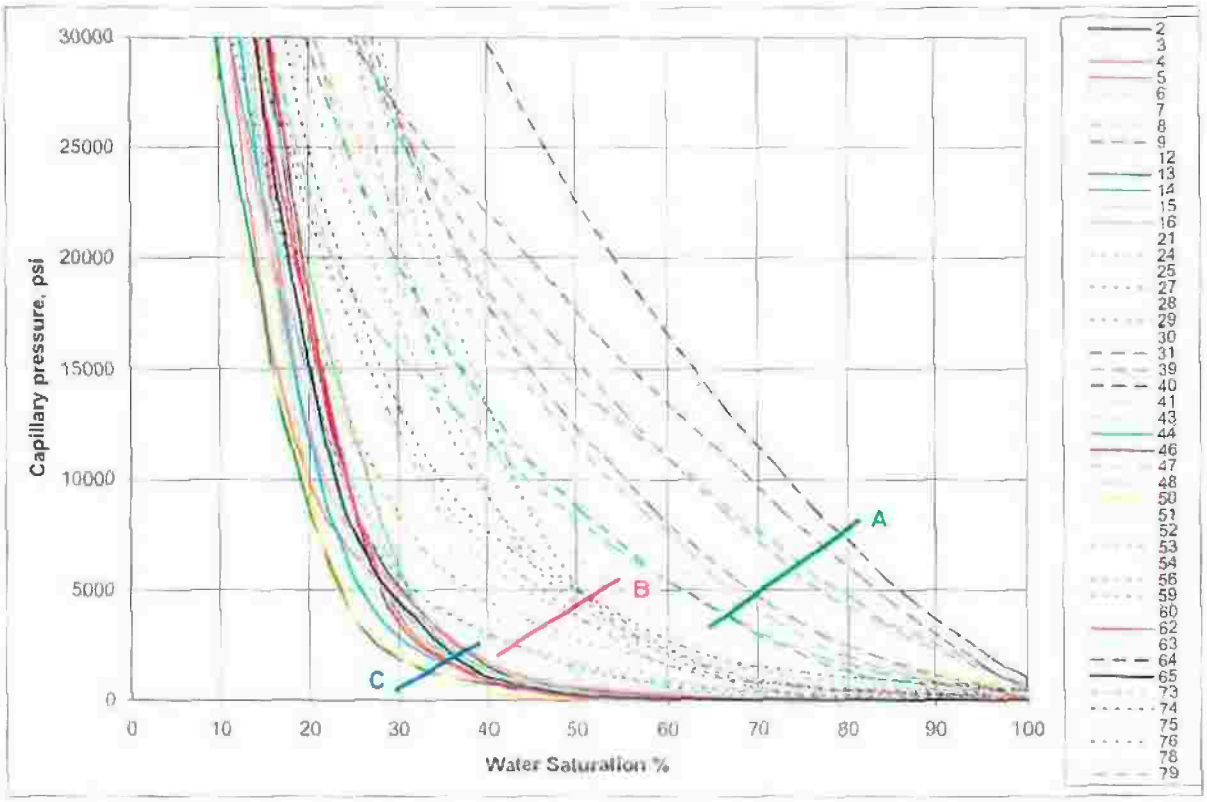

Fig. (5.1): Capillary pressure by mercury injection of L. Bahariya, BED1-11 well.

When comparing the groups of this figure and those of the porosity-permeability relation (Fig. 4.9), we found out a semi-identical relation between them and this assures the accurate classification of the samples based on porosity-permeability relation and also the anisotropy between the samples resulted from the lithological heterogeneity.

PLATE (5.1): The Lower part of the Bahariya Fm., BED1-11 well

Fig. (A): Sandstone, very fine grains, moderately sorted, highly cemented. Porosity is predominantly secondary in origin and filled with kaolinite and chlorite. Sample 21, PPL. ϕ=6.3%, k=0.03 md

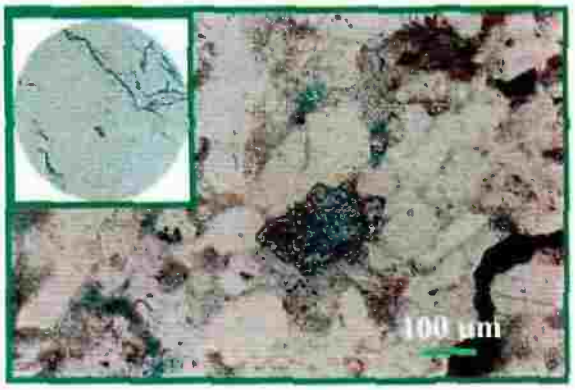

Fig. (B): Sandstone, very fine grains, moderate to well sorted with pore filling kaolinite. Quartz grains are the major framework grains with partly pore filling euhedral quartz overgrowth around detrital grains. Sample 73, PPL. ϕ=8.0%, k=0.11 md

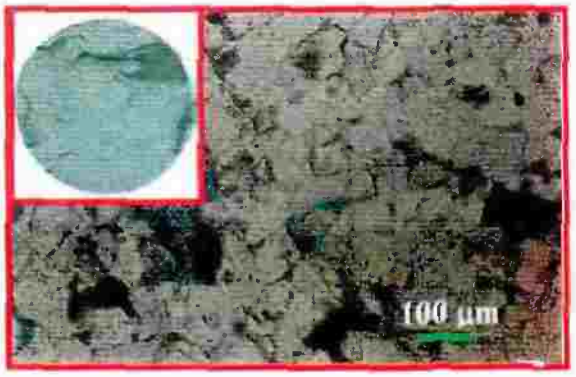

Fig. (C): Sandstone, very fine grains, moderately sorted with pore lining and pore filling kaolinite and chlorite rim cement. Quartz grains are dominantly corroded. Note the patchy ferroan dolomite partly filling pores. Sample 51, PPL. ϕ=17.3%, k=61.7 md

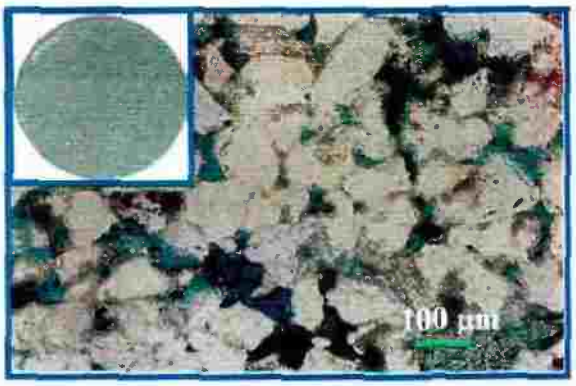

The capillary pressure curves of the studied samples of TSW-7 well (the upper part of the Bahariya Formation), have been grouped in figure (5.2). These curves have been classified into three groups. Groups (A), (B) and (C) are represented petrographically by plate (5.2), (Figs. A, B and C respectively). Sample (42) has a medium position between groups (A) and (B).

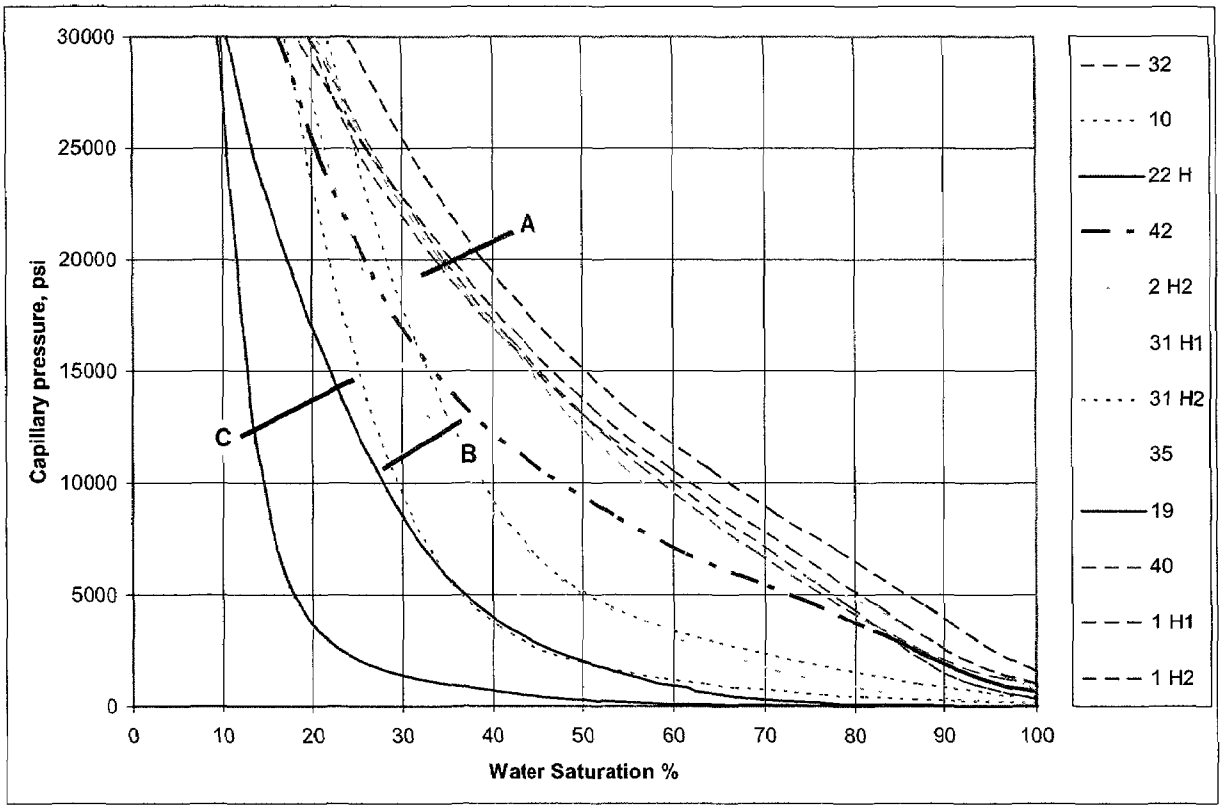

Fig. (5.2): Capillary pressure by mercury injection of U. Bahariya, TSW-7 well.

PLATE (5.2): The Upper part of the Bahariya Fm., TSW-7 well

Fig. (A): Sandstone, very fine to fine grains, poorly sorted, grains floating in glauconitic clay matrix, cemented by clays and carbonates, some iron oxides, visible porosity mainly secondary porosity, Sample 32, PPL. ϕ=11.9%, k=0.3 md.

Fig. (B): Sandstone, very fine grains, well sorted, cemented by clays and iron oxides, visible porosity mainly primary with contribution of secondary porosity, interlamination of silt and clay sometimes smeared by carbonaceous materials. Sample 2H2, PPL. ϕ=14.6%, k=1.02 md.

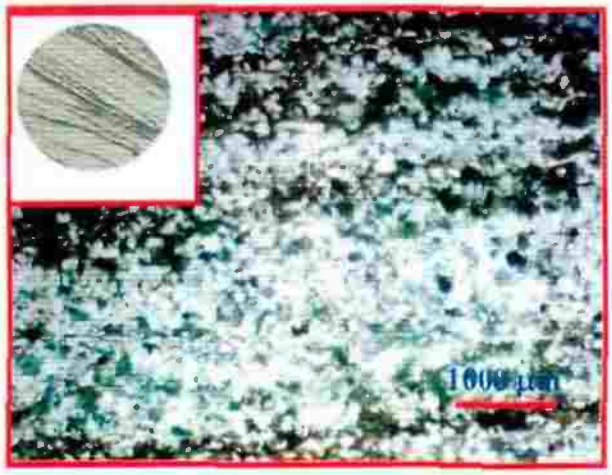

Fig. (C): Sandstone, fine grains, well sorted, cemented by clays and iron oxides, detrital clay, some glauconite, calcite pockets, visible porosity mainly intergrauular. Sample 22H, PPL. ϕ=16.4%, k=4.06 md.

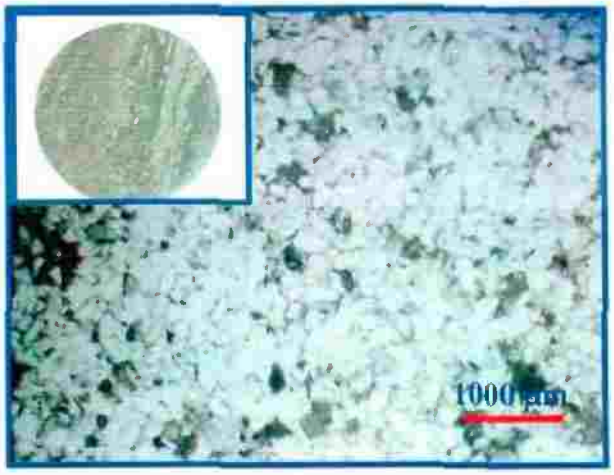

Figure (5.3) shows the capillary pressure curves of Abu Roash `F` samples obtained from TSW-8 well. In this well all the samples have the same shape of capillary pressure curve and this reflects the similarity in petrophysical characteristics, so samples of this well belong to one group (group A). Samples of this well represented petrographically by plate (5.3), (Fig. A).

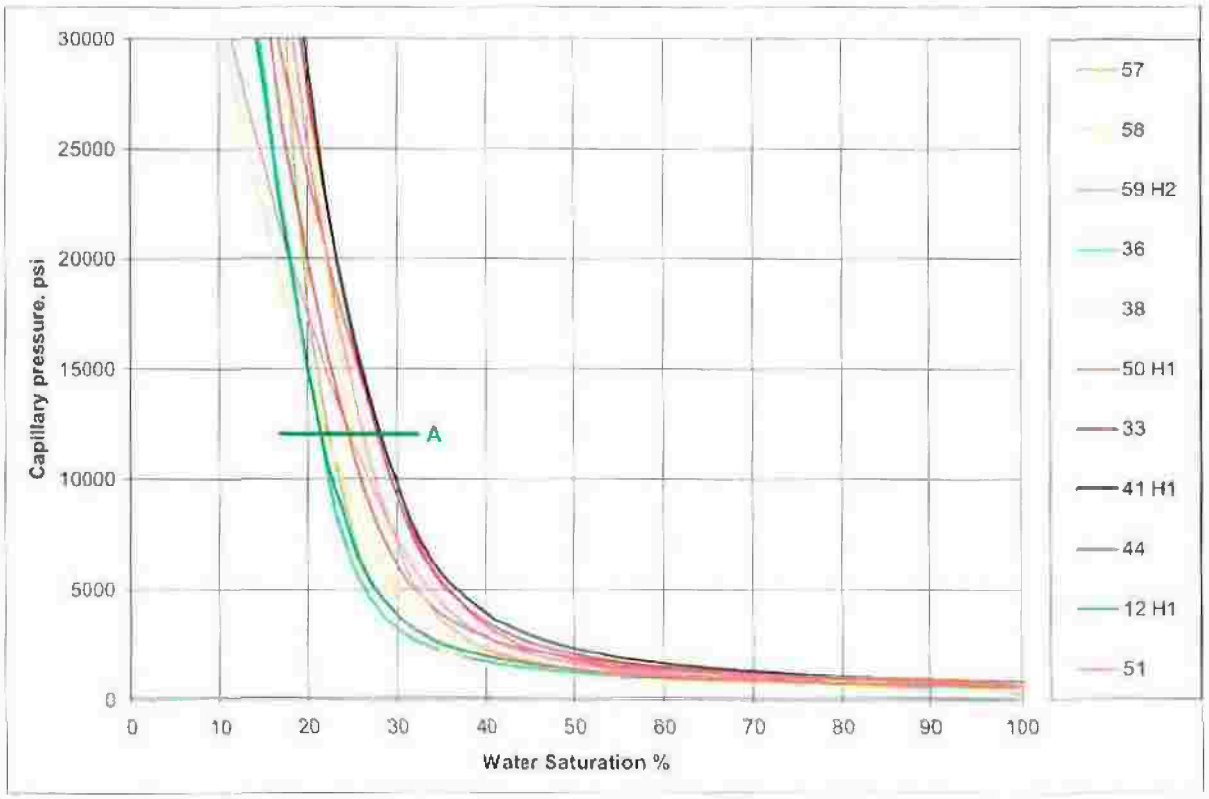

Fig. (5.3): Capillary pressure by mercury injection of Abu Roash `F`, TSW-8 well.

PLATE (5.3): Abu Roash `F`, TSW-8 well

Fig. (A): Marl, the ground mass is composed mainly of argillaceous micrite and sparry calcite, fossils and shell fragments are disseminated in the ground mass, some quartz grains are disseminated in the ground mass, no visible porosity. Sample 58, PPL. ϕ=18.7%, k=0.045 md.

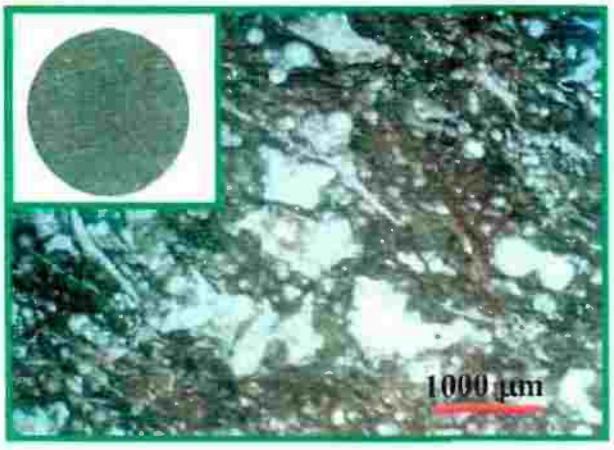

Concerning TSW-13 well (the upper part of the Bahariya Formation), the capillary pressure curves of the tested samples have been grouped and displayed in figure (5.4). Samples of this well have nearly the same shape of capillary pressure curve, hence similarity to great extent in petrophysical characteristics, so samples of this well belong to one group (group A). Samples of this well represented petrographically by plate (5.4), (Fig. A).

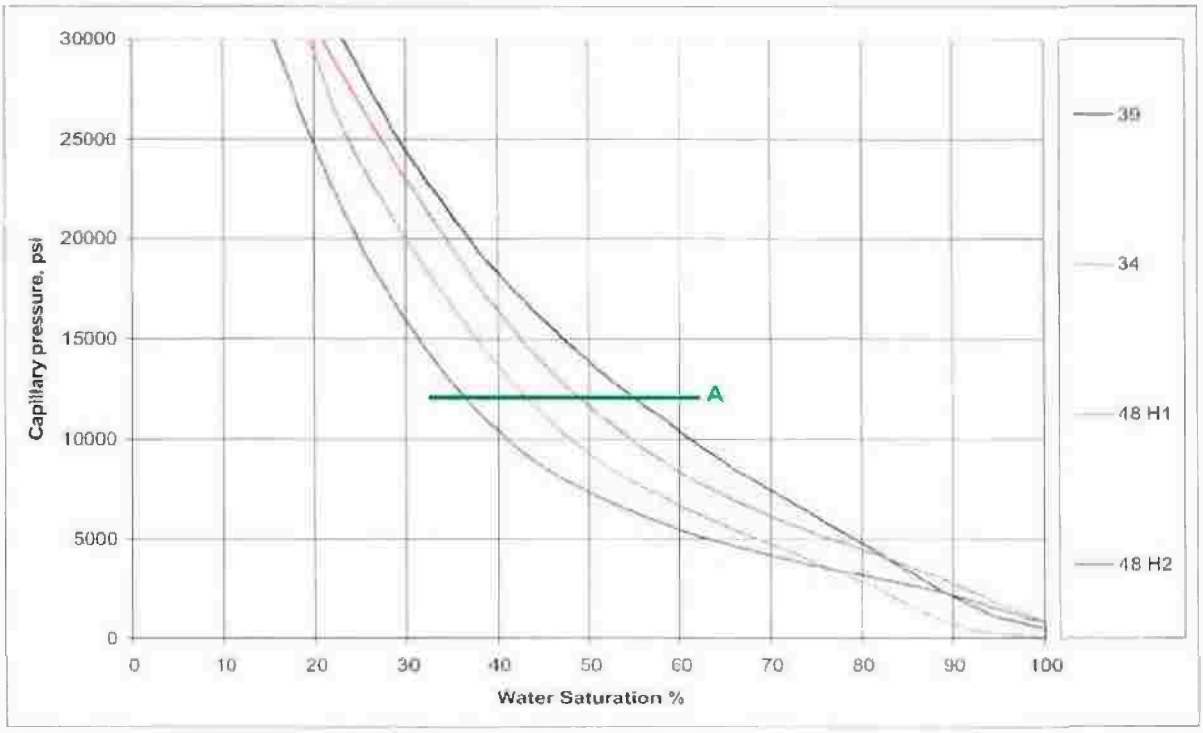

Fig. (5.4): Capillary pressure by mercury injection of U. Bahariya, TSW-13 well.

PLATE (5.4): The Upper part of the Bahariya Fm., TSW-13 well

Fig. (A): Sandstone, very fine to fine grains, grains floating in clay matrix, cemented by clays and carbonates, some iron oxides, visible porosity. Sample 48H2, PPL. ϕ=16.1%, k=0.19 md.

The capillary pressure curves of TSW-15 well (the upper part of the Bahariya Formation), have been grouped in figure (5.5). The different groups are represented petrographically by plate (5.5), (Figs. A, B and C).

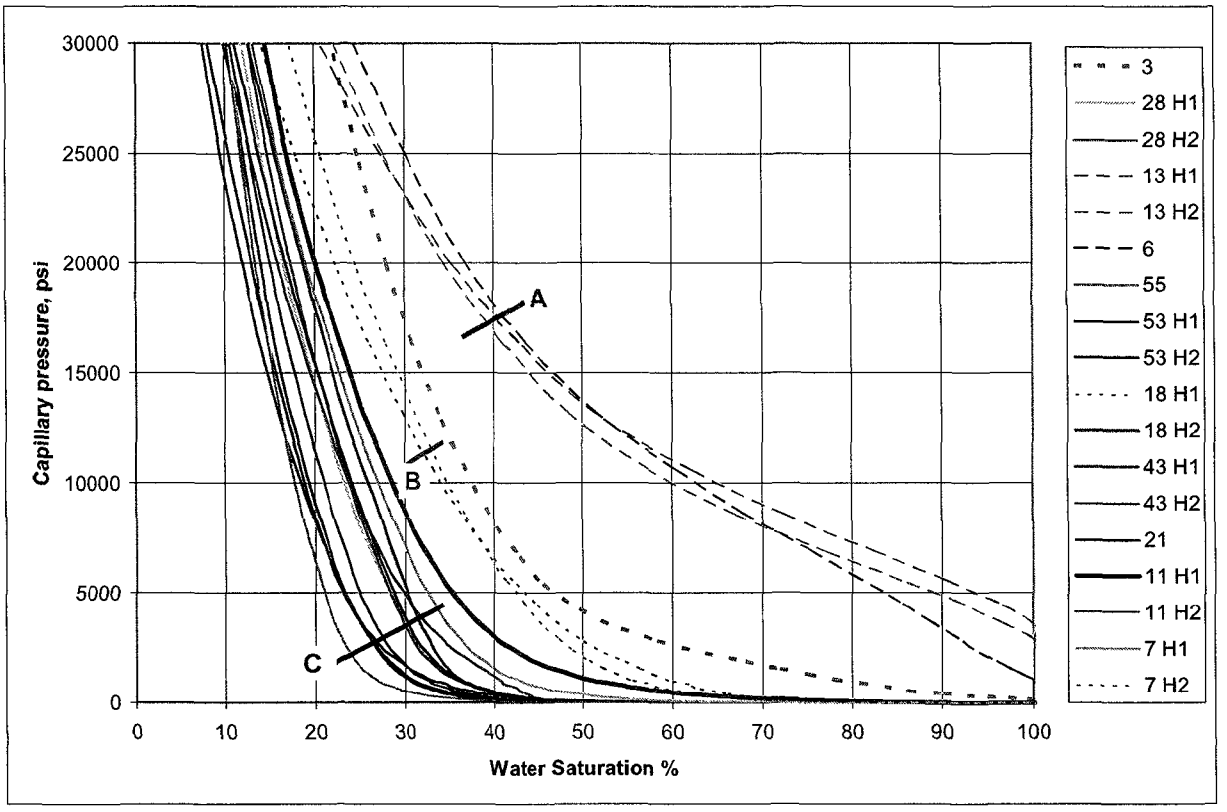

Fig. (5.5): Capillary pressure by mercury injection of U. Bahariya, TSW-15 well.

Samples (3 and 11H1) with heavy lines (dotted and solid), have their shapes of the capillary pressure curves so they don't follow any group.

PLATE (5.5): The Upper part of the Bahariya Fm., TSW-15 well

Fig. (A): Sandstone, fine to medium grains, moderately sorted, angular cemented by clays and iron oxides, visible porosity mainly secondary porosity due to leaching. Sample 6, PPL. ϕ=10.4%, k=0.1 md.

Fig. (B): Sandstone, fine to medium grains, moderately sorted, cemented by clays and iron oxides, glauconite, abundant detrital clays, visible porosity mainly primary intergranular, quartz grains are monocrystaline. Sample 11H1, PPL. ϕ=20.2%, k=14.5 md.

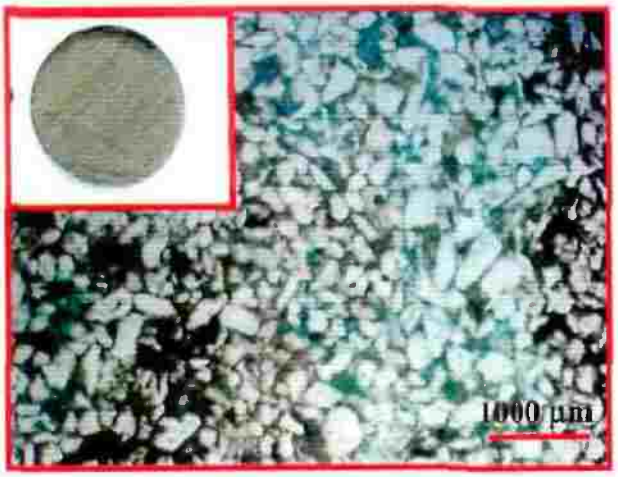

Fig. (C): Sandstone, fine to medium grains, some iron oxides, some detriral clay, visible porosity mainly primary intergranular porosity, Sample 43H2, PPL. ϕ=25.3%, k=238 md.

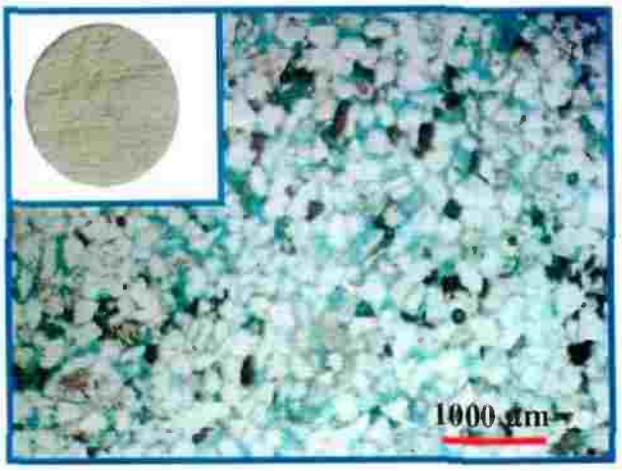

The same relation in TSW-21 well (Abu Roash `G` Member and the upper part of the Bahariya Formation), is displayed in figure (5.6), the two groups are represented petrographically by plate (5.6), (Figs. A and C).

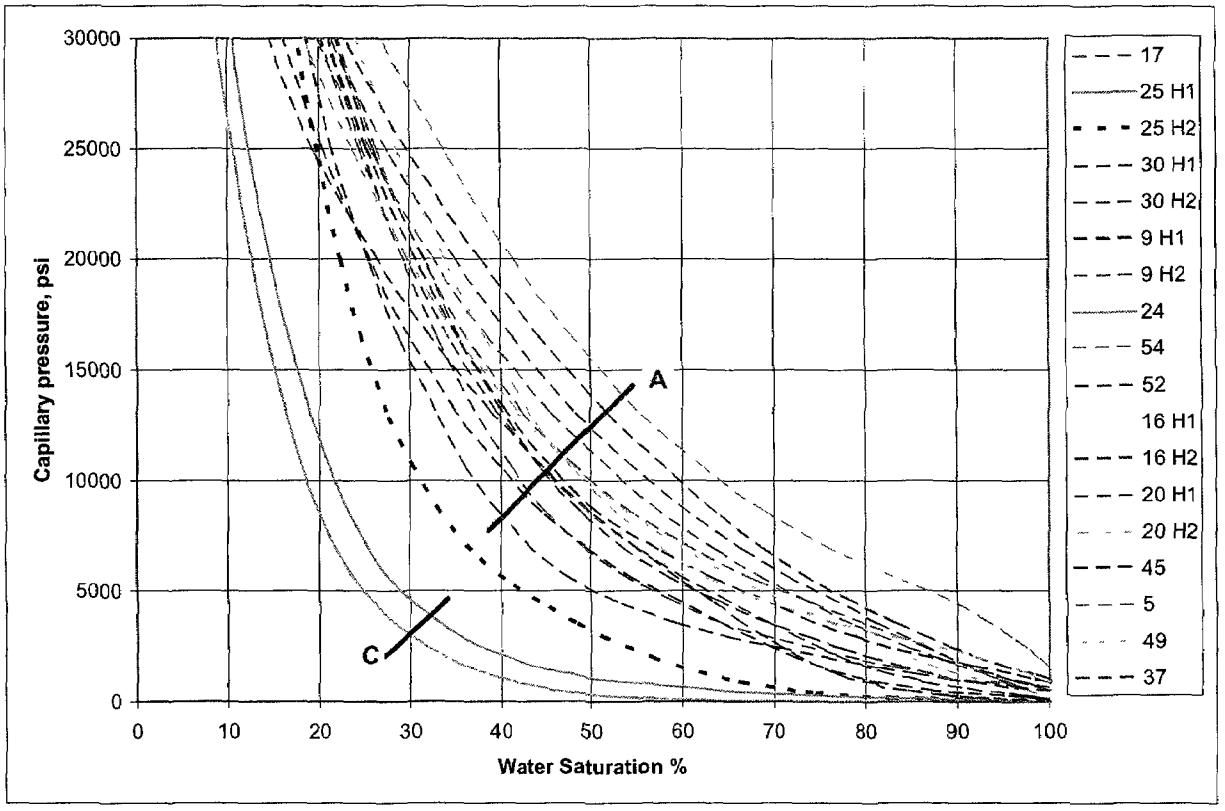

Fig. (5.6): Capillary pressure by mercury injection of TSW-21 well, Abu Roash `G` and U. Bahariya.

PLATE (5.6): The Upper part of the Bahariya Fm. and Abu Roash `G` Member, TSW-21 well

Fig. (A): Sandstone, very fine to medium grains, majority is fine grains, moderately well sorted, grains floating in clay matrix, cemented by clays, some iron oxides, glauconite are present, visible porosity mainly secondary porosity. Sample 49, PPL. ϕ=14.3%, k=0.043 md.

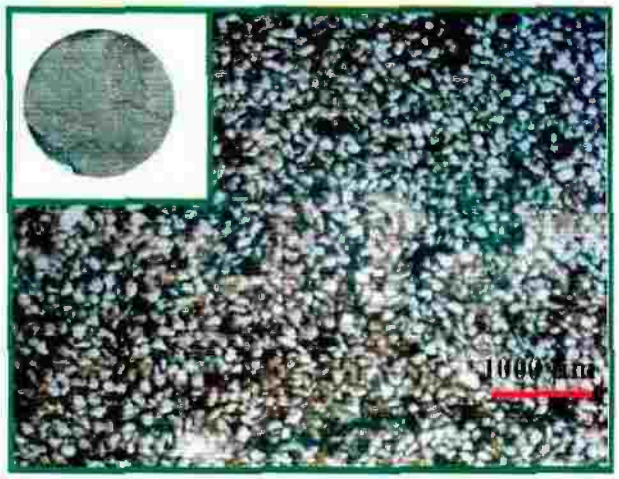

Fig. (C): Sandstone, fine grains, well sorted, cemented, some glauconite, abundant detrital clays, some iron oxides and, visible porosity about intergranular porosity, Sample 25H1, PPL. ϕ=24.6%, k=20.2 md.

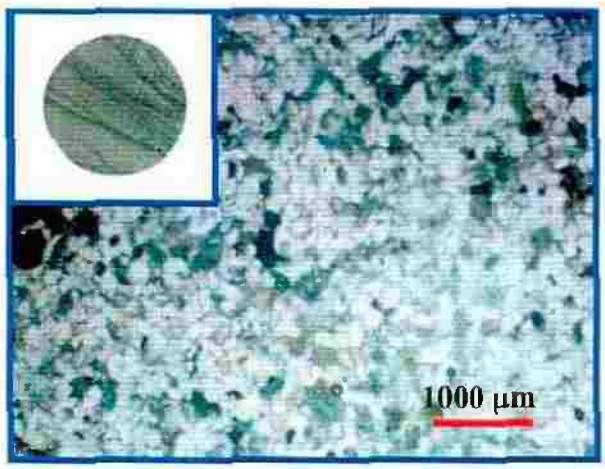

Like TSW-21 well, samples of Abu Roash `G` in same well differentiated into two groups (Fig. 5.7). The two groups are represented petrographically by plate (5.7), (Figs. A and C).

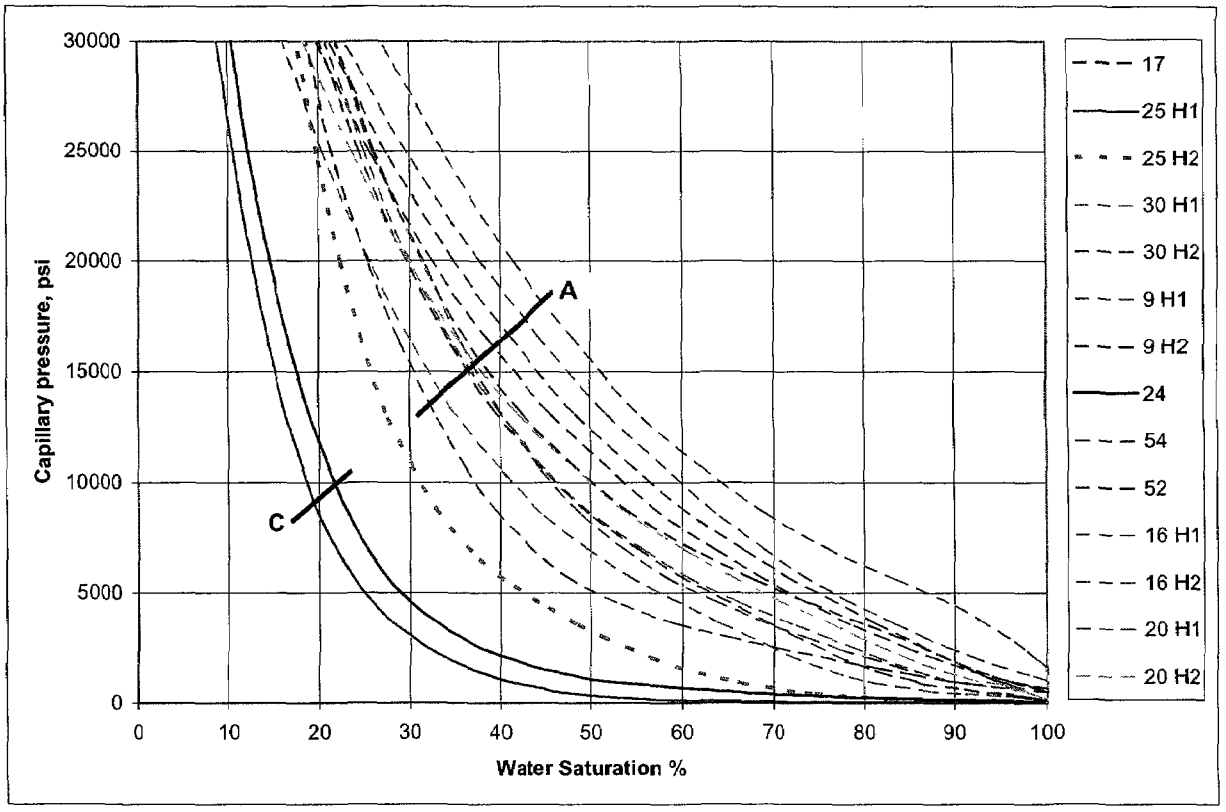

Fig. (5.7): Capillary pressure by mercury injection of Abu Roash `G`, TSW-21 well.

PLATE (5.7): Abu Roash `G` Member, TSW-21 well

Fig. (A): Sandstone, very fine grains, grains floating in clay matrix, cemented by clays and iron oxides, abundant detrital clays, glauconite, visible porosity mainly secondary due to leaching of some clay lamina, Sample 9H1, PPL. ϕ=11.1%, k=0.13 md.

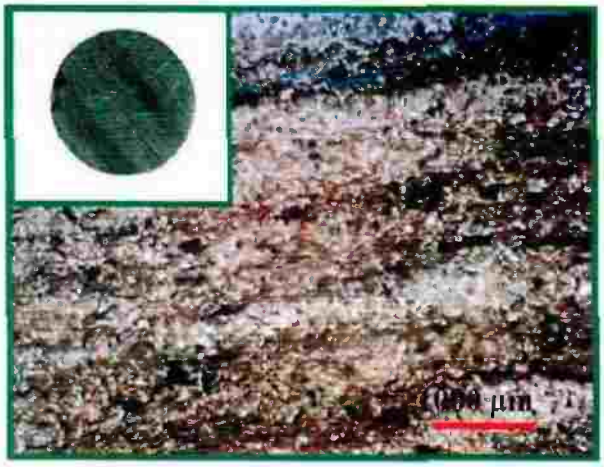

Fig. (C): Sandstone, fine grains, well sorted, cemented, some glauconite, abundant detrital clays, some iron oxides and, visible porosity about intergranular porosity, Sample 25H1, PPL. ϕ=24.6%, k=20.2 md.

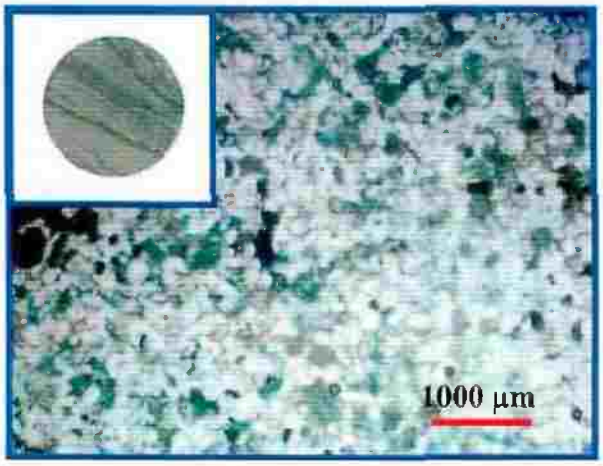

Figure (5.8) shows the capillary pressure curves of the studied samples of the upper part of the Bahariya Formation obtained from TSW-wells (TSW-7, 13, 15 and 21), the curves of the collected samples have been classified into three groups. These groups are represented petrographically by plate (5.8), (Figs. A, B and C).

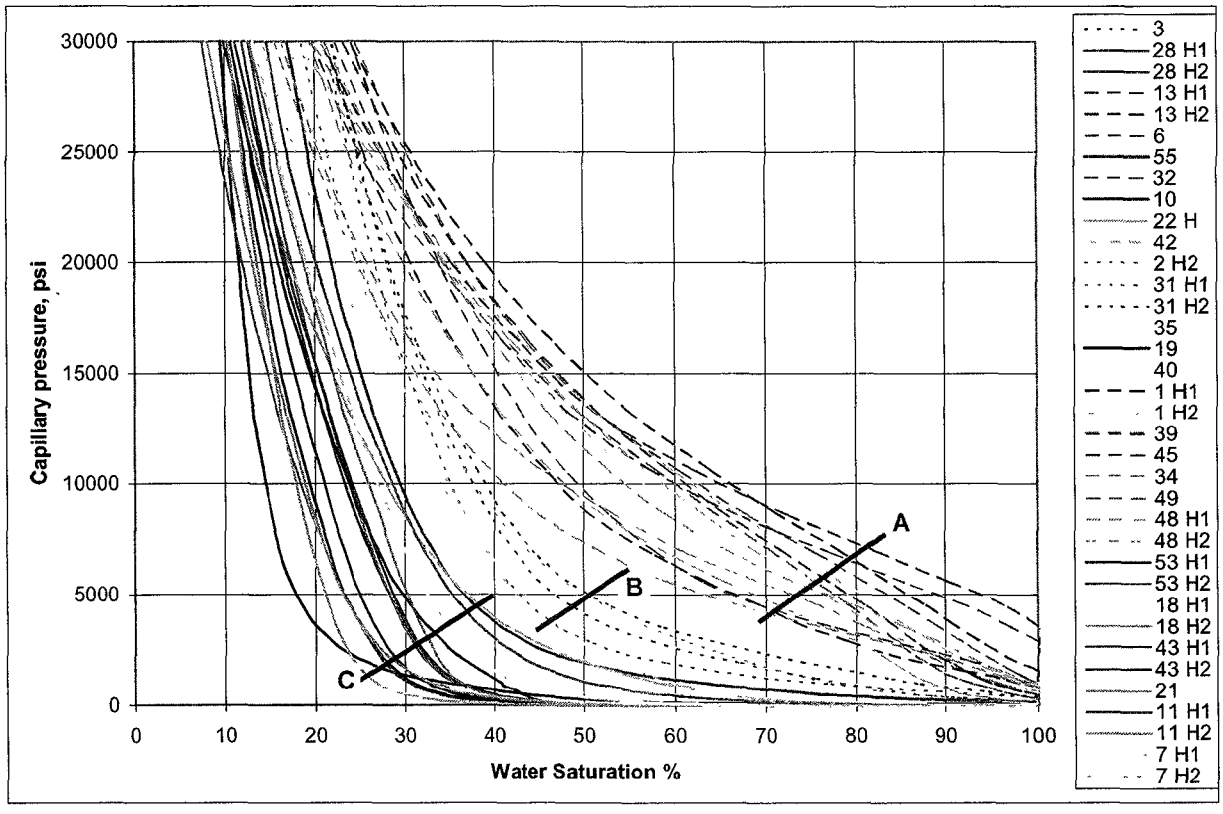

Fig. (5.8): Capillary pressure by mercury injection of U. Bahariya, TSW-7, 13, 15 and 21 wells.

PLATE (5.8): The Upper part of the Bahariya Fm. compiled from TSW-wells

Fig. (A): Sandstone, very fine to fine grains, majority is fine grains, well sorted, grains floating in clay matrix, cemented by clays and carbonates, some iron oxides, visible porosity. Sample 48H2, TSW-13 well, PPL. ϕ=16.1%, k=0.19 md.

Fig. (B): Sandstone, very fine grains, well sorted, cemented by clays and iron oxides, visible porosity mainly primary with contribution of secondary porosity, interlamination of silt and clay sometimes smeared by carbonaceous materials. Sample 2H2, TSW-7 well, PPL. ϕ=14.6%, k=1.02 md.

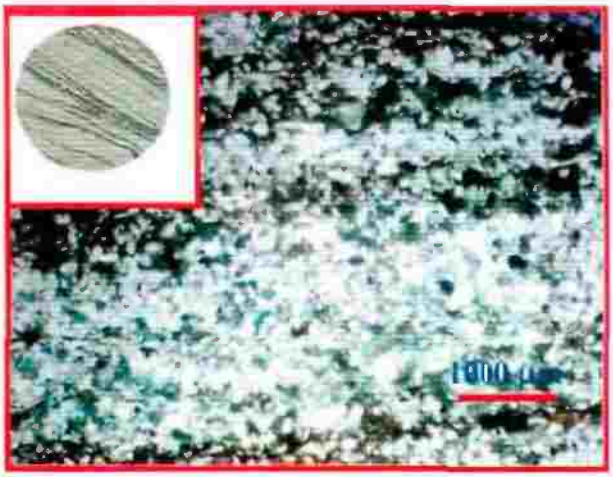

Fig. (C): Sandstone, fine to medium grains, some iron oxides, some detriral clay, visible porosity mainly primary intergranular porosity, Sample 43H2, TSW-15 well, PPL. ϕ=25.3%, k=238 md.

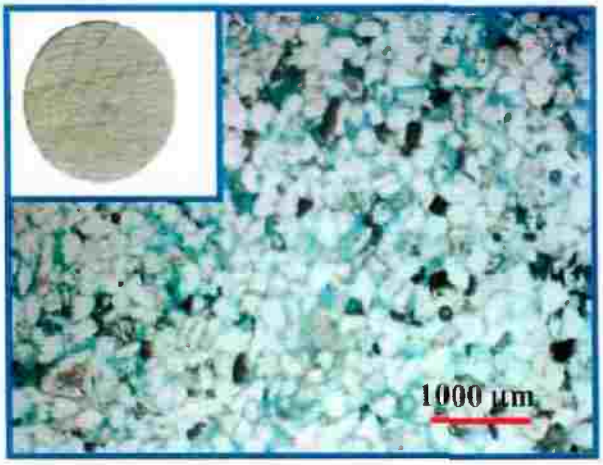

5.3.2 Capillary pressure results

Most of the capillary pressure curves can be divided into three segments. The first segment, if clearly distinguishable, occurs over a few percent of mercury saturation, has a generally steep slope, and represents the displacement pressure (Schowalter 1979). In the present study, this segment is absent because capillary data was corrected for conformance, the process by which mercury fills surface irregularities, (Vavra et al., 1992). The second segment ranges from a flat plateau defined by narrow range of capillary pressure values, to a sloping line covering a broader range of pressure values. The third segment is defined as the minimum unsaturated pore volume of the sample (Vavra, et al, 1992). Based on mercury-injection curve shapes, we found out the following:

The curves of the studied samples of the lower part of the Bahariya Formation in BED1-11 well are considered to be different in shape (Fig. 5.1). The percent of unsaturated pore volume varies from 9.2% to 27.7% except one sample has 39.6% unsaturated pore volume, also the same behavior present in the studied samples of TSW-wells where the percent of unsaturated pore volume varies from 9.5% to 23.9% in TSW-7 well (Fig. 5.2), from 7.4% to 24.4% in TSW-15 well (Fig. 5.5), from 8.7% to 26.8% in TSW-21 well (Fig. 5.6) and Abu Roash `G` samples in TSW-21 well (Fig. 5.7) but the studied samples obtained from TSW-8 well (Abu Roash `F`) and TSW-13 well are considered to be not different in shape, the only difference in the curve shape is the percent of unsaturated pore volume, which varies from 10.4% to 19.6% in Abu Roash `F` (Fig. 5.3) and from 15.5% to 23.1% in TSW-13 well (Fig. 5.4). Figure (5.8) displays the unsaturated pore volume of the studied samples of the upper part of the Bahariya Formation collected from all TSW wells, it varies from 7.4% to 24.4%.

5.4 Capillary pressure derived parameters

Many different parameters have been derived from capillary pressure test by mercury injection. Tracing the different groups (A, B and C) that resulted from porosity-permeability has been done through these different parameters to show the distinctive properties of each group. In our study we will concentrate mainly on the results of Bahariya Formation (lower and upper parts) and Abu Roash Members (`F` and `G`).

5.4.1 Displacement pressure (Pd)

The displacement pressure is defined as the pressure at which mercury first enters the samples after the mercury has filled any surface irregularities on the samples (Vavra, et al., 1992). El Sayed, (1997), has introduced a new definition of the displacement pressure as the pressure required to push fluids firstly into the rock pore spaces.

5.4.2 Displacement pressure results

The measured displacement pressures were of varied values for the different studied units. Table (5.1) shows the displacement pressure varies in a high range from a minimum of 15 psia up to a maximum value of 1290 psia with an average value 241 psia for the samples of the lower part of the Bahariya Formation in BED1-11 well. In TSW-wells the displacement pressure varies in a high range from 24 psia to 1985 psia with an average value 658 psia in TSW-7 well (Table 5.2), from 447 psia to 1032 psia with an average value 759 psia in TSW-8 well (Abu Roash `F`), (Table 5.3) and from 115 psia to 1032 psia with an average value 717 psia, in TSW-13 well (Table 5.4). In TSW-15 well, the range of the displacement pressure becomes very wide from a minimum of 12 psia up to a maximum value of 4569 psia with an average value 553 psia (Table 5.5). The samples of TSW-21 well shows a wide ranges of the displacement pressure from 40 psia to 1985 psia with an average value 625 psia (Table 5.6), the same behavior present in samples of

Abu Roash 'G' in TSW-21 well but with an average value of 599 psia (Table 5.7). Table (5.8) displays the displacement pressure results which differ in a very high range from a minimum of 12 psia up to a maximum value of 4569 psia with an average value 621 psia for the studied samples of the upper part of the Bahariya Formation obtained from TSW-wells.

5.4.3 Displacement pressure versus permeability relations

Figure (5.9) displays displacement pressure-permeability relation of the samples of the lower part of the Bahariya Formation in BED1-11 well.

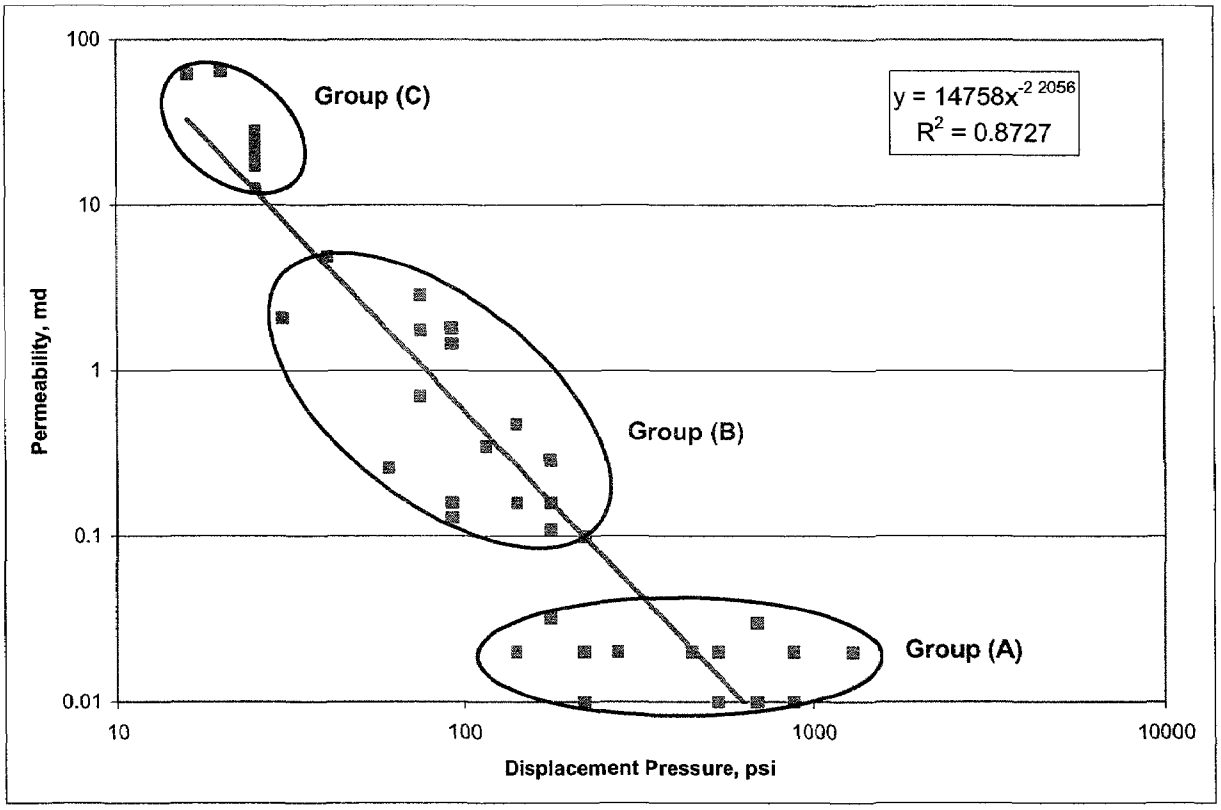

Fig. (5.9): Displacement pressure vs. permeability of L. part of Bahariya Fm., BED1-11 well.

The studied samples have a power relation which is expressed by the equation:

$$K = 14758\ dp^{-2.2056} \qquad (5.3)$$

$$R = 0.93$$

The very excellent value of correlation coefficient has revealed the possibility of permeability prediction with a high precision. Table (5.9) displays the characteristics of the displacement pressure for groups (A, B and C).

Figure (5.10) is a composite figure displays displacement pressure-permeability relations of the studied TSW-wells (TSW-7, TSW-8 (Abu Roash `F`), TSW-13, TSW-15 and TSW-21.

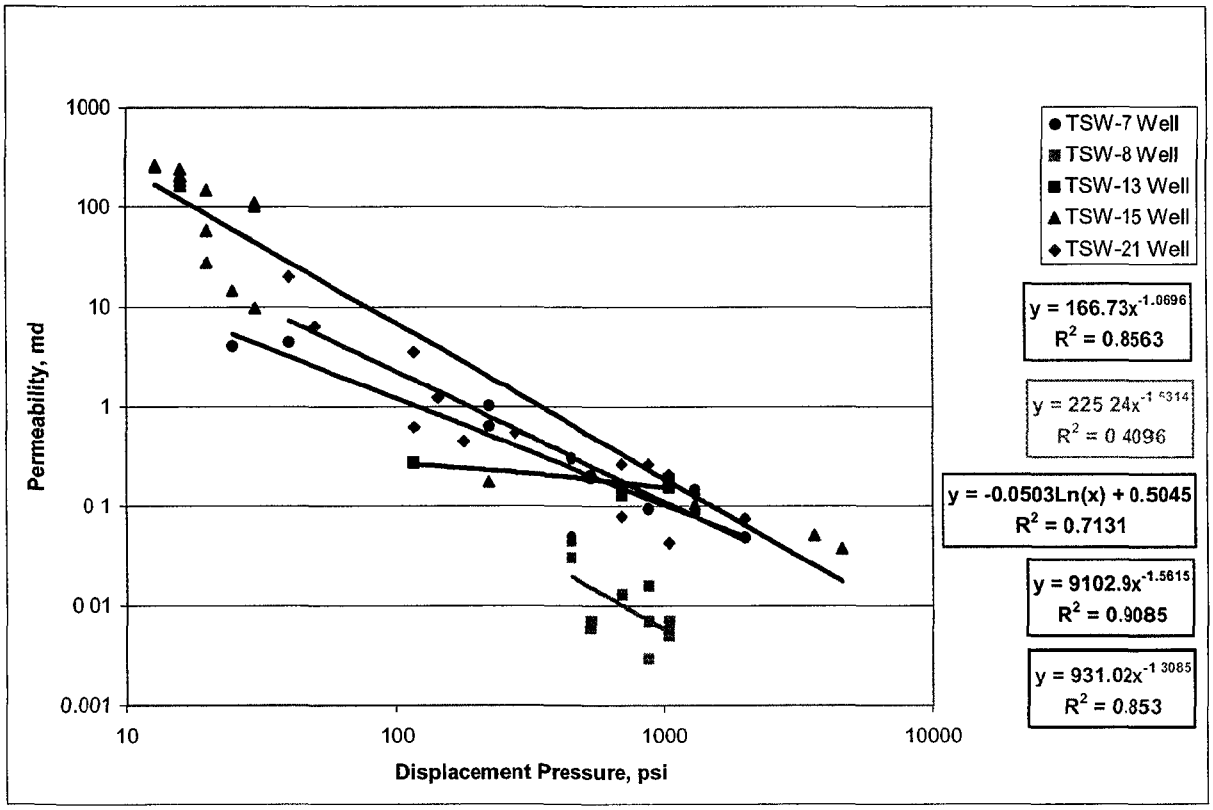

Fig. (5.10): Displacement pressure vs. permeability of all TSW wells.

The studied samples in TSW-7 well have a relation which is expressed by the equation:

$$K = 166.73\ dp^{-1.0696} \qquad (5.4)$$

$$R = 0.93$$

Where the relation in TSW-8 well (Abu Roash `F`) is expressed by the equation:

$$K = 225.24\ dp^{-1.5314} \qquad (5.5)$$

$$R = 0.64$$

The value of correlation coefficient indicates the low possibility of permeability prediction, this is due to the very narrow range of the permeability in this well, so no sensed differences in displacement pressure values. Table (5.10) displays the characteristics of the displacement pressure of samples of this well.

On the other hand samples of TSW-13 well have a relation which is expressed by the equation:

$$K = -0.0503 \text{ Ln } (dp) + 0.5045 \qquad (5.6)$$

$$R = 0.84$$

For samples of TSW-15 well, they have a relation which is expressed by the equation:

$$K = 9102.9\ dp^{-1.5615} \qquad (5.7)$$

$$R = 0.95$$

The same relation in TSW-21 well and is expressed by the equation:

$$K = 931.02\ dp^{-1\ 3085} \qquad (5.8)$$

$$R = 0.92$$

The previous relations with excellent values of correlation coefficients revealed the possibility of permeability prediction with a high precision in wells (TSW-7, TSW-15 and TSW-21).

Figure (5.11) displays displacement pressure-permeability relation of Abu Roash `G` samples obtained from TSW-21 well.

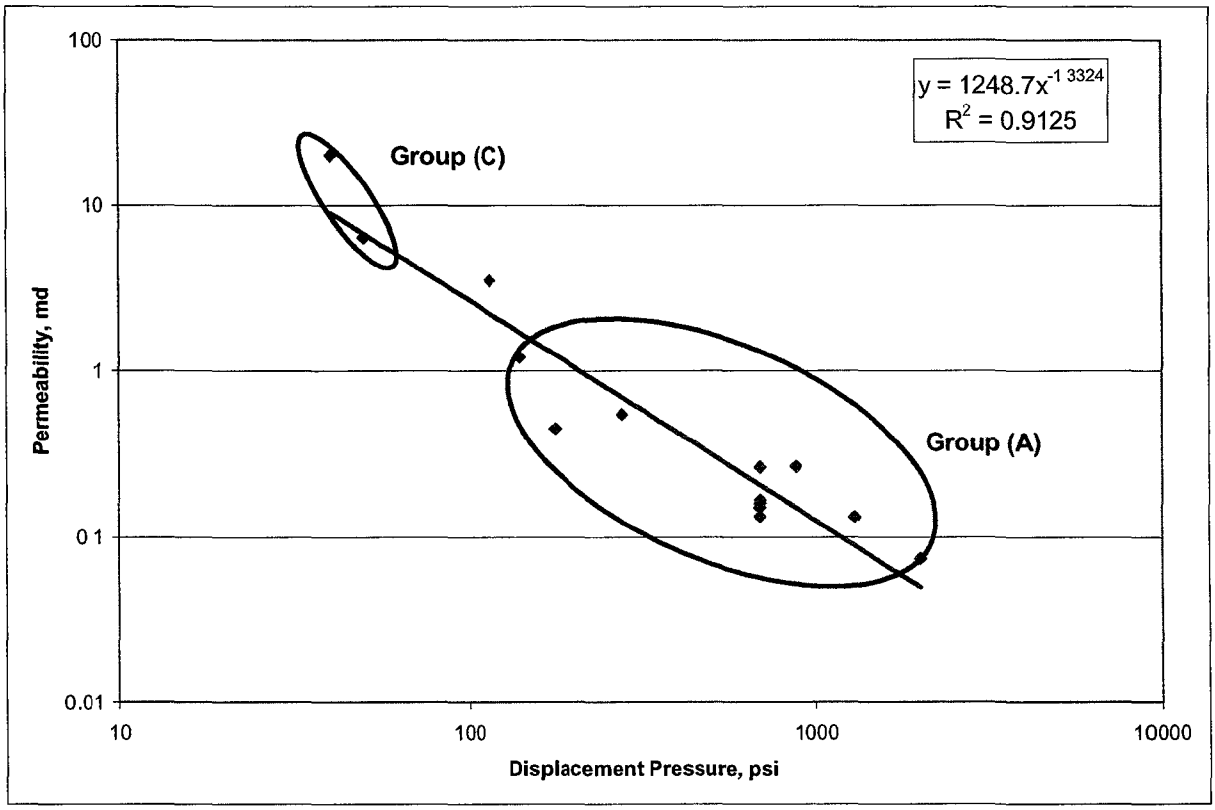

Fig. (5.11): Displacement pressure vs. permeability of Abu Roash `G`, TSW-21 well.

The studied samples have an outstanding relation which is expressed by the equation:

$$K = 1248.7\ dp^{-1.3324} \qquad (5.9)$$

$$R = 0.96$$

The previous equation is very reliable to predict the permeability with a very high precision. Table (5.11) displays the characteristics of the displacement pressure for groups (A and C).

Figure (5.12) displays displacement pressure-permeability relation of the studied samples of the upper part of the Bahariya Formation collected from wells (TSW-7, 13, 15 and 21).

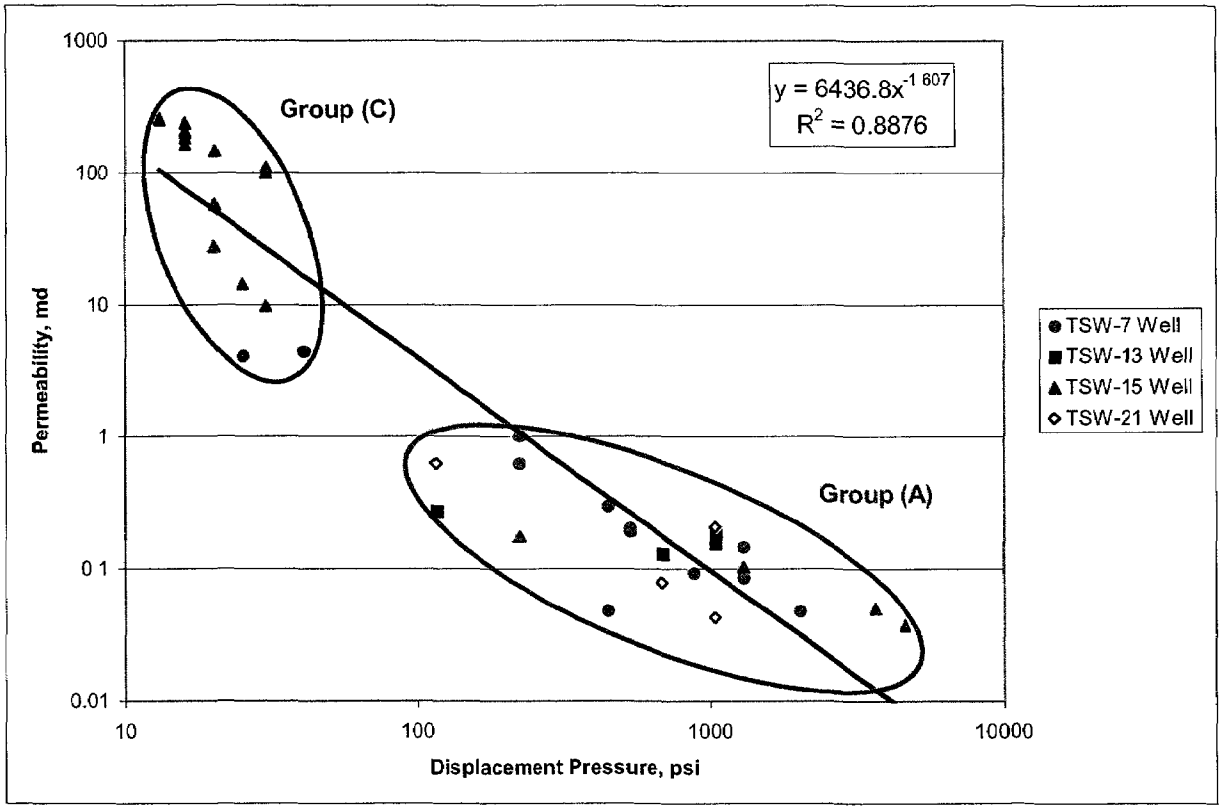

Fig. (5.12): Displacement pressure vs. permeability of U. part of Bahariya Fm., TSW-7, 13, 15 and 21 wells.

The relation of the studied samples is expressed by the equation:

$$K = 6436.8\ dp^{-1.607} \qquad (5.10)$$

$$R = 0.94$$

The outstanding value of correlation coefficient of the permeability-displacement pressure relation shows the possibility of permeability prediction with a high precision. Table (5.12) displays the characteristics of the displacement pressure for groups (A and C).

5.4.4 Unsaturated pore volume (Sw_{irr})

As mentioned previously, irreducible water saturation (percent of unsaturated pore volume), was estimated as the percentage of pore spaces volume not filled with mercury. In the present study, the pressure of 30000 psi was selected to determine the unsaturated pore volume of the studied samples. Although the percentage of unsaturated pore volume dose not exactly measure irreducible water saturation (Vavra et al., 1992), but it reflects the amount of micropores which are controlled with smaller pore-throats. These micropores (of pore-throats lower than 0.0035 microns in radius in our study) require very high capillary pressure to displace the wetting phase. This amount of pore throats radius (lower than 0.0035 microns in radius) which contribute only to develop microporosity should be taken into account when determining the values of permeability and porosity cutoffs for the net pay calculation. This microporosity can not be differentiated on logs from other pore types (Bliefnick et al., 1996). The up-to-date techniques of Nuclear Magnetic Resonance (NMR), has the capability to measure the distribution of pore size in rocks and hence determine a cutoff value which is equivalent to irreducible water saturation in a given reservoir rock.

5.4.5 Unsaturated pore volume (Sw_{irr}) results

The measured (Sw_{irr}) was of varied values for the studied samples as follows: Table (5.13) displays the values of (Sw_{irr}) which varies in a very high range from a minimum of 9.2 % up to a maximum value of 39.6 % with an average value 17.5 % for the samples of the lower part of the Bahariya Formation in BED1-11 well, also tables (5.14) through (5.19) show respectively the same parameter which differ from 9.5 % to 23.9 % with an average value 18.0 % (TSW-7 well), from 10.4 % to 19.6 % with an average value 16.0 % (TSW-8 well (Abu Roash `F` Member), from 15.5 % to 23.1 % with an average value 19.7 % (TSW-13 well), from 7.4 % to 24.4 % with an average value 14.0 %

(TSW-15 well), from 8.7 % to 26.8 % with an average value 19.1 % (TSW-21 well) and from 8.7 % 26.8 % with an average value 18.9 % (Abu Roash 'G' in TSW-21 well). Table (5.20) displays the values of (Sw_{irr}) of the studied samples of the upper part of the Bahariya Formation obtained from TSW-wells where they vary in a high range from a minimum of 7.4 % up to a maximum value of 24.4 % with an average value 16.8 %.

5.4.6 Unsaturated pore volume (Sw_{irr}) versus permeability relations

Figure (5.13) displays irreducible water saturation-permeability relation for the studied samples of the lower part of the Bahariya Formation in BED1-11 well.

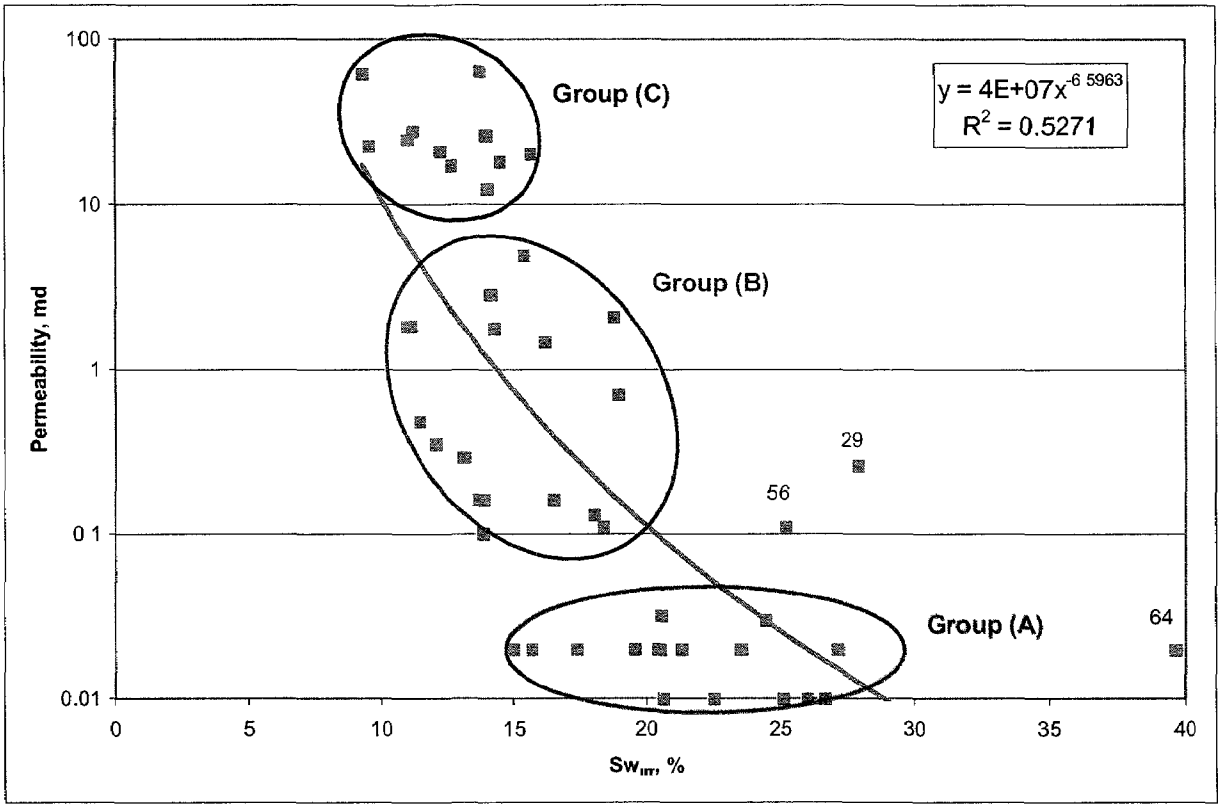

Fig. (5.13): Sw_{irr} vs. permeability of L. part of Bahariya Fm., BED1-11 well.

The studied samples of the lower part of Bahariya Formation have a relation which is indicated by the equation:

$$K = 4E+07Sw_{irr}^{-6.5963} \qquad (5.11)$$

$$R = 0.73$$

The value of correlation coefficient has revealed the possibility of permeability prediction to some extent in BED1-11 well. Table (5.21) displays the characteristics of irreducible water saturation of groups (A, B and C). Due to their high irreducible water saturation values hence shifting away from the general trend line, so sample (64) was excluded from group (A) and samples (29 and 56) were excluded from group (B).

Figure (5.14) is a composite figure displays irreducible water saturation-permeability relations of wells TSW-7, TSW-8 (Abu Roash `F`), TSW-13, TSW-15 and TSW-21.

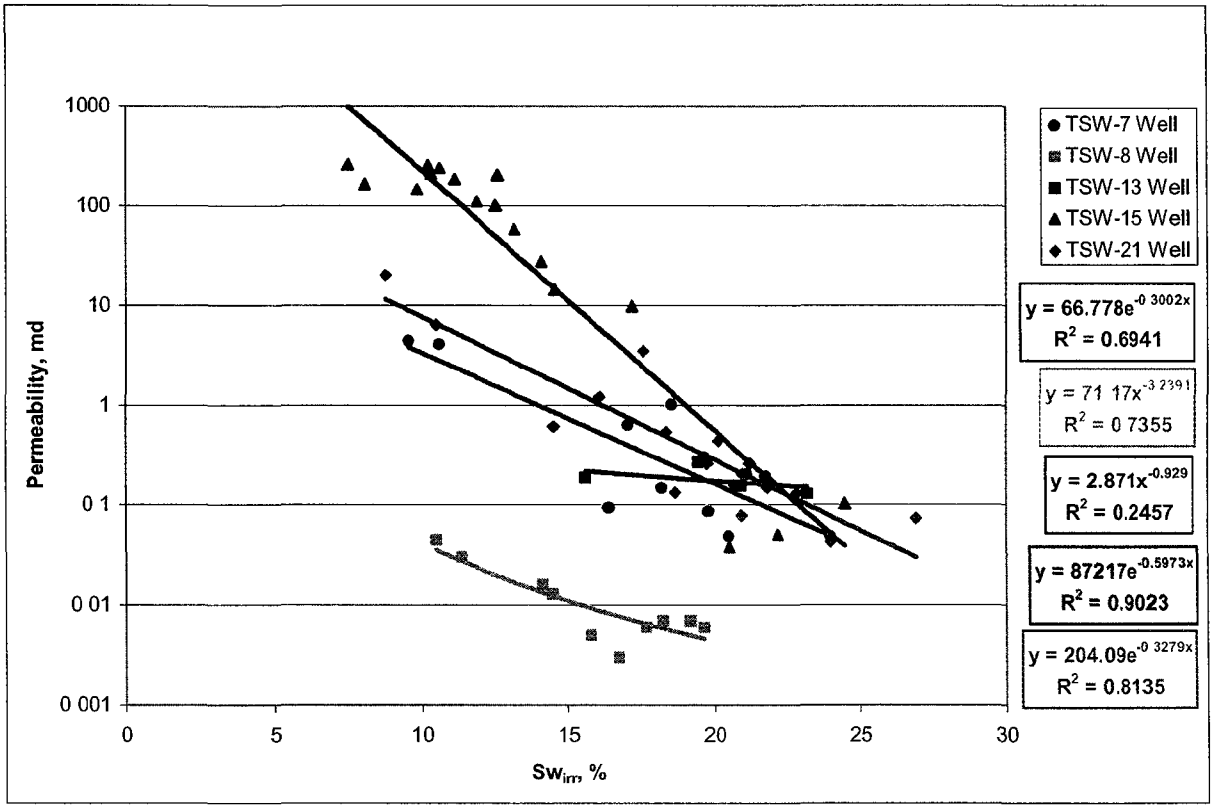

Fig. (5.14): Sw_{irr} vs. permeability of all TSW wells.

The studied samples (TSW-7 well) have a relation indicated by the equation:

$$K = 66.778e^{-0.3002Swirr} \qquad (5.12)$$

$$R = 0.83$$

Samples of TSW-8 well (Abu Roash `F`) have a relation which is indicated by the equation:

$$K = 71.17\ Sw_{irr}^{-3.2391} \qquad (5.13)$$

$$R = 0.86$$

The good value of correlation coefficient displayed the ability of permeability prediction to great extent. Table (5.22) displays the characteristics of the irreducible water saturation for this well.

The relation in TSW-13 well is weak and indicated by the equation:

$$K = 2.871\ Sw_{irr}^{-0.929} \qquad (5.14)$$

$$R = 0.50$$

The relation in TSW-15 well is very strong and indicated by the equation:

$$K = 87217e^{-0.5973Swirr} \qquad (5.15)$$

$$R = 0.95$$

Similarly in TSW-21 well, the studied samples have a relation which is indicated by the equation:

$$K = 204.09e^{-0.3279Swirr} \qquad (5.16)$$

$$R = 0.90$$

The excellent values of correlation coefficient of the previous two wells revealed the possibility of permeability prediction with a high precision.

Figure (5.15) displays irreducible water saturation-permeability relation of Abu Roash `G` in TSW-21 well.

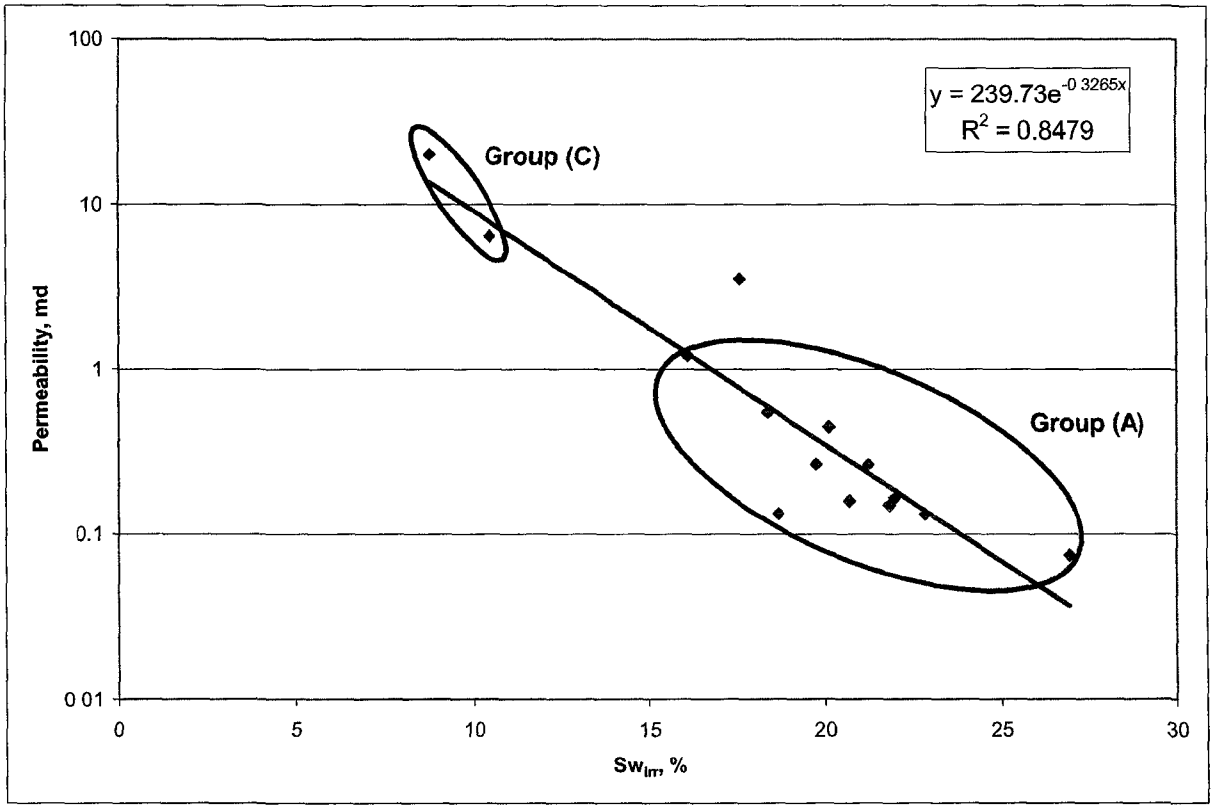

Fig. (5.15): Sw_{irr} vs. permeability of Abu Roash `G`, TSW-21 Well.

The excellent relation is indicated by the equation:

$$K = 239.73e^{-0.3265Swirr} \qquad (5.17)$$

$$R = 0.92$$

Table (5.23) displays the characteristics of the irreducible water saturation of groups (A and C).

Figure (5.16) displays irreducible water saturation-permeability relation of the upper part of the Bahariya Formation samples that were collected from TSW-7, 13, 15 and 21 wells.

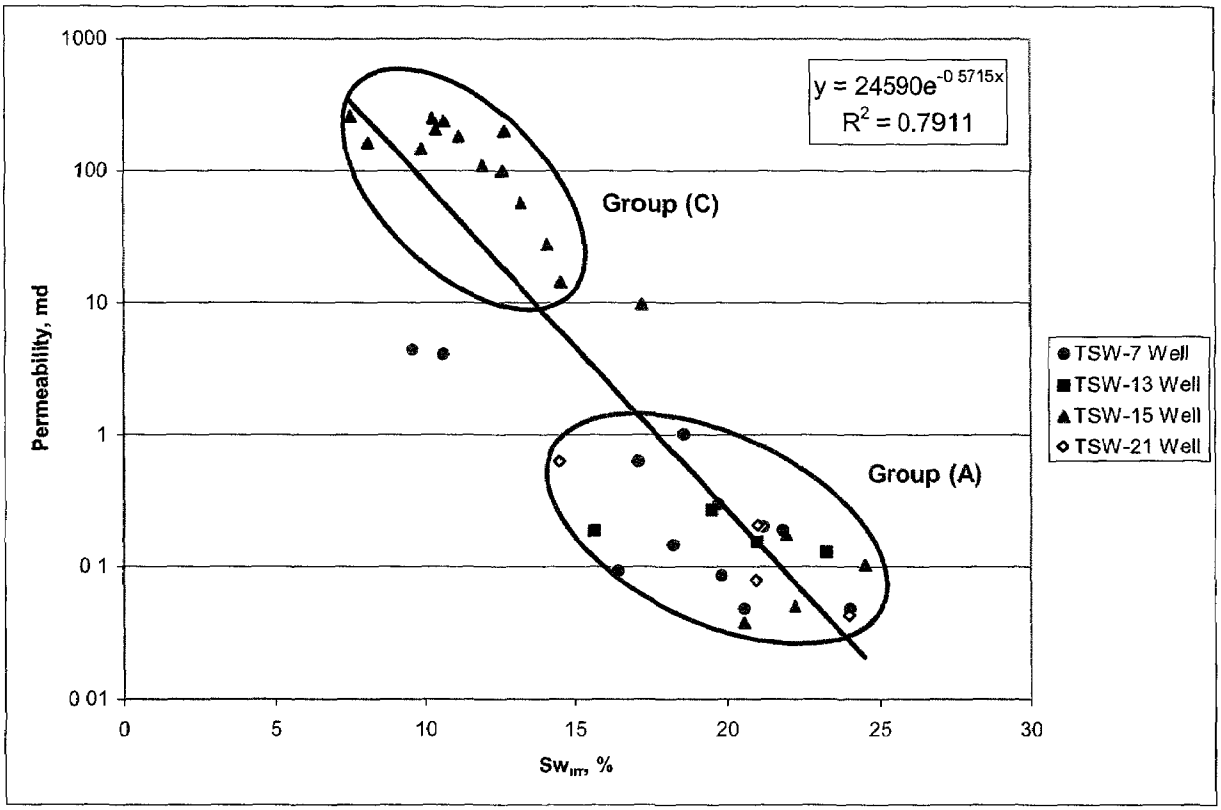

Fig. (5.16): Sw_{irr} vs. permeability of U. Bahariya Fm., TSW-7, 13, 15 and 21 wells.

The previous relationship is indicated by the equation:

$$K = 24590e^{-0.5715Swirr} \qquad (5.18)$$

$$R = 0.89$$

The obtained value of correlation coefficient indicates the equation is reliable to great extent to predict the permeability. Table (5.24) displays the characteristics of the displacement pressures for groups (A and C).

5.4.7 Pore-throat size distribution

Determination of pore-throat size distribution contributes to assess the performance of reservoir rocks. The study of the pore-throat size distribution of the reservoir rocks has a great importance for investigating secondary hydrocarbon migration and entrapment, (Schowalter, 1979). The correlation of pore-throat size with either reservoir porosity or permeability is important because pore-throat distribution controls all reservoir parameters (El Sayed, 1997). In the present study, the pore-throat size distribution was determined to relate the reservoir rock pore-spaces to its petrophysical properties. Consequently, the pore-throat size distribution is used to predict permeability, enhance the permeability-porosity relationship.

5.4.7.1 Calculation of pore-throat size distribution

Pore-throat size distribution can be calculated from the data of capillary pressure curves. These data can be used to approximate the distribution of pore volume accessible by throat of a given effective size using the equation adapted from Washburn (1921).

$$r = (2\gamma \cos\theta) / P_c \qquad (5.19)$$

Where:

r = pore-throat radius, microns.

γ = interfacial tension of the air/mercury system, 485 dynes/cm.

θ = air/mercury/solid contact angle, 140°.

P_c = capillary pressure, dynes/cm^2.

5.4.7.2 Classification of pore-throat size distribution

The ultimate aim of reservoir description is the characterization of reservoir heterogeneities. The overall pore network in a rock is the key factor in understanding the performance of reservoir rocks through the different measured petrophysical parameter. In turn, these petrophysical parameters are much controlled by the pore geometry. Much of the inter sample variability in

reservoir physics is associated with changes in pore type abundance, (Ehrlich et al., 1991). Moreover, the pore-throat size distribution controls all reservoir parameters (El Sayed and Kiss, 1997). If the pore system of a rock is modeled as a bundle of circular capillary tubes, the shapes and dimensions of the pore-throat size distribution could serve as a fingerprint of the reservoir rock pore types. Pore types and throat-size information derived from thin section and mercury injection was used to construct a simple physical model for permeability and electrical conductivity (Ehrlich et al, 1991). Toledo (1994) stated that: the interpretation of the fingerprint is still the subject of active research work. While El Sayed and Kiss (1997) have introduced a rock pore space model (Fig. 5.17) depending on the capillary pressure measurements of more than 500 sandstones samples. They classified the rock pore space frame work into 7 classes (PVC1 up to PVC7) of bundles of circular capillary tubes ranged from pore volume corresponding to radius started from 0.0075 to 7.5 microns.

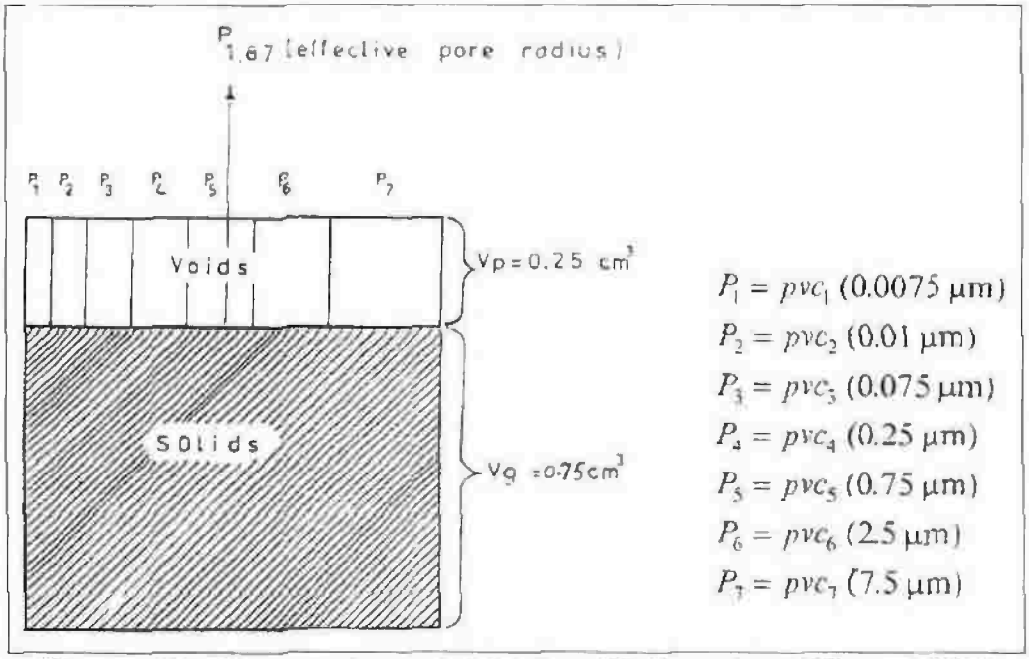

Fig. (5.17): Reservoir model (After, El Sayed and Kiss, 1997)

They also considered that the rock–effective pore radius contributing for water, oil and gas transportation is equal to 1.87 μm. This classification has been used by the authors for clean sandstone, clayey sandstone and marly sandstone facies discrimination

5.4.7.3 Results of pore-throat size distribution

The pore-throat size distribution data are presented in form of frequency cumulative curves. The results of the pore-throat size distribution of the lower part of the Bahariya Formation in BED1-11 well are presented in figure (5.18). The results of pore-throat size distribution of TSW-wells (TSW-7, 8, 13, 15 and 21) are presented in figures (5.19) through (5.23) respectively. On the other hand the results of Abu Roash `G` in TSW-21 well are presented in figure (5.24) where the results of the upper part of the Bahariya Formation samples obtained from wells TSW-7, 13, 15 and 21 are presented in figure (5.25).

(Fig. 5.18) display the studied samples of BED1-11 well (the lower part of the Bahariya Formation), the samples classified into three groups: A, B and C. Some samples (heavy lines) have intermediate positions between groups (B) and (C) but nearer to group (B).

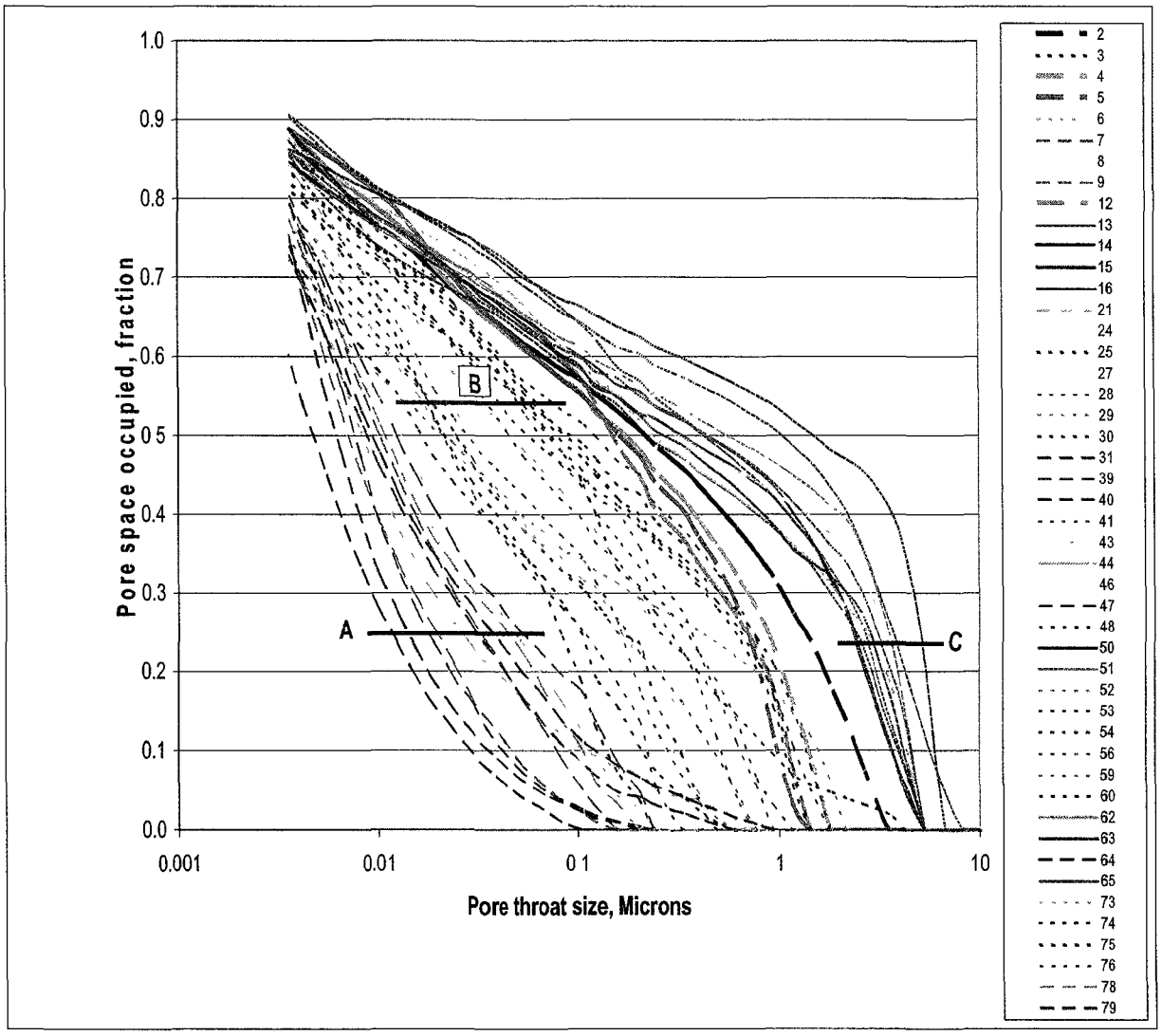

Fig. (5.18): Pore throat size distribution from mercury injection data of L. part of Bahariya Fm., BED1-11 well.

Figures (5.19-5.23) show the pore size distribution of TSW-wells where figure (5.24) displays the pore size distribution of Abu Roash `G` in TSW-21 well, the same relation exhibited in figure (5.25) for the studied samples of the upper part of the Bahariya Formation obtained from TSW-wells as follows:

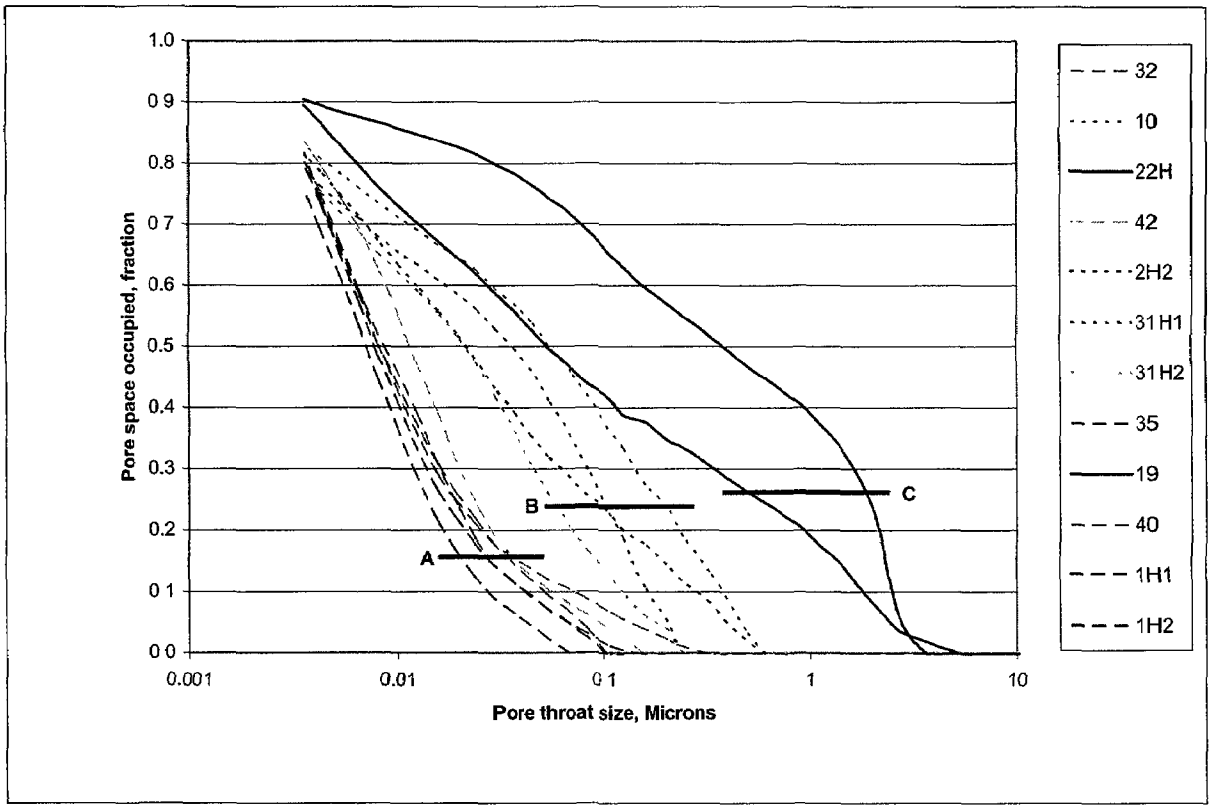

Fig. (5.19): Pore throat size distribution from mercury injection data, TSW-7 well.

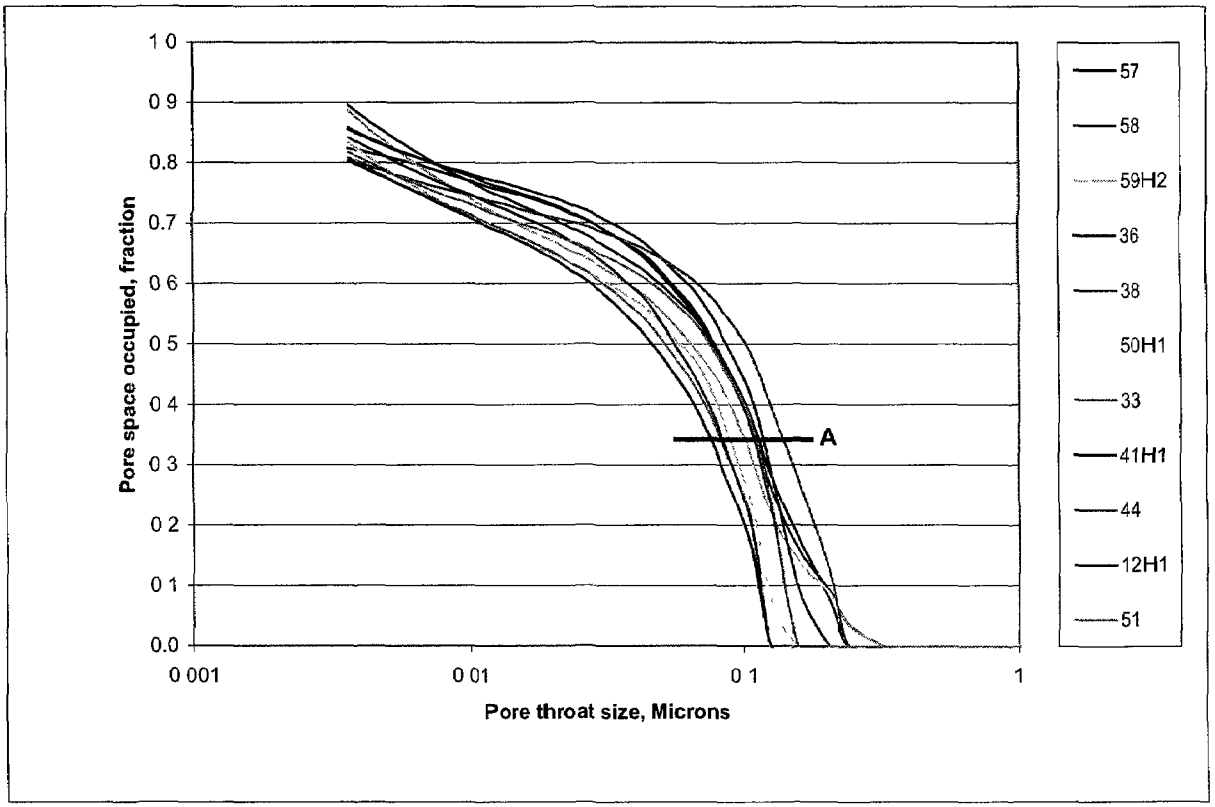

Fig. (5.20): Pore throat size distribution from mercury injection data, TSW-8 well.

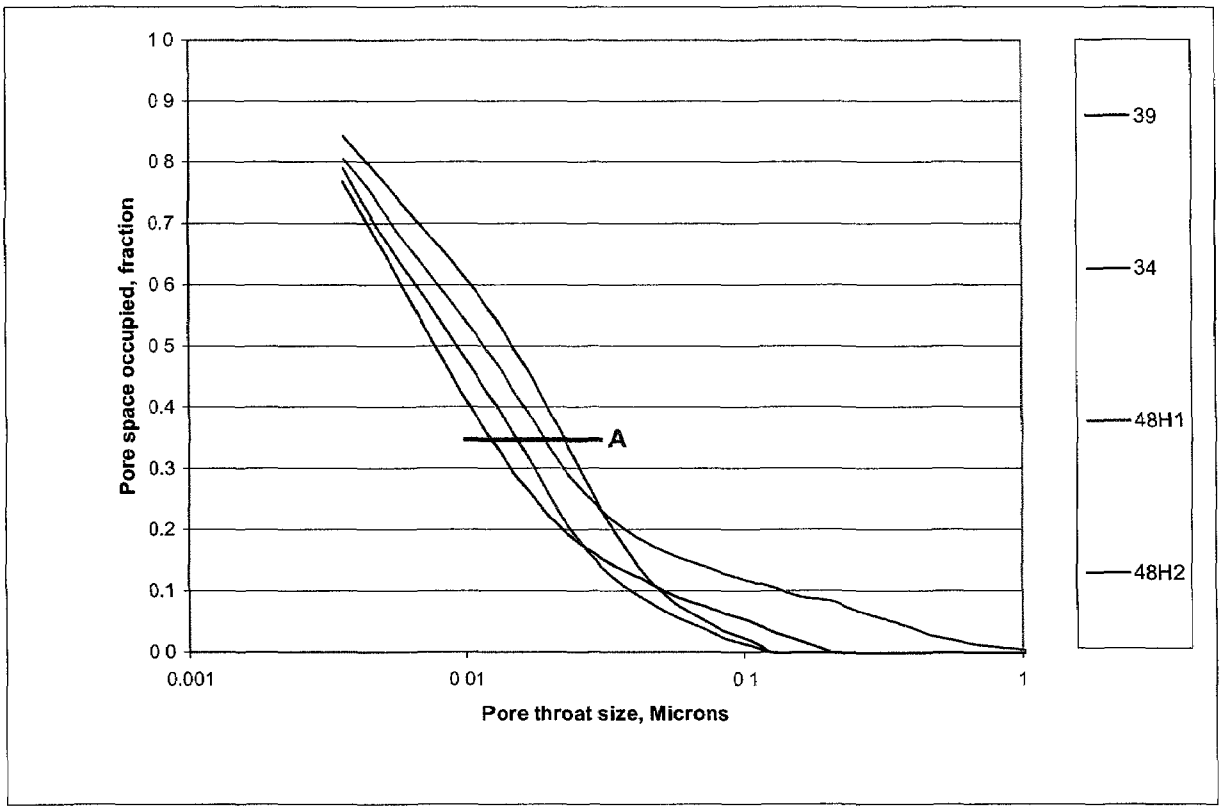

Fig. (5.21): Pore throat size distribution from mercury injection data, TSW-13 well.

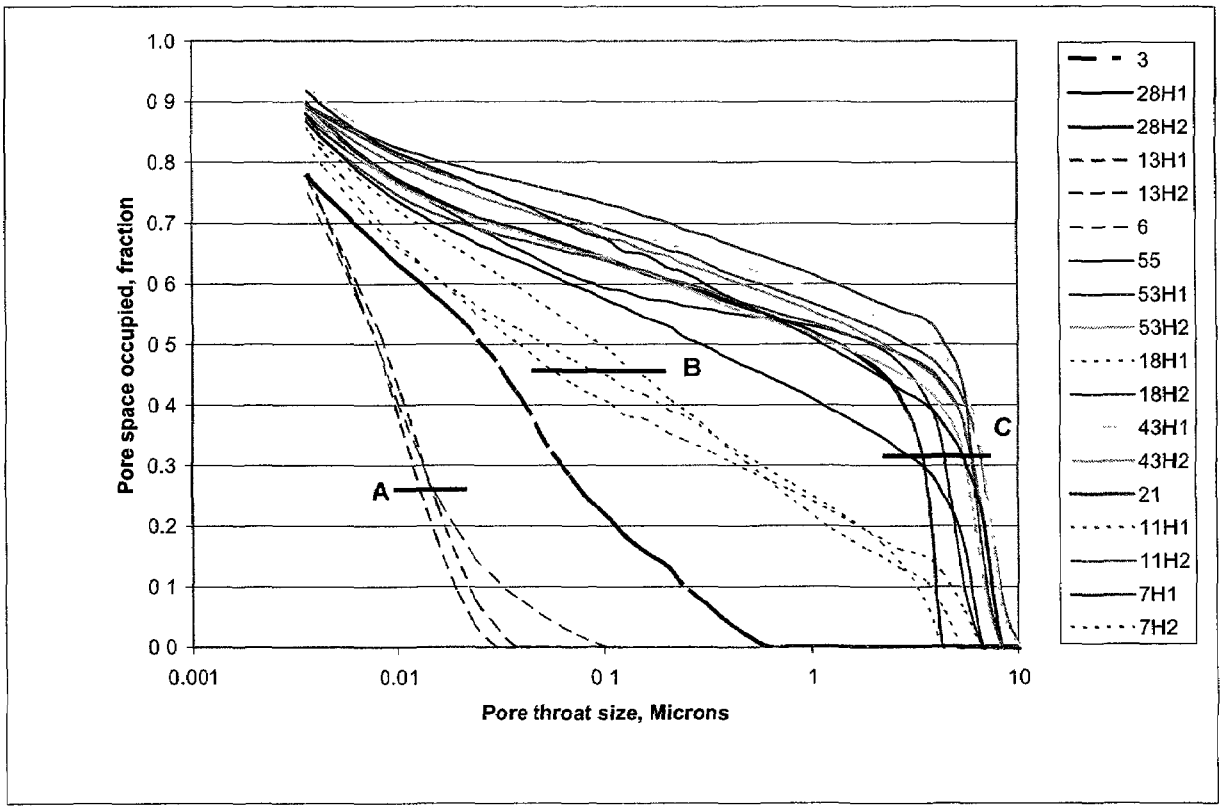

Fig. (5.22): Pore throat size distribution from mercury injection data, TSW-15 well.

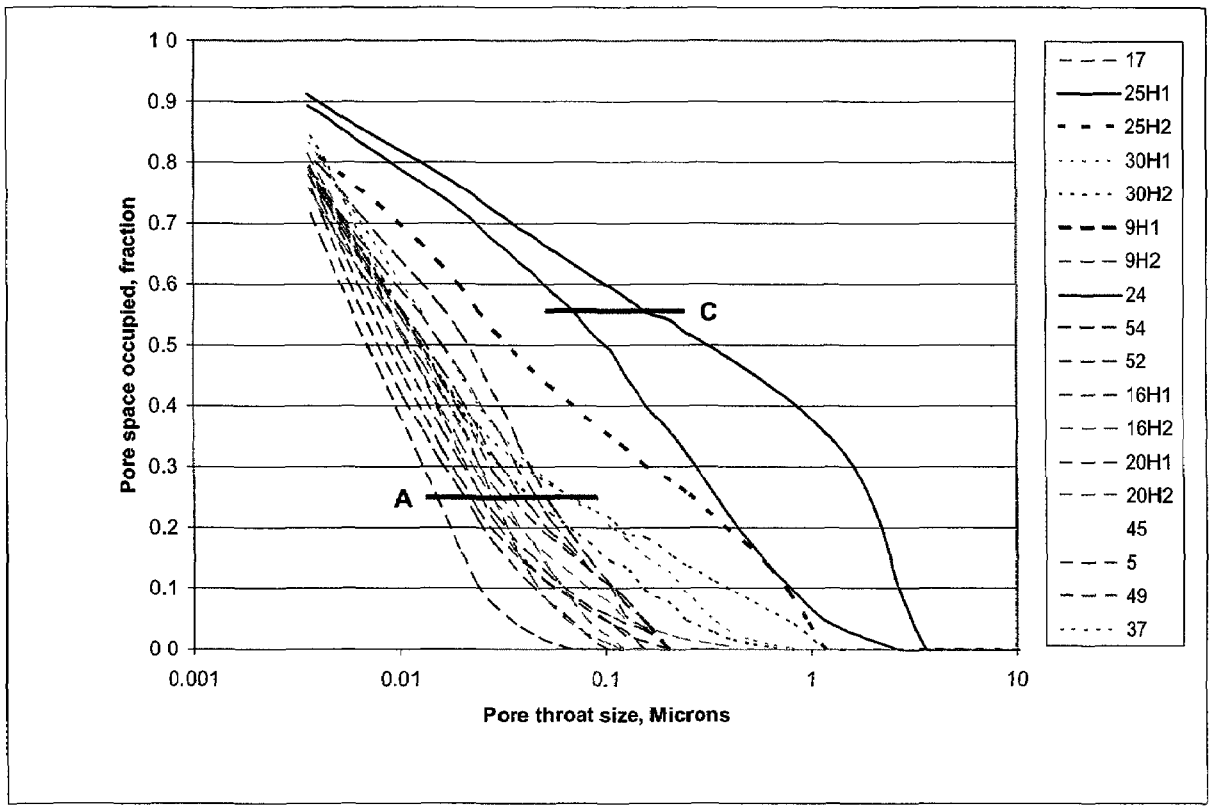

Fig. (5.23): Pore throat size distribution from mercury injection data, TSW-21 well.

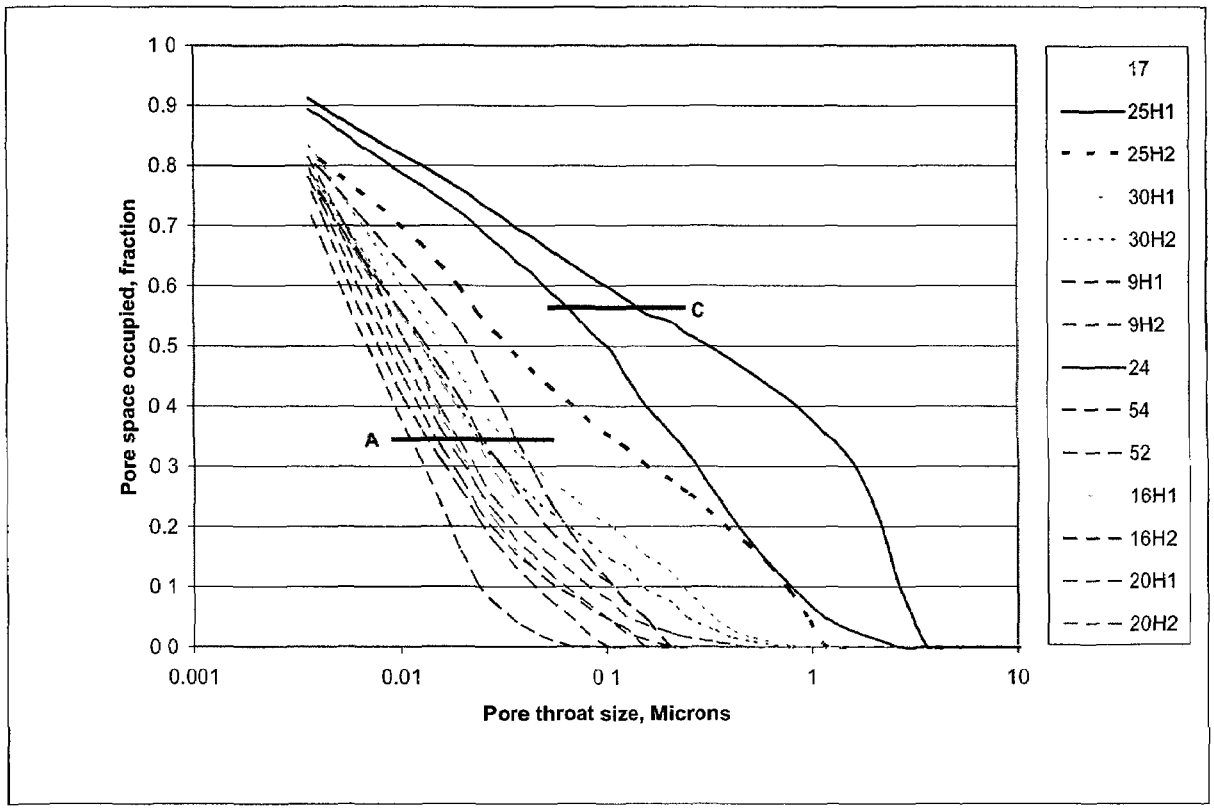

Fig. (5.24): Pore throat size distribution from mercury injection data of Abu Roash `G`, TSW-21 well.

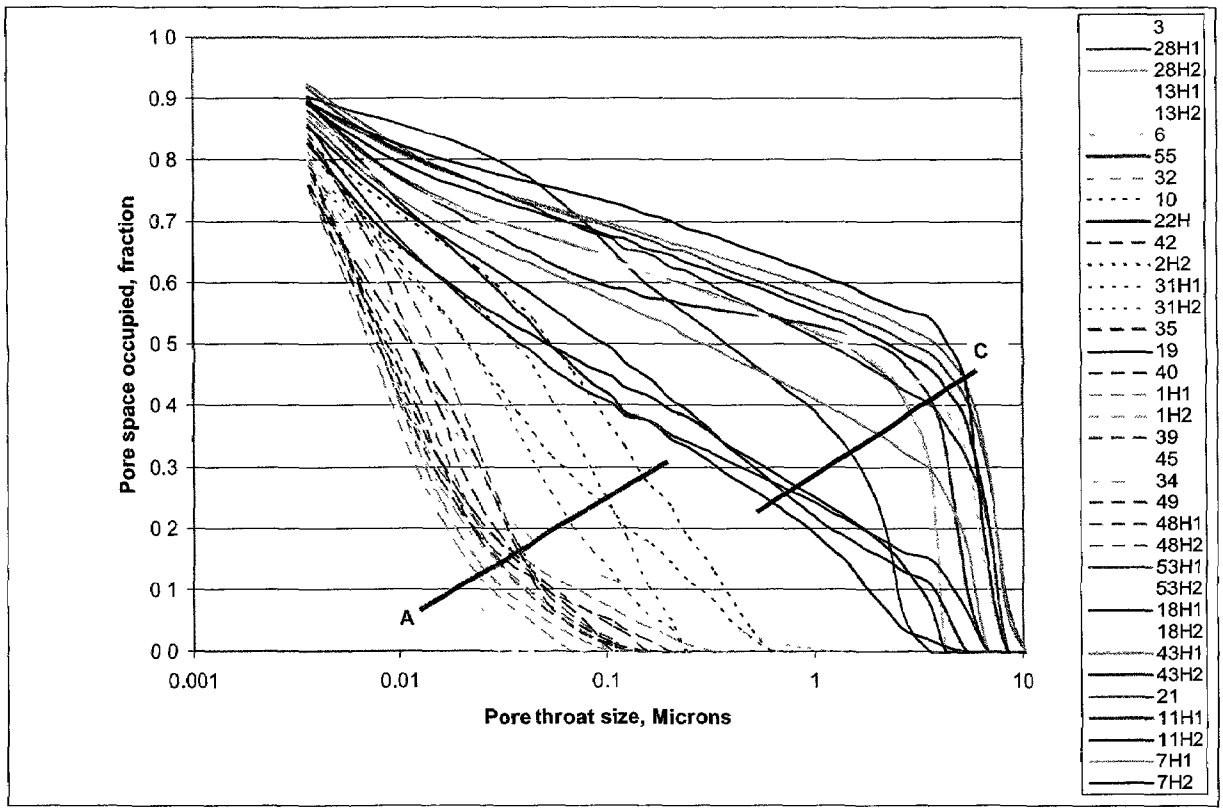

Fig. (5.25): Pore throat size distribution from mercury injection data of U. Bahariya, TSW-7, 13, 15 and 21 wells.

5.5 Pore-throat size distribution derived parameters

5.5.1 PVC

According to El Sayed and Kiss (1997), PVC means a pore volume that corresponding to a certain pore radius. Values of (PVC1-PVC7) have been determined for all samples and it is found out that (PVC2) that corresponding to 0.01 Microns has the best relation with permeability in the lower part of the Bahariya Formation in BED1-11 well, TSW-wells (7, 15 and 21), Abu Roash 'G' Member in TSW-21 well and the upper part of the Bahariya Formation that compiled from TSW-wells. Also it is found out that (PVC1) that corresponding to 0.0075 Microns has the best relation with the permeability only in wells TSW-8 and TSW-13, although (PVC3) and (PVC2) constitute the majority of PVC's in wells TSW-8 and TSW-13 respectively.

5.5.1.1 PVC's results

The results of PVC's displayed in tables for the different studied units, these tables show the percent of each PVC but we will concentrate on the results of PVC2 and PVC1 that gave the best results with the permeability as previously mentioned. Table (5.25) displays the wide range of (PVC2) from a minimum of 15.2% to a maximum value of 73.9% with an average value 38.9% for the studied samples of the lower part of the Bahariya Formation in BED1-11 well. For TSW-8 well (Abu Roash `F`), (PVC1) varies from a minimum of 2% up to a maximum value of 4.5% with an average value 3.1% (Table 5.27). Also (PVC1) varies from 11% to 19.9% with an average value 14.6% for TSW-13 well, Table (5.28). (PVC2) values differ in a high range from a minimum of 18.1% up to a maximum value of 76.2% with an average 57.3% for TSW-7 well (Table 5.26), from a minimum of 7.9% up to a maximum value of 78.8% with an average value 27.9% for TSW-15 well (Table 5.29), from 23% up to 83.8% with an average value 62.8% for TSW-21 well (Table 5.30), from 23% up to a maximum value of 79.9% with an average value 60.7% for Abu Roash `G` in TSW-21 well (Table 5.31) and from 7.9% up to a maximum value of 83.8% with an average value 41.5% for the studied samples of the upper part of the Bahariya Formation (Table 5.32).

5.5.1.2 PVC's versus permeability relations

Figure (5.26) displays PVC2-permeability relation for studied samples of the lower part of the Bahariya Formation obtained from BED1-11 well.

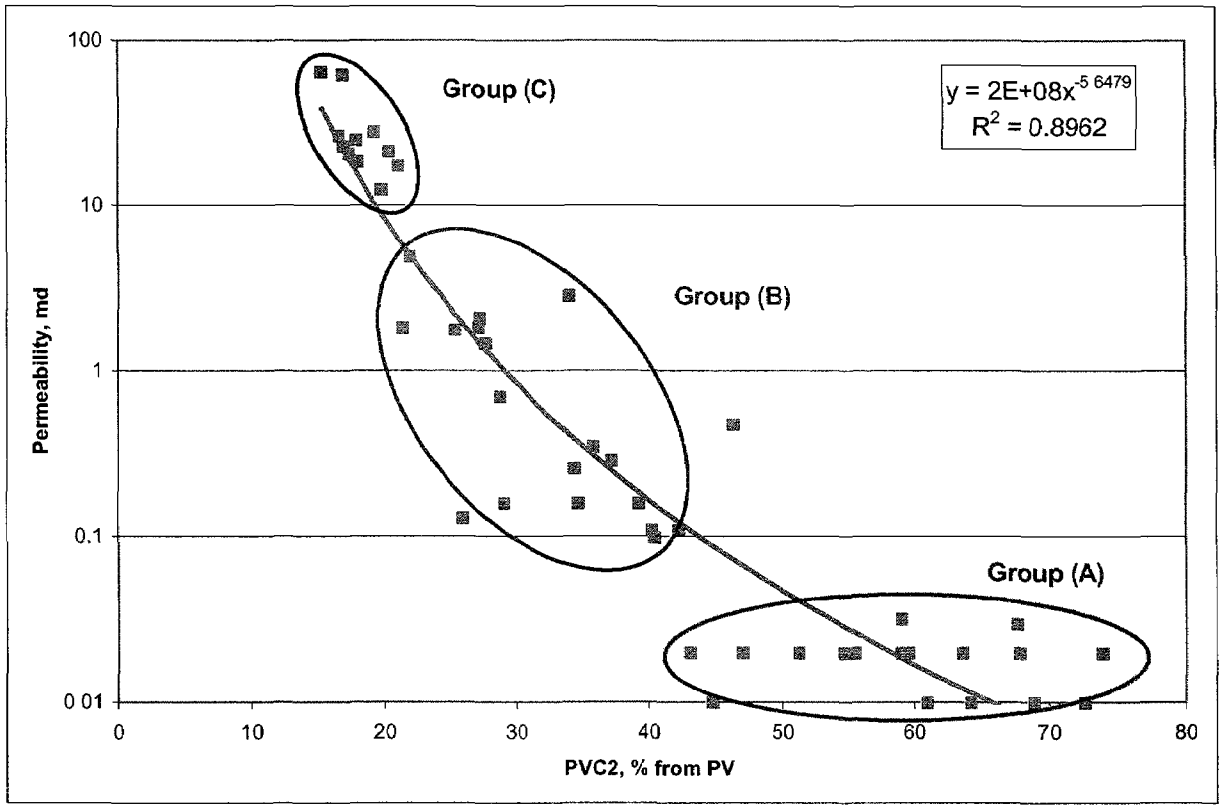

Fig. (5.26): PVC2 vs. permeability of L. Bahariya, BED1-11 well.

The relation is expressed by the equation:

$$K = 2E+08(PVC2)^{-5.6479} \qquad (5.20)$$

$$R = 0.95$$

The excellent value of correlation coefficient revealed the possibility of permeability prediction with a high accuracy. Table (5.33) displays the characteristics of PVC2 of groups (A, B and C).

Figure (5.27) shows PVC1-permeability relations of wells TSW-8 (Abu Roash `F`) and TSW-13, although (PVC3) and (PVC2) constitute the major percents in wells TSW-8 and TSW-13 respectively.

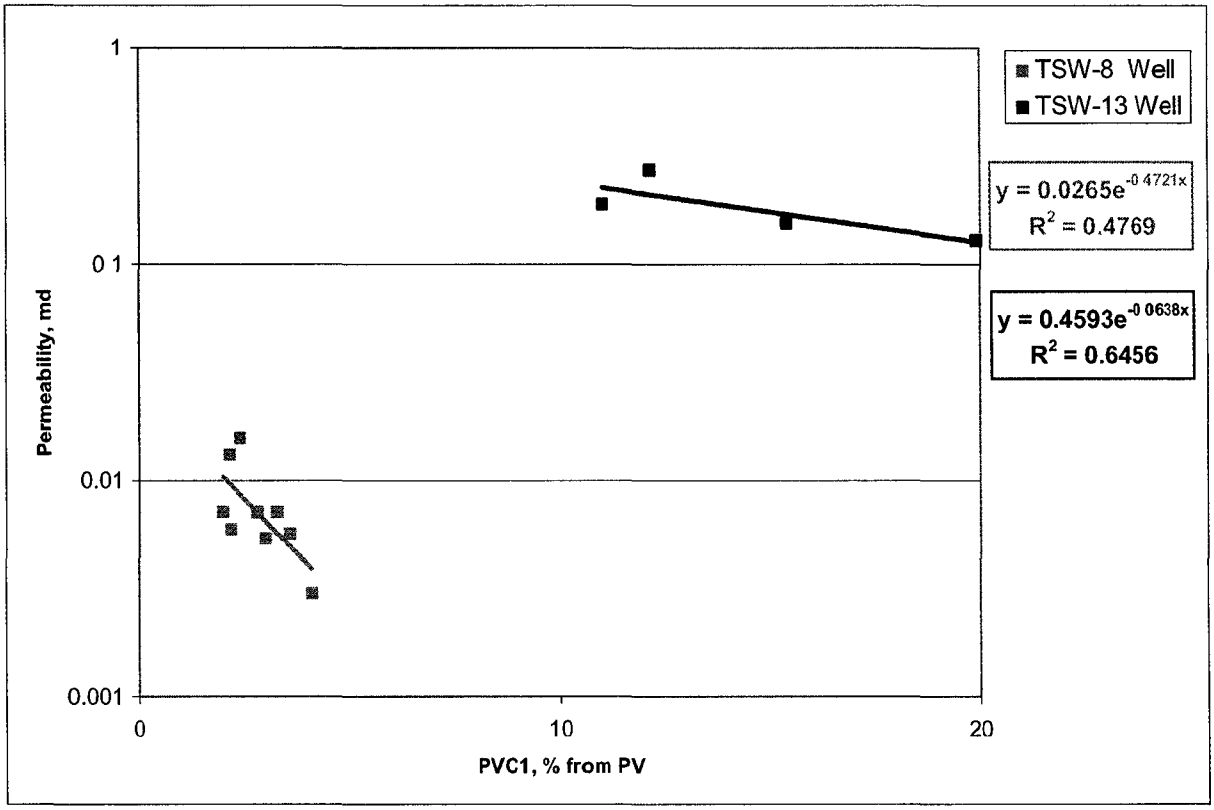

Fig. (5.27): PVC1 vs. permeability of wells TSW-8 and TSW-13.

The previous relation for TSW-8 well is expressed by the equation:

$$K = 0.0265e^{0.4721(PVC1)} \qquad (5.21)$$

$$R = 0.69$$

Samples (58) and (59) were canceled due to their abnormal values.

The relation for TSW-13 well is expressed by the equation:

$$K = 0.4593e^{0.0638(PVC1)} \qquad (5.22)$$

$$R = 0.80$$

The values of correlation coefficients indicate the possibility of permeability prediction to some extent. Figure (5.27) shows that all samples of TSW-8 well have nearly the same PVC1 values. Table (5.34) displays the characteristics of (PVC1) of this well.

Figure (5.28) displays PVC2-permeability relations for wells TSW-7, 15 and 21.

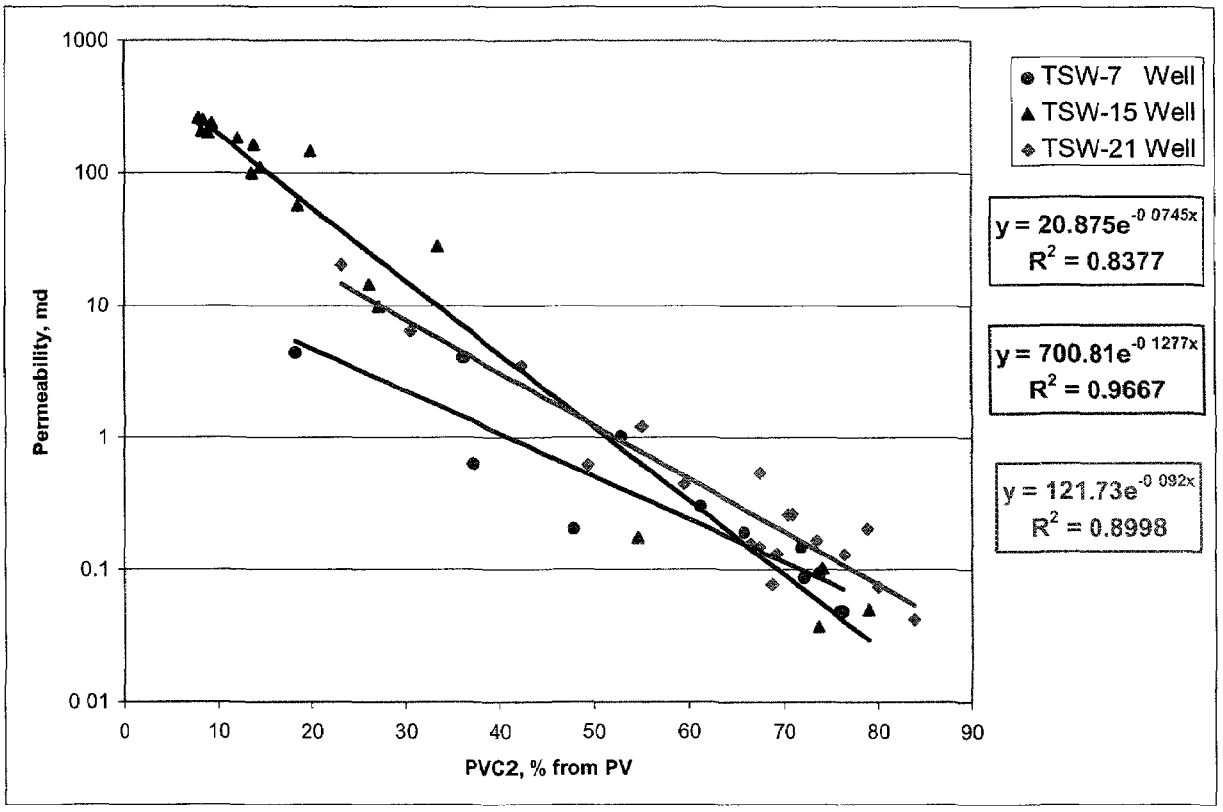

Fig. (5.28): PVC2 vs. permeability of TSW-7, 15 and 21 wells.

The outstanding relations were found and are expressed by the following equations:

For TSW-7 well:

$$K = 20.875e^{-0.0745(PVC2)} \qquad (5.23)$$

$$R = 0.92$$

For TSW-15 well:

$$K = 700.81e^{-0.1277(PVC2)} \qquad (5.24)$$

$$R = 0.98$$

For TSW-21 well:

$$K = 121.73e^{-0.092(PVC2)} \qquad (5.25)$$

$$R = 0.95$$

Similarly for Abu Roash `G` in TSW-21 well (Fig. 5.29), an outstanding relation was found where it is expressed by the equation:

$$K = 154.96e^{-0.0946(PVC2)} \qquad (5.26)$$

$$R = 0.97$$

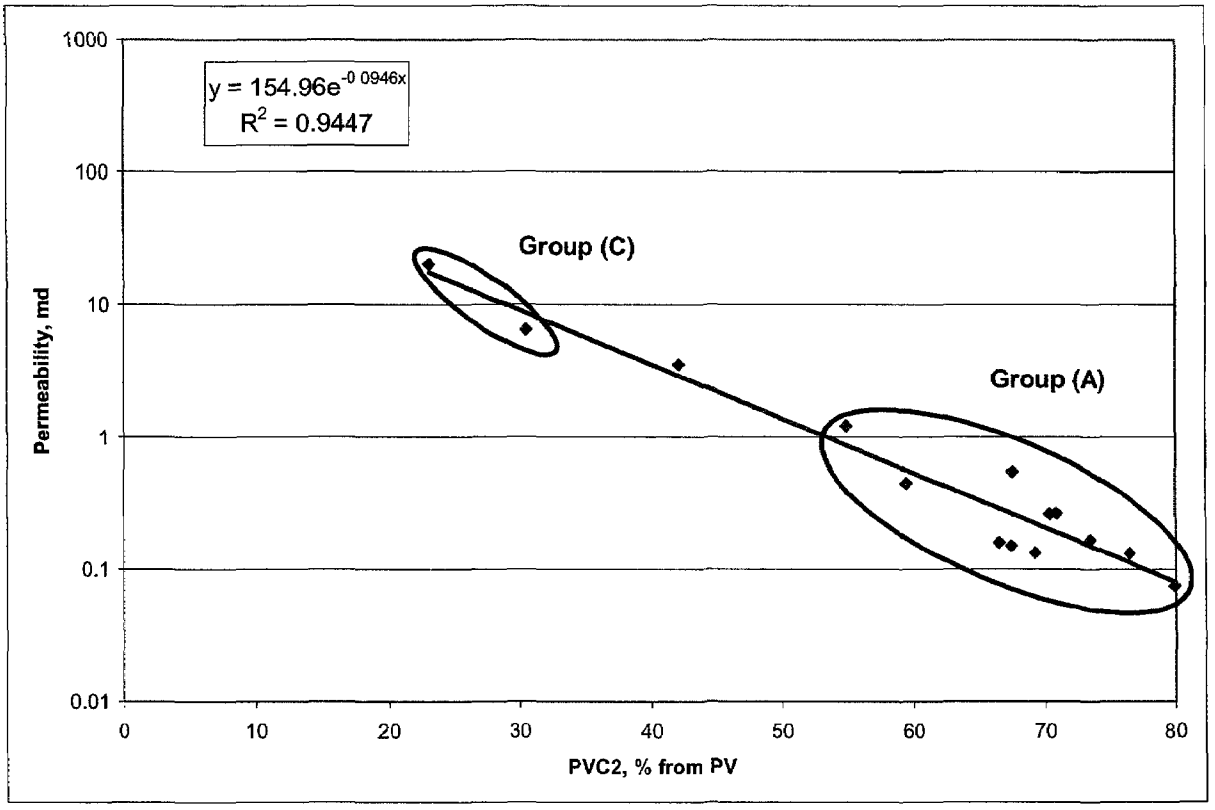

Fig. (5.29): PVC2 vs. permeability of Abu Roash `G`, TSW-21 well.

Table (5.35) displays the characteristics of PVC2 of groups (A and C)

Figure (5.30) displays PVC2-permeability relation for the studied samples of the upper part of the Bahariya Formation, obtained from TSW-wells.

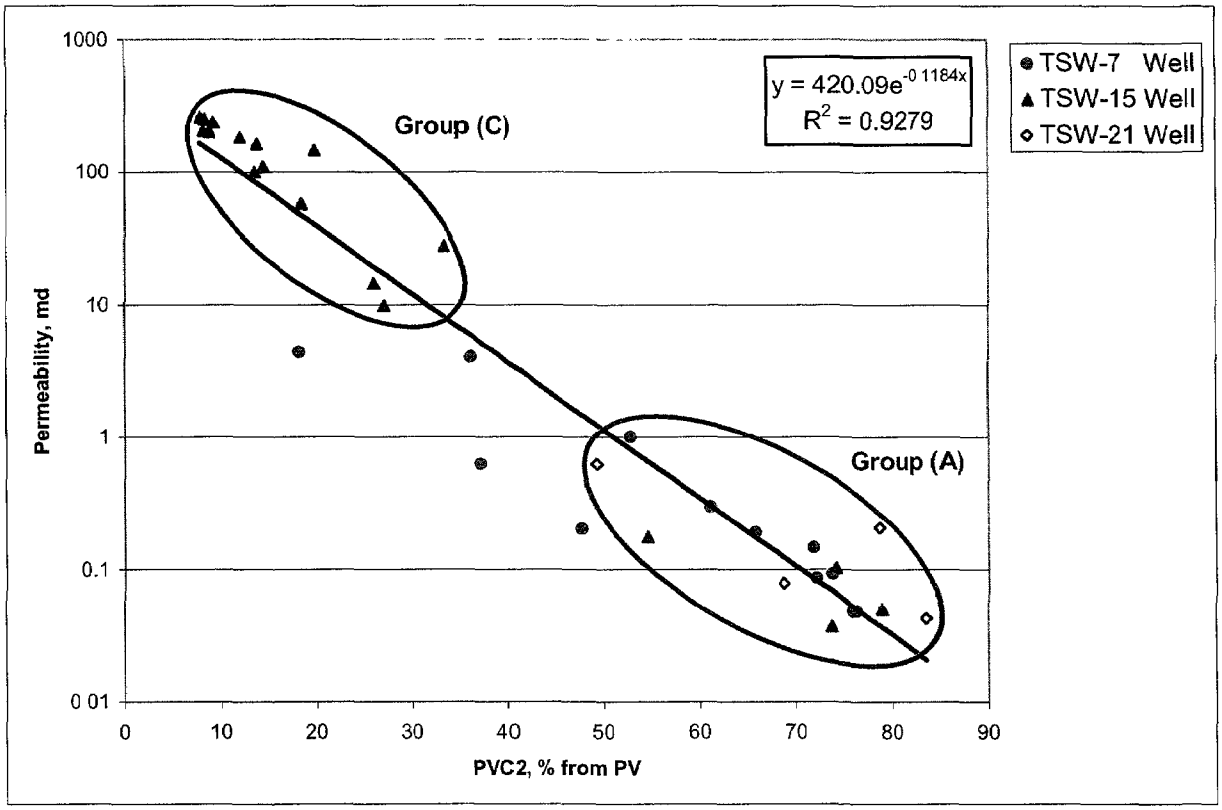

Fig. (5.30): PVC2 vs. permeability of U. Bahariya in TSW-7, 15 and 21 wells.

The relation is expressed by the equation:

$$K = 420.09e^{-0.1184(PVC2)} \qquad (5.27)$$

$$R = 0.96$$

The outstanding value of correlation coefficient assures that the equation is very reliable to predict the permeability with a high precision. Table (5.36) displays the characteristics of PVC2 of groups (A and C). The different PVC's against depth relations for the studied units are displayed in figures (5.31) to (5.35).

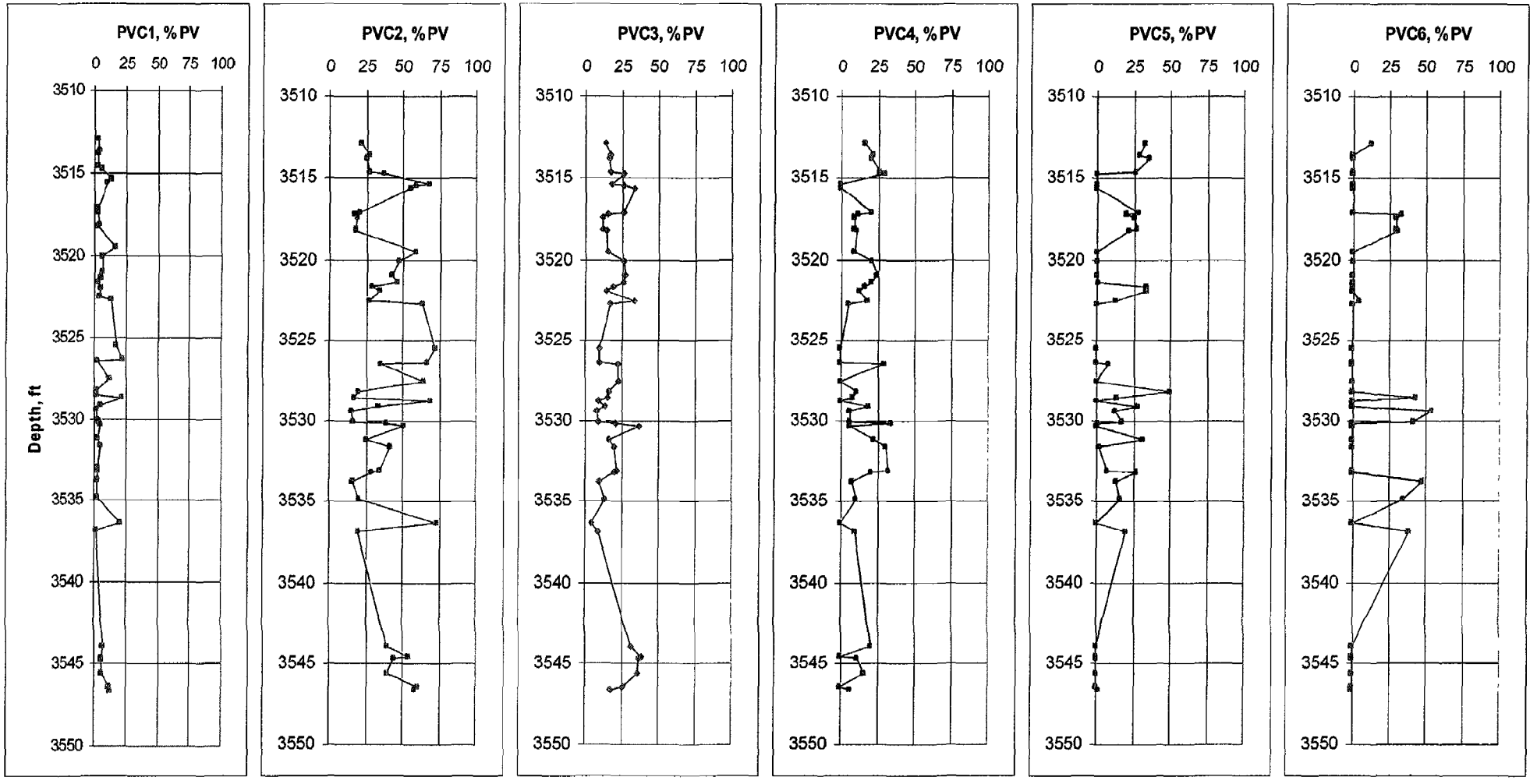

Fig. (5.31): Different PVC's percents vs. depth of L. Bahariya, BED1-11 well.

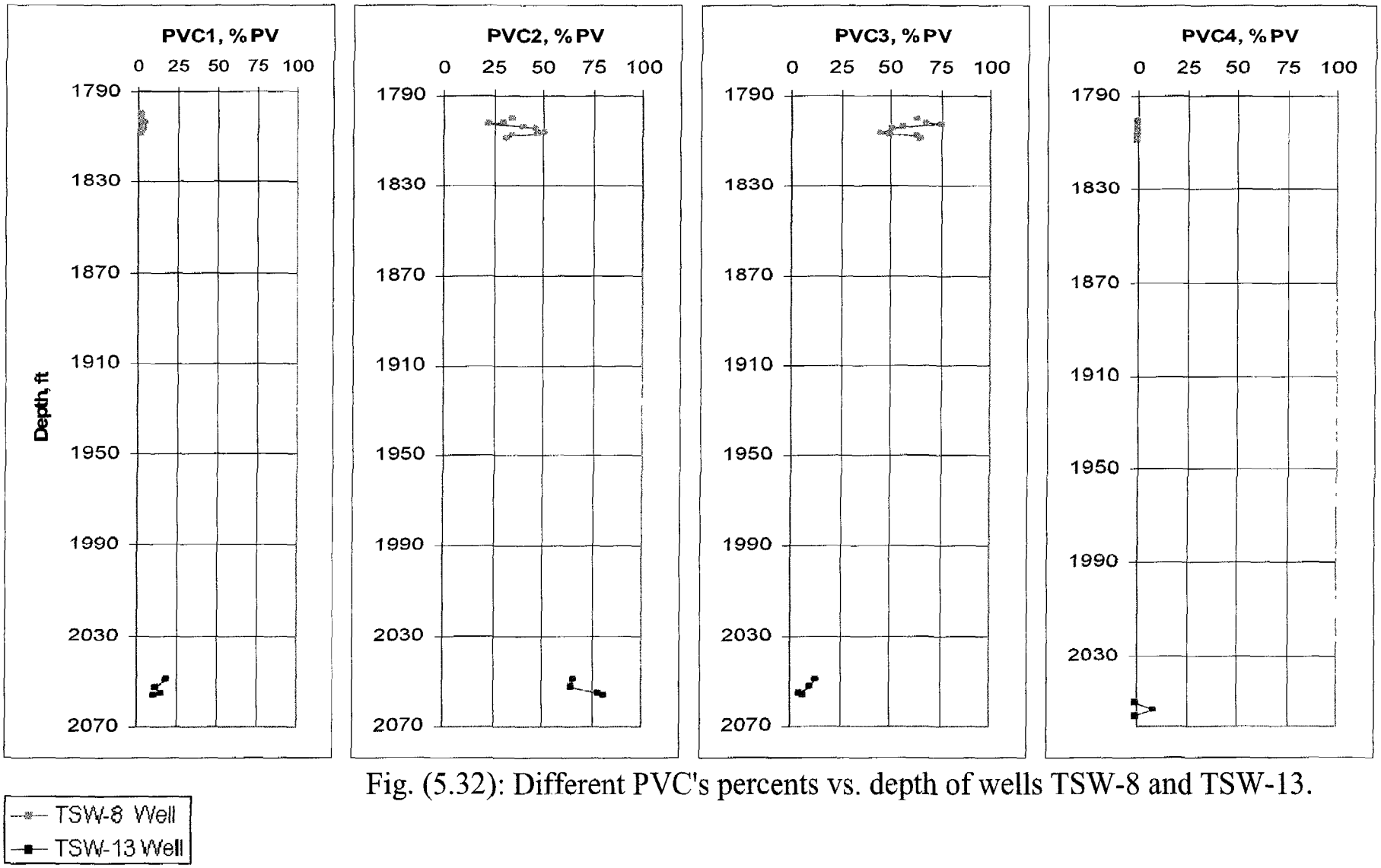

Fig. (5.32): Different PVC's percents vs. depth of wells TSW-8 and TSW-13.

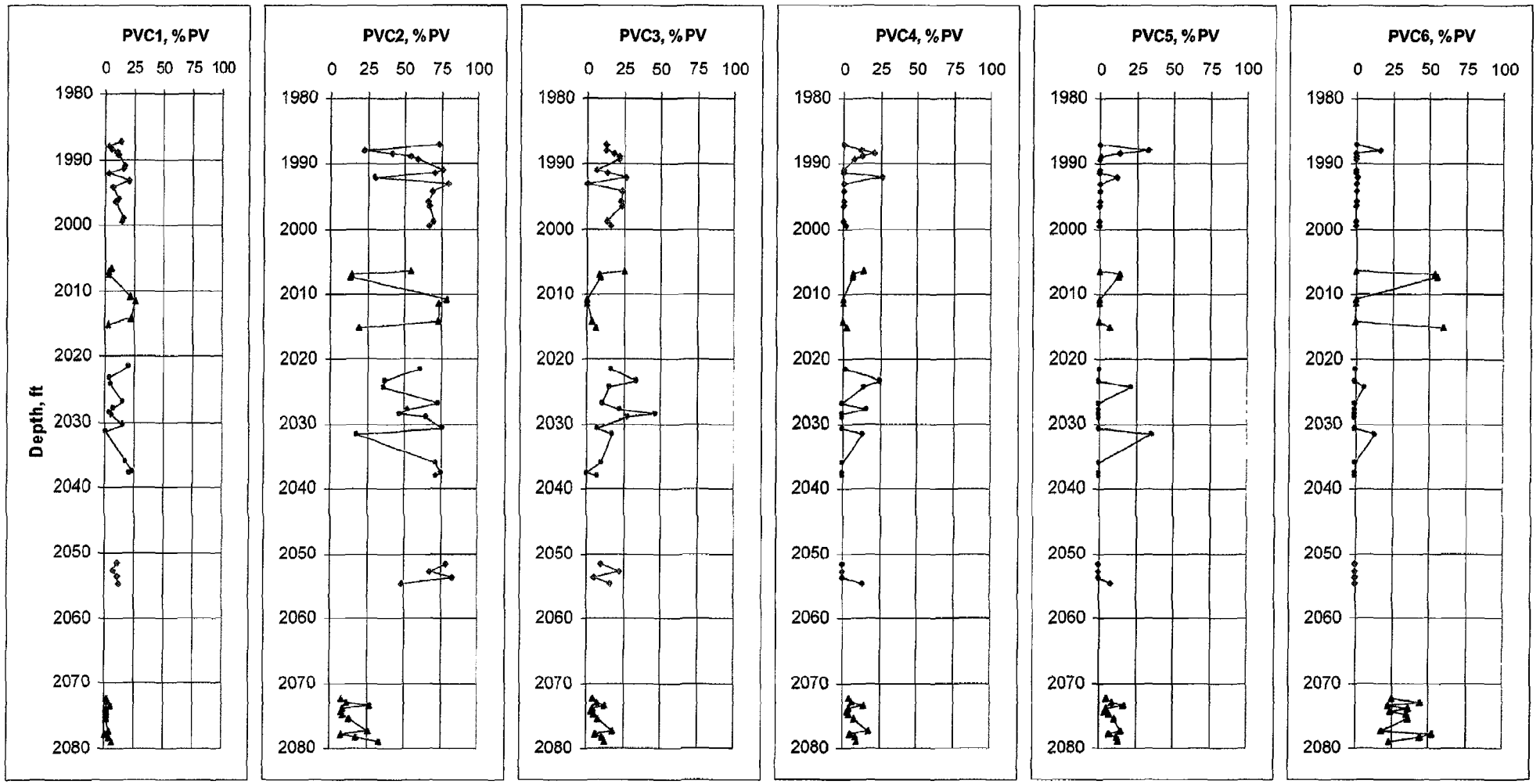

Fig. (5.33): Different PVC's percents vs. depth of wells (TSW-7, 15 and 21).

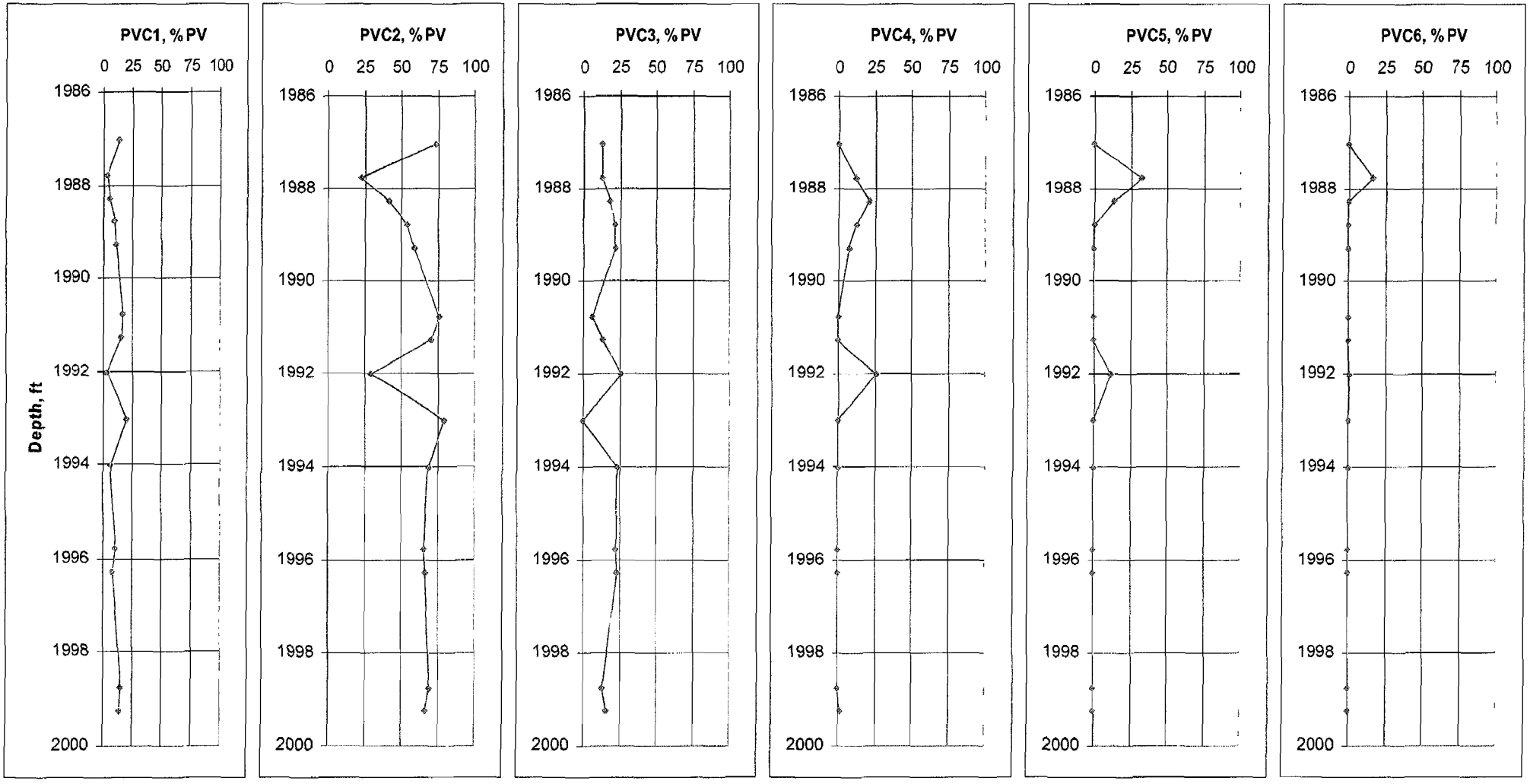

Fig. (5.34): Different PVC's percents against depth of Abu Roash `G` Member, TSW-21 well.

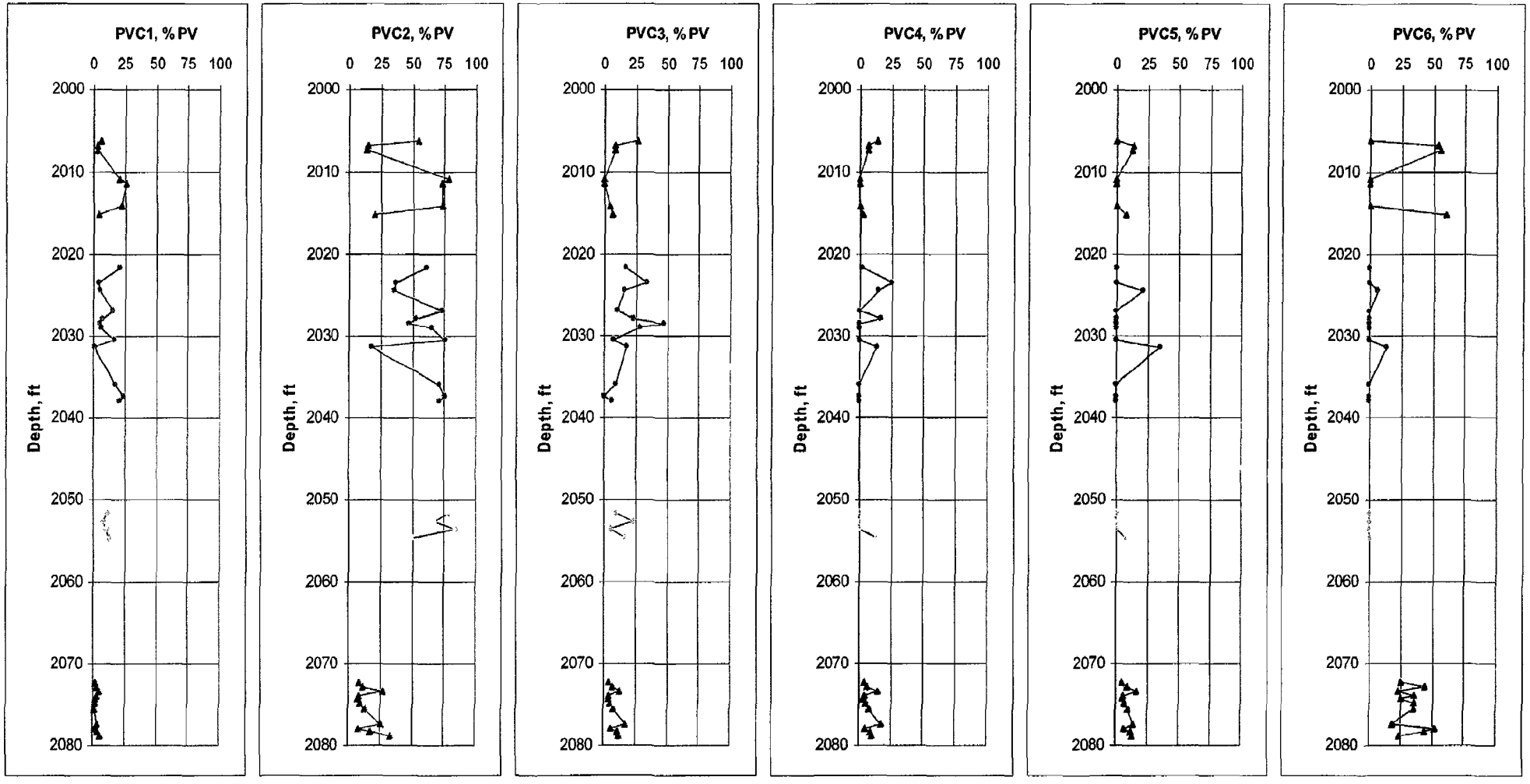

Fig. (5.35): Different PVC's percents against depth of U. Bahariya, TSW-7, 15 and 21 wells.

5.5.2 Mean hydraulic radius (MHR)

Mean hydraulic radius is defined as the ratio of a conduit's cross-sectional area to the wetted perimeter. It means the ratio of the rock pore open volume for fluid flow to the volume of the wetted area in pore spaces.

$$Mhr = (\text{volume open to flow}) / (\text{wetted surface area}) \qquad (5.28)$$

For a circular, cylindrical capillary tube

$$Mhr = r/2 \qquad (5.29)$$

Mean hydraulic radius (mhr) is the average pore size of the sample and is given by:

$$Mhr = (\sum ri^2 \ \Delta Si)^{½} \qquad (5.30)$$

Where:

ri (mean throat radius) = [(ri-1) + ri] / [2].

ΔSi (change in mercury saturation) = [(Si+1) – (Si-1)].

5.5.3 Median pore-throat size (Md)

Median pore-throat radius is defined as that radius above and below which 50% of the pore volume exists. It can be obtained by entering the cumulative pore-throat size distribution curve at 50% pore spaces occupied and determine the median value from the x-axis.

5.5.4. R35

R35 is defined as the pore aperture corresponding to a mercury saturation of 35% pore volume. The term was introduced by Winland who developed an empirical relationship among porosity, air permeability and pore aperture corresponding to a mercury saturation of 35% (R35) for a mixed suit of sandstones and carbonates. The Winland's equation was used and published by Kolodzie (1980).

$$\log r35 = 0.732 + 0.588 \log k_{air} - 0.864 \log \phi \qquad (5.31)$$

Where:

r35 = the pore aperture radius corresponding to the 35th percentile.

K_{air} = the uncorrected air permeability (md).

ϕ = porosity (%).

Winland also has showed, through several field examples, that r35 could be used to delineate commercial hydrocarbon accumulations of stratigraphic traps. One of Winland's examples was the Terry Sandstone at Spindle field, Colorado. Pittman (1989), using some of the same cored wells as Winland, has showed that the net feet of sandstone having an r35 greater than 0.5 μm was useful for delineating the trap. Up dip dry holes have no net sandstone with an r35 >0.5 μm. whereas, a good well in the field has 39 ft (11.9 m) of net sandstone with an r35 >0.5 μm. The obtained results of the median of the pore-throat size distribution, the mean hydraulic radius and R35 for all the studied samples are presented in tables as follows: Table (5.37) displays the results of the studied samples of the lower part of the Bahariya Formation obtained from BED1-11 well. Tables (5.38) through (5.42) display the results of TSW-7, 8, 13, 15 and 21 wells respectively. Table (5.43) displays the results of Abu Roash `G`, TSW-21 well. Table (5.44) displays the results of the studied samples of the upper part of the Bahariya Formation collected from TSW-7, 13, 15 and 21 wells.

5.6. Mean hydraulic radius results

Samples of the lower part of the Bahariya Formation in BED1-11 well show a wide range of MHR varies from 0.03 micron up to 4.54 microns with an average value 1.09 microns (Table 5.37). For TSW-wells, TSW-7 well have MHR range differs from 0.025 micron up to 2.05 microns with an average value 0.386 micron (Table 5.38), TSW-8 well (Abu Roash `F`) displays a very narrow range of MHR varies from a minimum of 0.087 micron up to a maximum value of 0.175 micron with an average value 0.129 micron and this reflected in the tight properties of this well (Table 5.39), similarly in TSW-13 well, where MHR varies in a range from a minimum of 0.039 micron up to a maximum value of 0.221 micron with an average value 0.091 micron (Table 5.40). TSW-15 well displays the widest range of MHR from 0.018 micron up to 7.61 microns with an average value 3.65 microns (Table 5.41). The range of MHR varies from 0.024 micron up to 1.99 microns with an average value 0.262 micron in TSW-21 well (Table 5.42), the same behavior for Abu Roash `G`, TSW-21 well but the average value is 0.299 micron (Table 5.43). Like TSW-15 well, the studied samples of the upper part of the Bahariya Formation obtained from TSW-wells have a the widest range of MHR differs from 0.018 micron up to 7.61 microns with an average value 1.87 microns, (Table 5.44).

5.6.1 Mean hydraulic radius versus permeability relations

Figure (5.36) displays mean hydraulic radius-permeability relation of the lower part of the Bahariya Formation in BED1-11 well.

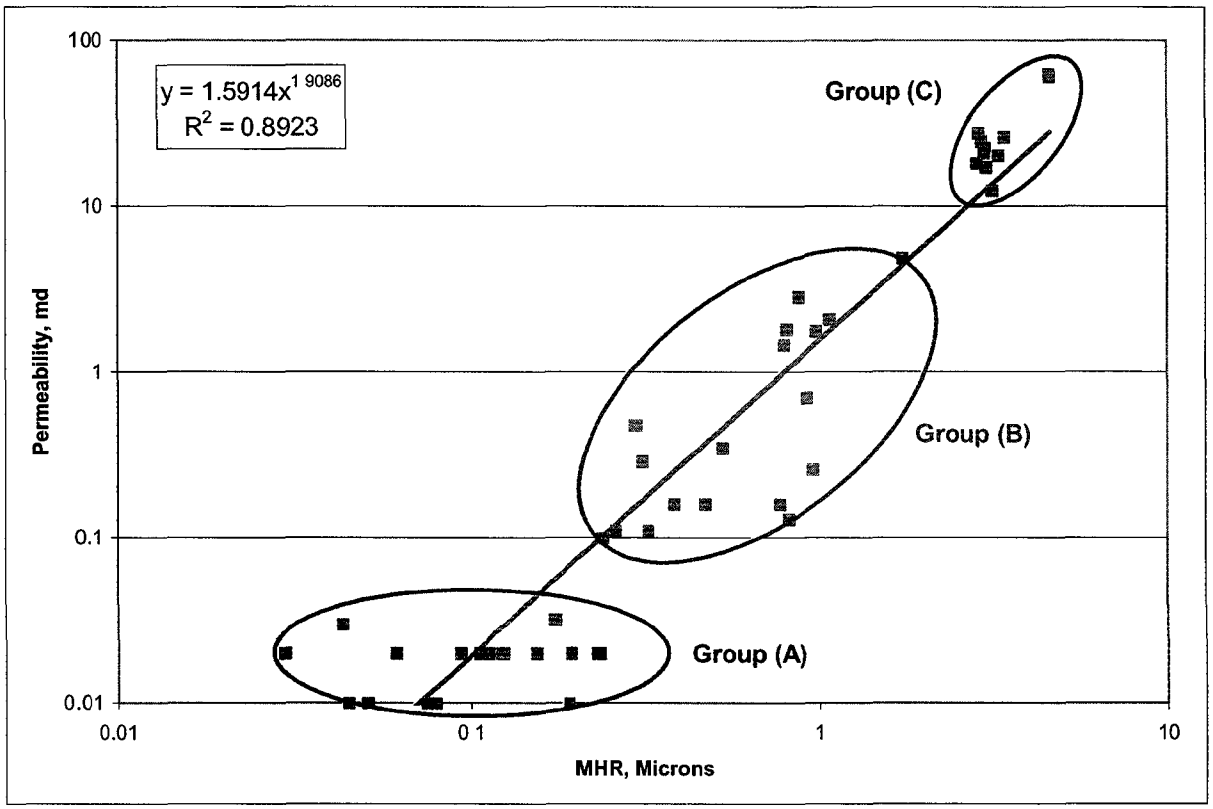

Fig. (5.36): Mean hydraulic radius vs. permeability of L. Bahariya, BED1-11 well.

The excellent relation is expressed by the equation:

$$K = 1.5914 mhr^{1.9086} \qquad (5.32)$$

$$R = 0.94$$

The previous equation revealed the possibility of permeability prediction with a high precision. Table (5.45) displays the characteristics of MHR of groups (A, B and C).

Figure (5.37) is a composite figure displays mean hydraulic radius-permeability relations of the studied samples in wells TSW-7, TSW-8 (Abu Roash `F`), TSW-13, TSW-15 and TSW-21.

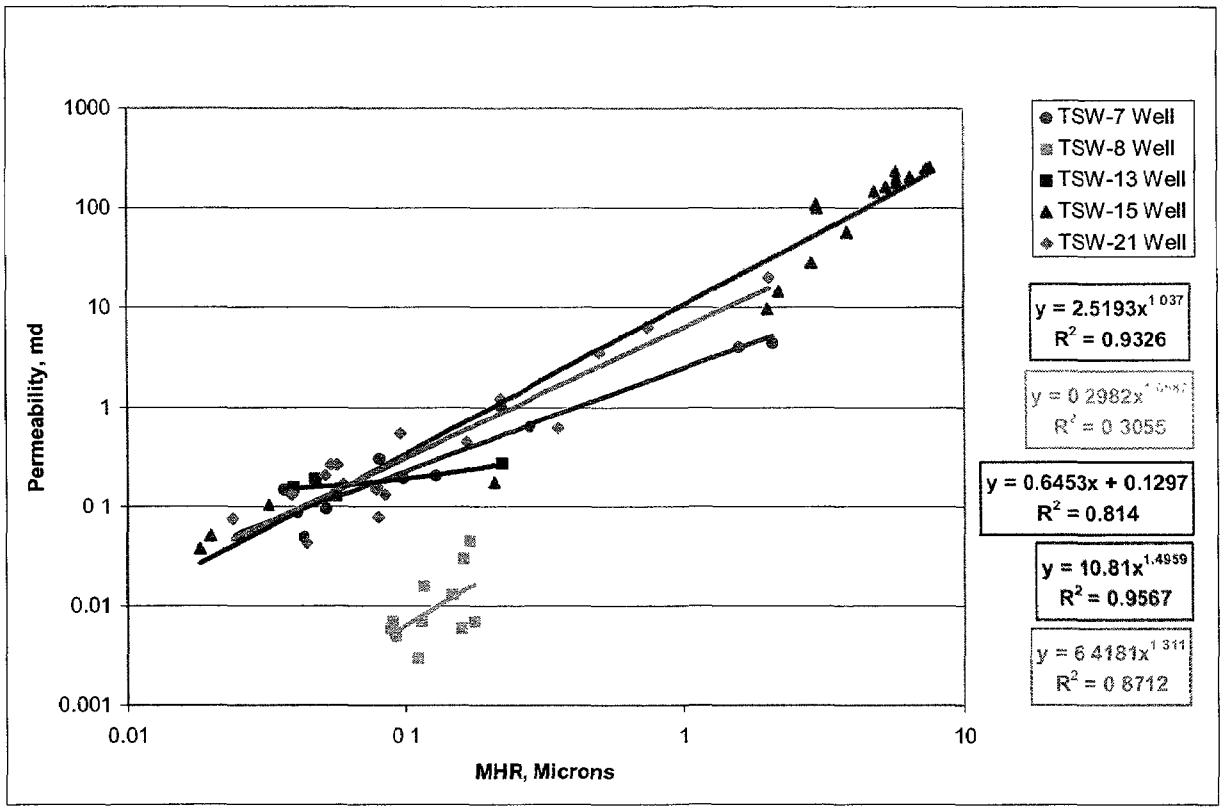

Fig. (5.37): Mean hydraulic radius vs. permeability of all TSW wells.

The majority of the studied wells gave very excellent results as follows:

Samples of TSW-7 well have a relation which is expressed by the equation:

$$K = 2.5193 mhr^{1.037} \qquad (5.33)$$

$$R = 0.97$$

The studied samples of TSW-8 well (Abu Roash `F`) have a relation which is expressed by the equation:

$$K = 0.2982 mhr^{1.6587} \qquad (5.34)$$

$$R = 0.55$$

The weak value of correlation coefficient indicate the low possibility of permeability prediction and this may be due to the very close values of

samples' permeability so there is no clear differences in MHR values. Table (5.46) displays the characteristics of TSW-8 well.

In TSW-13 well, the studied samples have a relation which is expressed by the equation:

$$K = 0.6453mhr + 0.1297 \qquad (5.35)$$

$$R = 0.90$$

For TSW-15 well, the studied samples have a relation which is expressed by the equation:

$$K = 10.81mhr^{1.4959} \qquad (5.36)$$

$$R = 0.98$$

In TSW-21 well, the studied samples have a relation which is expressed by the equation:

$$K = 6.4181mhr^{1.311} \qquad (5.37)$$

$$R = 0.93$$

The very excellent values of correlation coefficient (except TSW-8 well) revealed the possibility of permeability prediction with a high precision.

Figure (5.38) displays mean hydraulic radius-permeability relation of Abu Roash `G` in TSW-21 well.

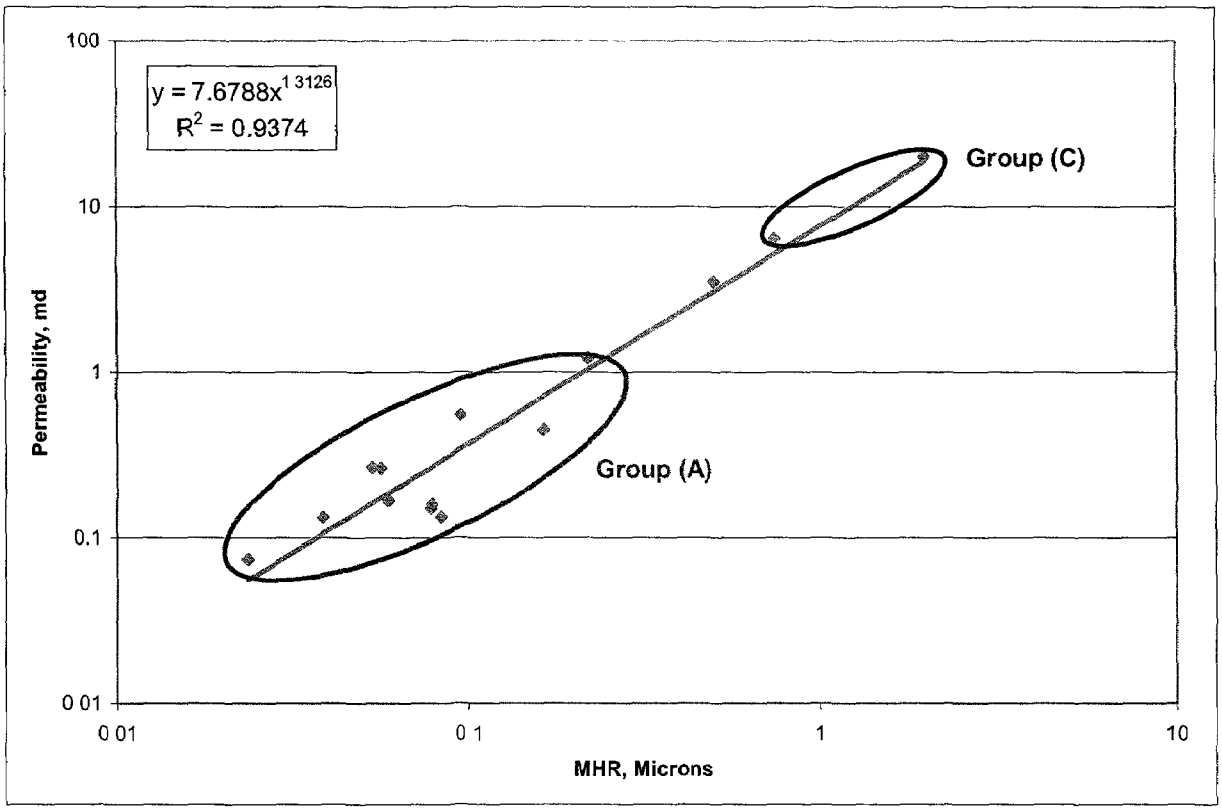

Fig. (5.38): Mean hydraulic radius vs. permeability of Abu Roash `G`, TSW-21 well.

The previous relation is expressed by the equation:

$$K = 7.6788 mhr^{1.3126} \qquad (5.38)$$

$$R = 0.97$$

The previous equation is very reliable to predict the permeability. Table (5.47) displays the characteristics of MHR of groups (A and C).

Figure (5.39) displays mean hydraulic radius-permeability relation of the studied samples of the upper part of the Bahariya Formation obtained from TSW-7, 13, 15 and 21 wells.

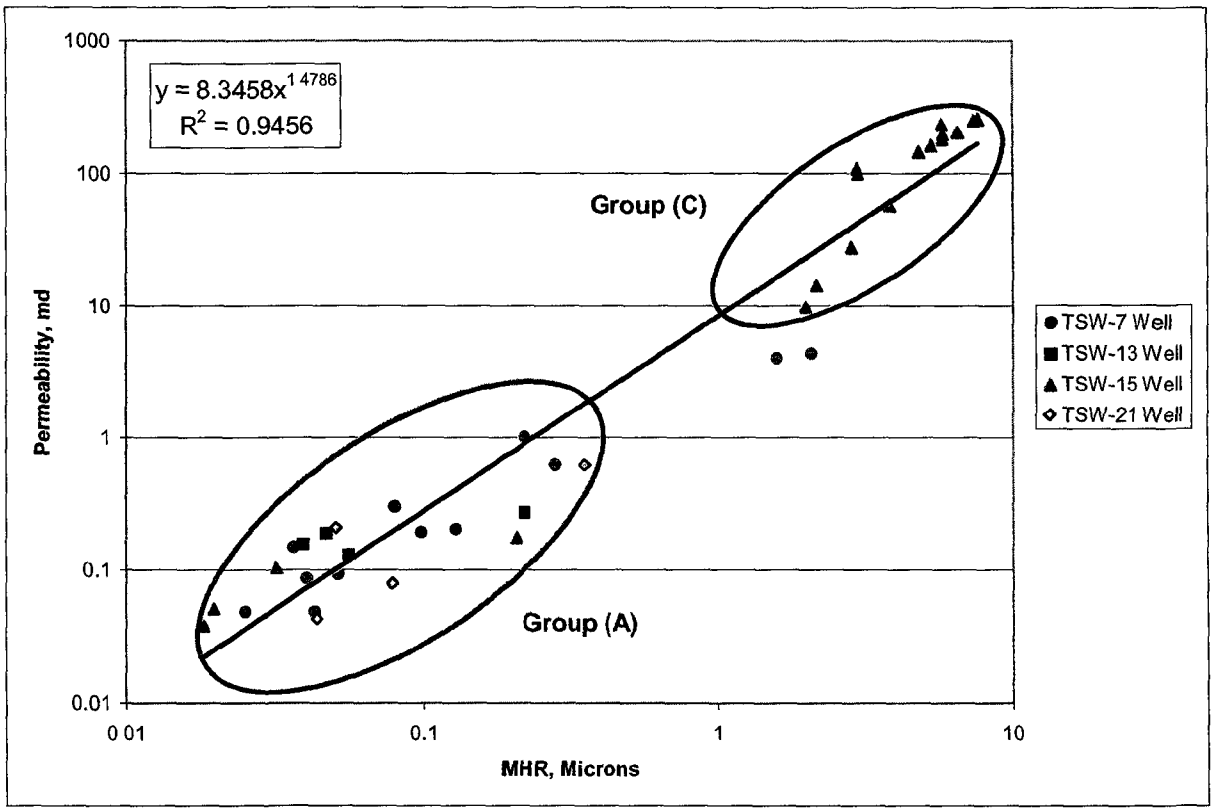

Fig. (5.39): Mean hydraulic radius vs. permeability of U. Bahariya, TSW-7, 13, 15 and 21 wells.

The previous relation is expressed by the equation:

$$K = 8.3458 mhr^{1.4786} \qquad (5.39)$$

$$R = 0.97$$

Also this equation is very reliable to predict the permeability with a high precision. Table (5.48) displays the characteristics of MHR of groups (A and C).

5.7 Median pore-throat size results

The measured (R50) was of varied values for each well and each formation as the following:

Table (5.37) show R50 varies in a high range from a minimum of 0.004 micron up to a maximum value of 1.51 microns with an average value 0.16 micron for the studied samples of the lower part of the Bahariya Formation in BED1-11 well where in TSW-7 well R50 varies from 0.007 micron up to 0.37 micron with an average value 0.05 micron (Table 5.38), the range becomes much narrow in TSW-8 well (Abu Roash `F`) where R50 varies in a range from 0.045 micron up to 0.1 micron with an average value 0.068 micron (Table 5.39), similarly in TSW-13 well where R50 varies in a range from 0.007 micron up to 0.014 micron with an average value 0.01 micron (Table 5.40), on the other hand in TSW-15 well R50 varies in a very high range from a minimum of 0.007 micron up to a maximum value of 4.42 microns with an average value 1.29 microns (Table 5.41), finally in TSW-21 well R50 varies in a range from 0.006 micron up to 0.31 micron with an average value 0.034 micron (Table 5.42). Abu Roash `G` in TSW-21 well display a range of R50 differs from 0.007 micron up to 0.31 micron with an average value 0.041 micron (Table 5.43). The studied samples of the upper part of the Bahariya Formation obtained from TSW wells have a very high range of R50 varies from a minimum of 0.007 micron up to a maximum value of 4.42 microns with an average value 0.63 micron (Table 5.44).

5.7.1 Median pore-throat size versus permeability relations

Figure (5.40) displays median pore throat-permeability relation of the studied samples of the lower part of the Bahariya Formation in BED1-11 well.

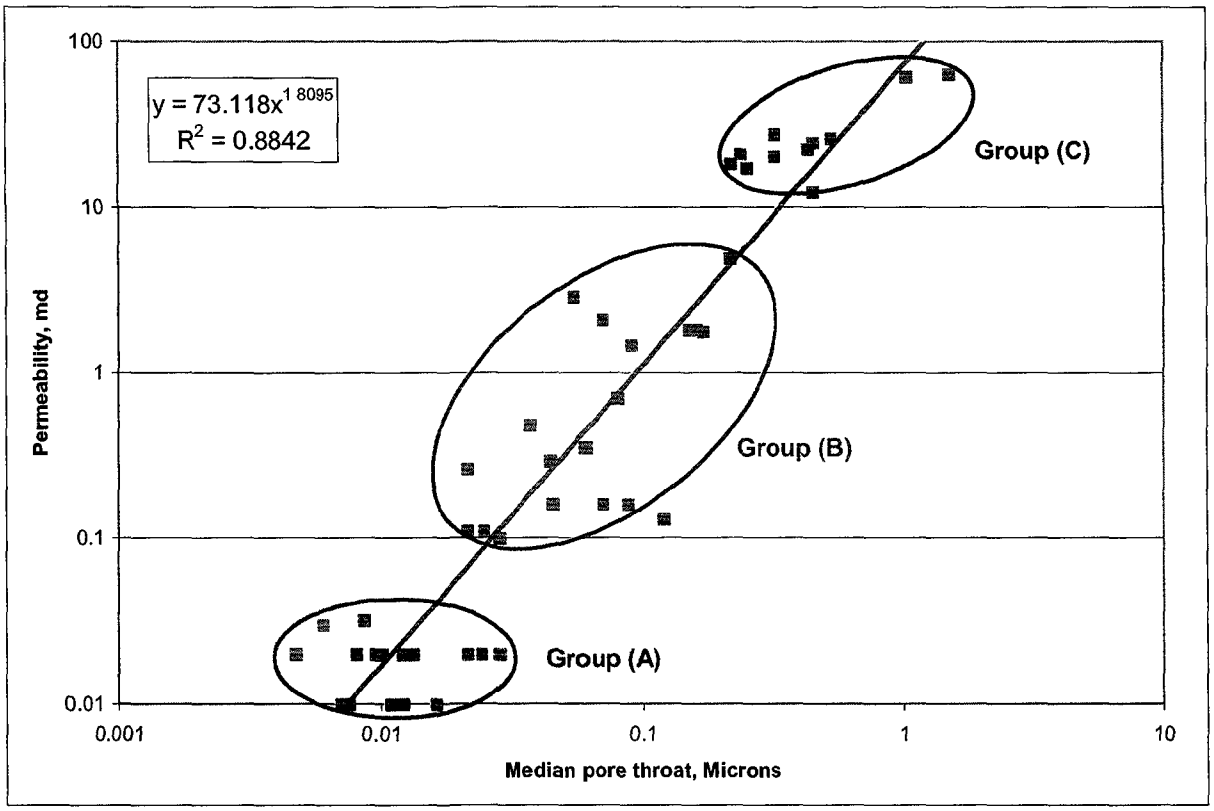

Fig. (5.40): Median pore throat vs. permeability of L. Bahariya, BED1-11 well.

The studied samples have an excellent relation which is expressed by the following equation:

$$K = 73.118\ md^{1.8095} \qquad (5.40)$$

$$R = 0.94$$

The previous equation is very reliable to predict the permeability with a high precision. Table (5.49) displays the characteristics of median for groups (A, B and C).

Figure (5.41) is a composite figure displays median pore throat-permeability relations for wells TSW-7, TSW-8 (Abu Roash 'F'), TSW-13, TSW-15 and TSW-21.

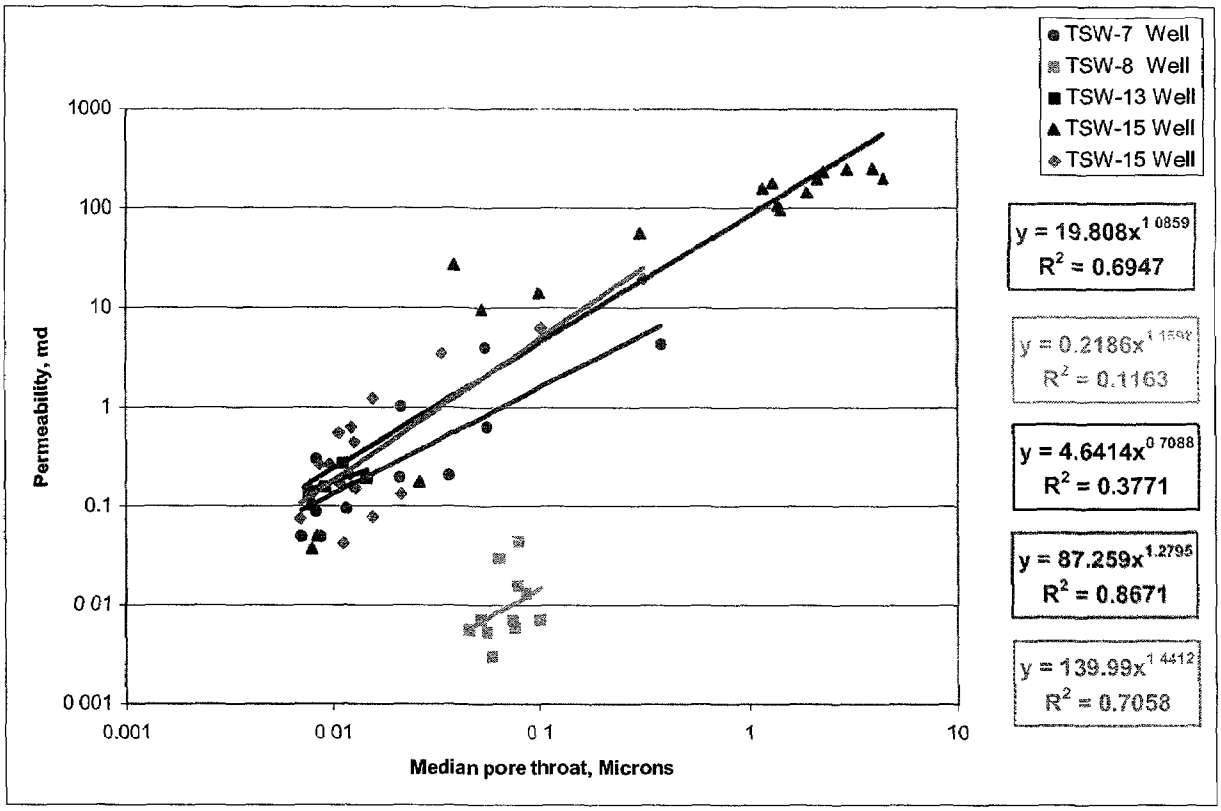

Fig. (5.41): Median pore throat vs. permeability of all TSW wells.

The studied samples of TSW-7 well have a relation which is expressed by the following equation:

$$K = 19.808\ md^{1.0859} \qquad (5.41)$$

$$R = 0.83$$

On the other hand in TSW-8 well (Abu Roash 'F'), the studied samples have no definite relation. The relation is expressed by the following equation:

$$K = 0.2186\ md^{1.1598} \qquad (5.42)$$

$$R = 0.34$$

The bad value of correlation coefficient may be due to the very close values of samples permeabilities so there are no clear differences in median values. Table (5.50) displays the characteristics of TSW-8 well samples.

Samples of TSW-13 well resemble to some extent well TSW-8 where the relation is weak and expressed by the following equation:

$$K = 4.6414\ md^{0.7088} \qquad (5.43)$$

$$R = 0.61$$

In contrast in TSW-15 well, the studied samples have an excellent relation which is expressed by the following equation:

$$K = 87.259\ md^{1.2795} \qquad (5.44)$$

$$R = 0.93$$

The studied samples of TSW-21 well have a relation which is expressed by the following equation:

$$K = 139.99\ md^{1.4412} \qquad (5.45)$$

$$R = 0.84$$

Figure (5.42) displays median pore throat-permeability relation of Abu Roash `G`, TSW-21 well.

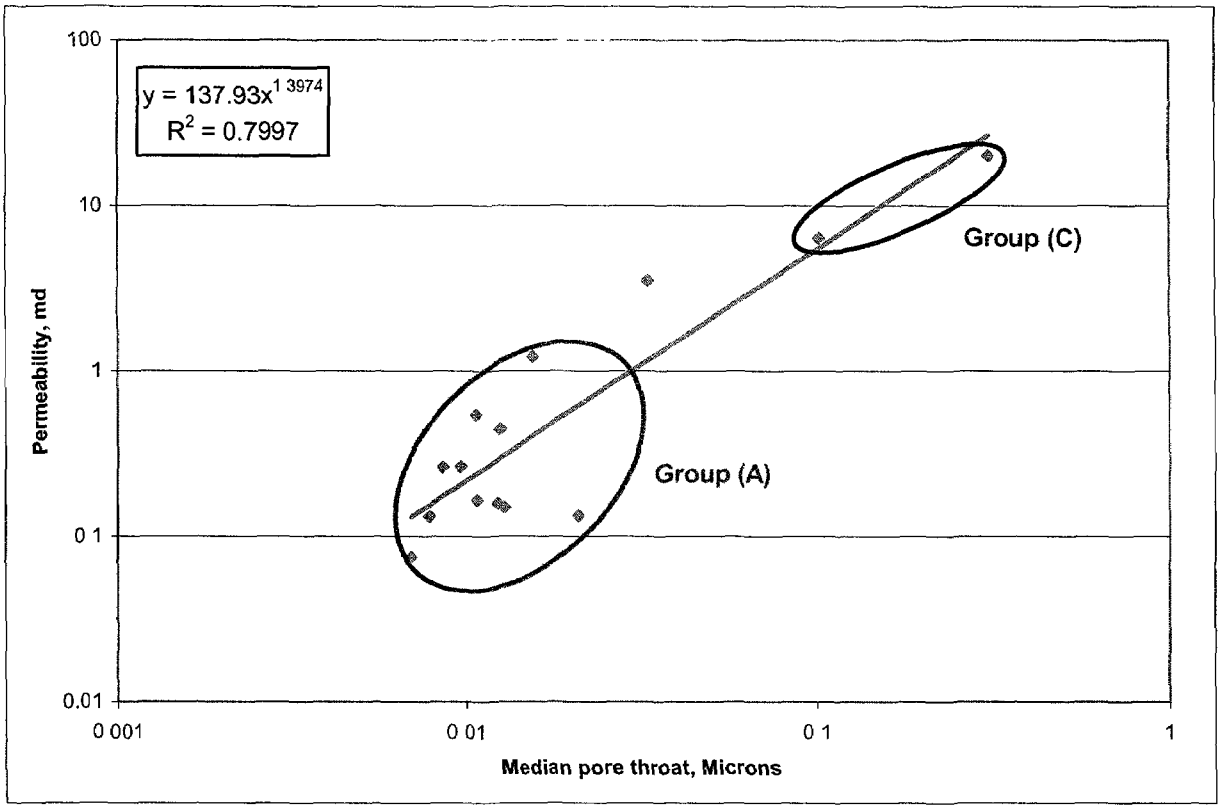

Fig. (5.42): Median pore throat vs. permeability of Abu Roash `G`, TSW-21 well.

The studied samples have a good relation which is expressed by the following equation:

$$K = 137.93\ md^{1.3974} \qquad (5.46)$$

$$R = 0.89$$

Table (5.51) displays the characteristics of median for groups (A and C).

Figure (5.43) displays median pore throat-permeability relationship for the upper part of the Bahariya Formation samples that collected from TSW-7, 13, 15 and 21 wells.

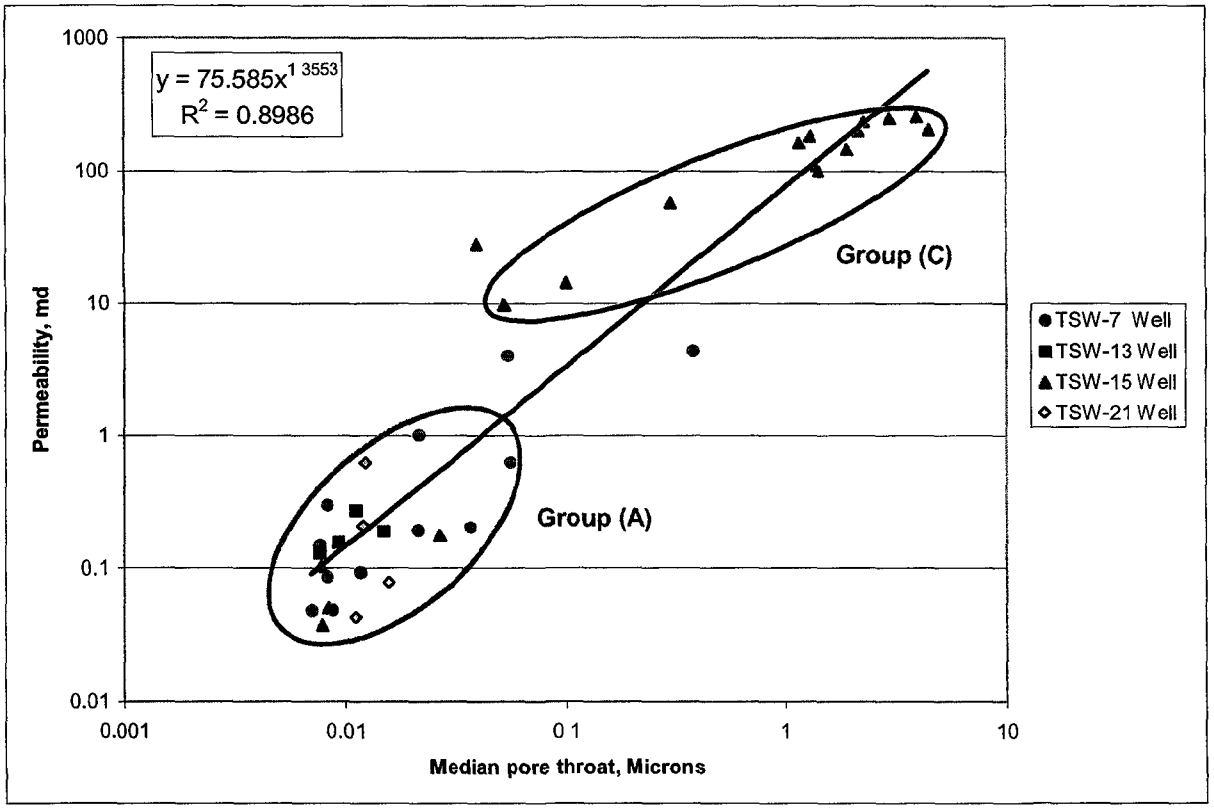

Fig. (5.43): Median pore throat vs. permeability of U. Bahariya, TSW-7, 13, 15 and 21 wells.

The studied samples have an excellent relation which is expressed by the following equation:

$$K = 75.585\ md^{1.3553} \qquad (5.47)$$

$$R = 0.95$$

The outstanding value of correlation coefficient has revealed the possibility of permeability prediction with a high precision. Table (5.52) displays the characteristics of median for groups (A and C).

5.8 R35

In the present study, the classification according to R35 values was used as a basis for reservoir rock zonation. This attempt was made to collect all the samples that having the same R35 irrespective to their lithology or their geologic age (stratigraphic unit) and use them to prove the validity of the reservoir rock zonation based on the R35. The reservoir rock zonation is defined in terms of petrophysical properties rather than sedimentological characteristics. In other words, the zonation concept is dealing directly with the rock pore network. Consequently, within a given lihtofacies unit, several zones can be defined with different pore network characteristics. Thus the defined reservoir rock zonation will ultimate reflect the similarity in the pore network rather than the similarity in sedimentological characteristics, e.g. grain size, texture, cementation and clay types. In other words, the reservoir rock zonation concept is dealing directly with the final product of geological and sedimentological effect on the reservoir rocks, i.e., different geological and sedimentological facies could produce the same reservoir rock zones and the same lithofacies could have different reservoir rock zones. The R35 of a given rock type both reflects its depositional and diagenetic fabric and influences fluid flow and reservoir performance (Hartmann and Coalson, 1990). Consequently, estimating R35 from core and logs, using the Winland's equation (Kolodzie, 1980), or directly from capillary pressure data (when available) provides the basis for a common zonation that can be used by both geologists and reservoir engineers. Flow units can be identified from the calculation of pore throat radii at the 35% pore volume (R35), using Winland's equation, so four petropysical flow units with different reservoir performances are distinguished by ranges of R35 (Martin et al. 1997).

(1) Megaport flow units: defined as having an R35 value above a threshold of 10 μm. Production of medium-gravity crudes can readily attain tens of

thousands of barrels per day from a megaport flow unit if zonal thickness and other factors are constant.

(2) Macroport flow units: defined as having an R35 ranging between 10 and 2 μm, with all other constraints held constant, are capable of production of thousands of barrels of oil per day.

(3) Mesoport flow units: defined as having an R35 ranging between 2 and 0.5 μm, this allows only hundreds of barrels of oil per day to our comparative completion, again with all other factors held constant.

(4) Microport flow units: defined as having an R35 of less than 0.5 μm. Although numerous tight gas reservoirs have these R35 properties, microport flow units are decidedly non-reservoir in this comparative completion of moderate thickness and medium gravity oil without mechanical constraints. Key wells with mostly microport flow units make at best few barrels of oil per day on pump.

5.8.1 R35 results

The measured (R35) was of different values for the studied units as follows:

Table (5.37) displays the results of R35 of the lower part of the Bahariya Formation in BED1-11 well, where it varies in a very wide range from a minimum value of 0.008 micron up to a maximum value of 4.26 microns with an average of 0.59 micron. In TSW-7 well (R35) varies in a high range from a minimum of 0.01 micron up to a maximum value of 1.27 microns with an average value 0.15 micron (Table 5.38). R35 in TSW-8 well (Abu Roash `F`) differs in a narrow range from 0.07 micron up to 0.13 micron with an average value 0.1 micron (Table 5.39), similarly in TSW-13 well where it varies from 0.012 micron up to 0.022 micron with an average value 0.017 micron (Table 5.40). R35 varies in a very high range from a minimum of 0.01 micron up to a maximum value of 6.4 microns with an average value 2.9 microns for TSW-15 well (Table 5.41). R35 varies from 0.01 micron up to

1.17 microns in TSW-21 well with an average value 0.1 micron (Table 5.42), the same behavior in Abu Roash 'G', TSW-21 well where R35 varies from 0.01 micron up to 1.17 microns with an average value 0.12 micron (Table 5.43). Also the studied samples of the upper part of the Bahariya Formation obtained from TSW-wells have the widest range of R35 where it differs from 0.01 micron to 6.4 microns with an average value 1.45 microns (Table 5.44).

5.8.2 R35 versus permeability relations

Figure (5.44) displays R35-permeability relation of the studied samples of the lower part of the Bahariya Formation in BED1-11 well.

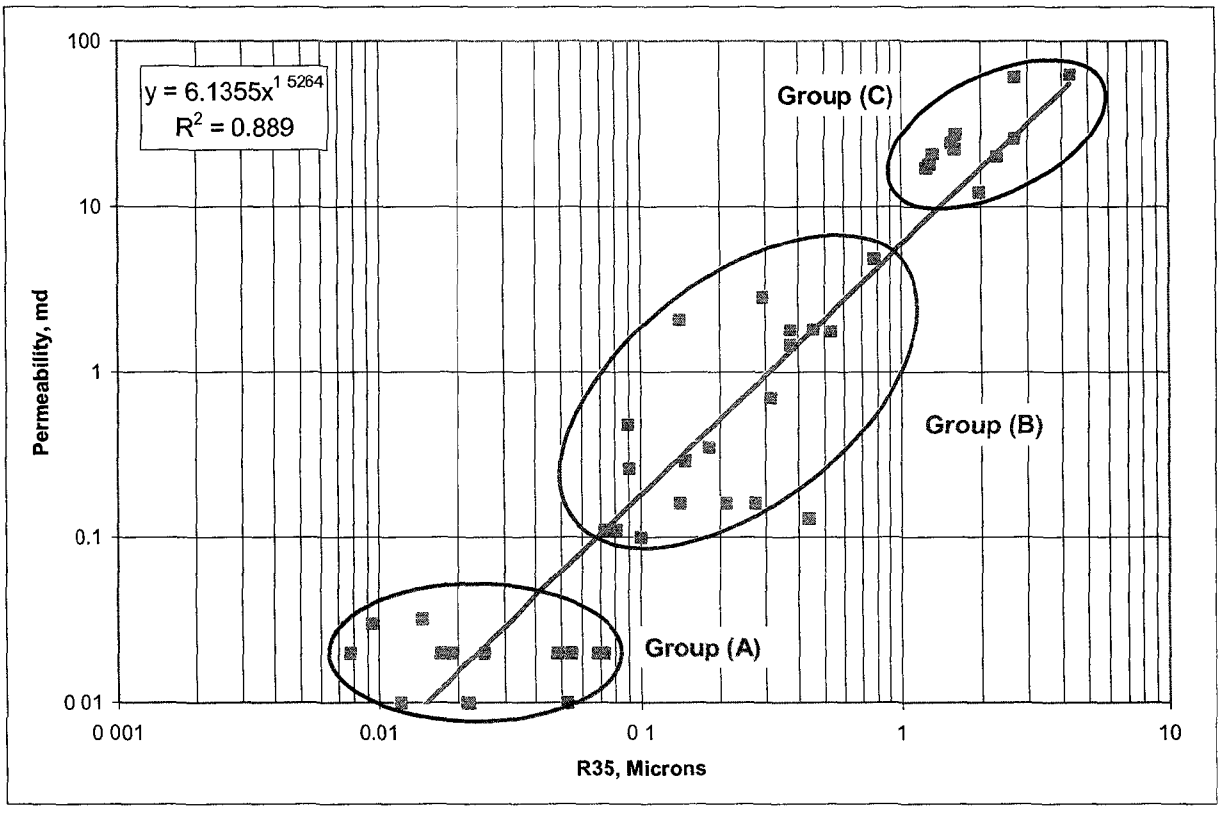

Fig. (5.44): R35 vs. permeability of L. Bahariya, BED1-11 well.

The studied samples have an excellent relation which is expressed by the following equation:

$$K = 6.1355(R35)^{1.5264} \qquad (5.48)$$

$$R = 0.94$$

According to the previous classification based on R35 values, three flow units could be identified as follows:

a-Microport flow units: having an R35 of less than 0.5 μm. the majority of samples related to this unit (groups A and B, 35 samples).

b-Mesoport flow units: having (0.5-2 μm) range of R35, (group C, 8 samples).

c-Macroport flow units: having (2-10 μm) range of R35 (group C, 4 samples).

Figure (5.45) is a composite figure displays R35-permeability relations for TSW-7, TSW-8 (Abu Roash 'F'), TSW-13, TSW-15 and TSW-21 wells.

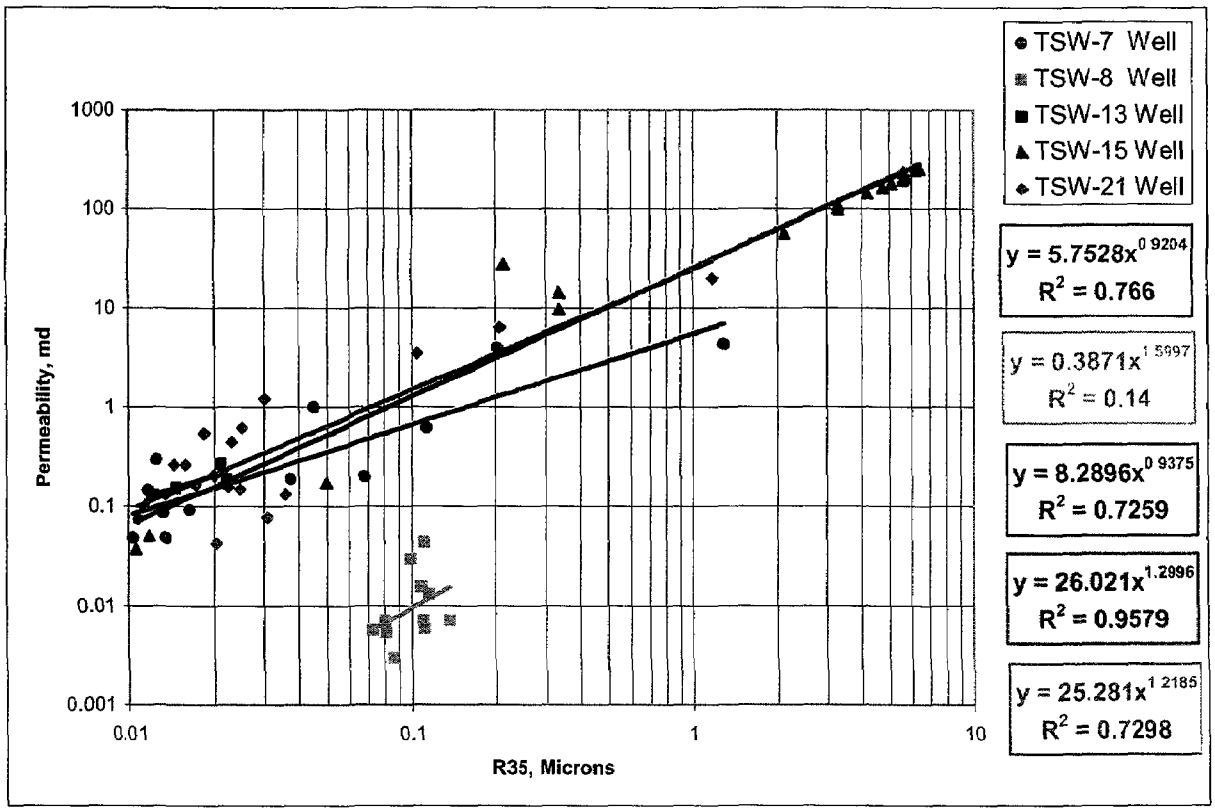

Fig. (5.45): R35 vs. permeability of all TSW wells.

The studied samples of TSW-7 well have a relation which is expressed by the following equation:

$$K = 5.7528(R35)^{0.9204} \qquad (5.49)$$

$$R = 0.88$$

On the other hand in TSW-8 well (Abu Roash `F`), the relation is bad and is expressed by the following equation:

$$K = 0.3871(R35)^{1.5997} \qquad (5.50)$$

$$R = 0.37$$

The bad value of correlation coefficient may be due to the very close values of samples' permeability so there are no clear differences between R35 values.

The same relation in TSW-13 well which is expressed by the following equation:

$$K = 8.2896(R35)^{0.9375} \qquad (5.51)$$

$$R = 0.85$$

Where the relation is very excellent in TSW-15 well which is expressed by the following equation:

$$K = 26.021(R35)^{1.2996} \qquad (5.52)$$

$$R = 0.98$$

The relation of the studied samples of TSW-21 well is expressed by the following equation:

$$K = 25.281(R35)^{1.2185} \qquad (5.53)$$

$$R = 0.85$$

Figure (5.46) displays R35-permeability relation for Abu Roash `G` samples in TSW-21 well.

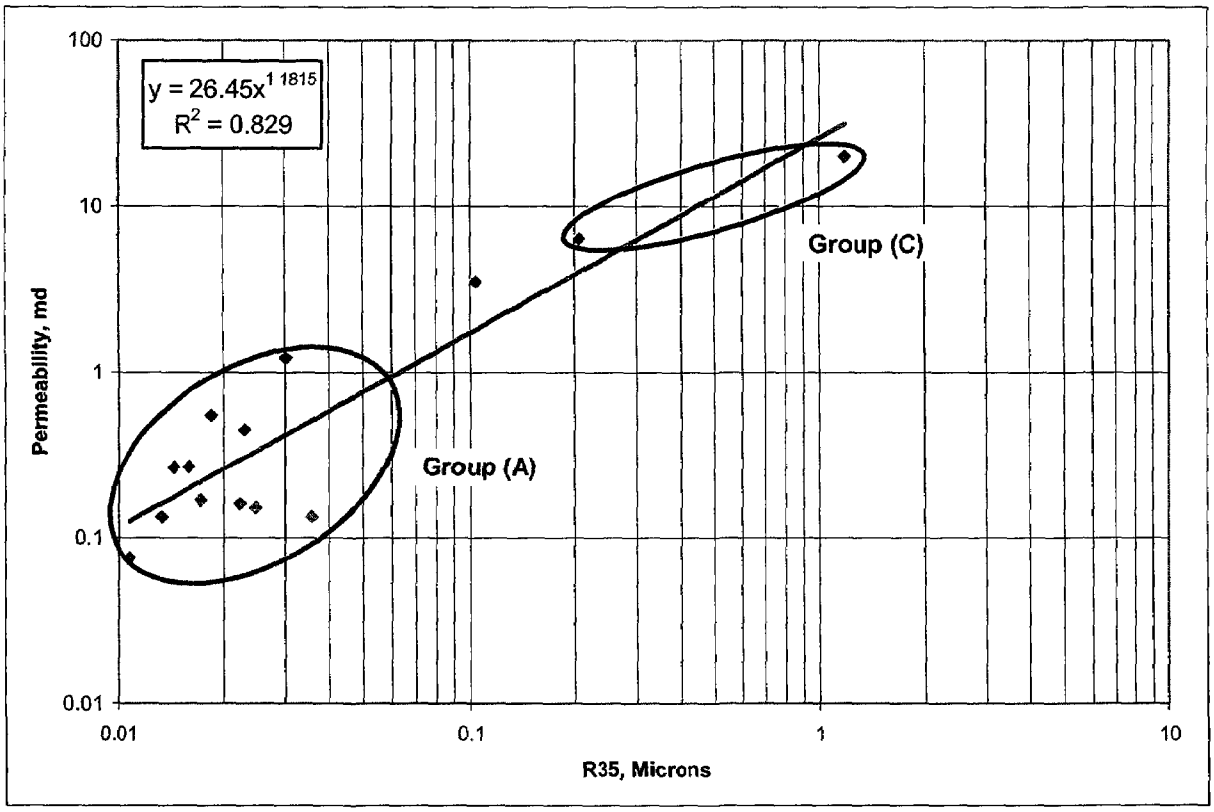

Fig. (5.46): R35 vs. permeability of Abu Roash `G`, TSW-21 well.

The studied samples have an excellent relation which is expressed by the following equation:

$$K = 26.45(R35)^{1.1815} \qquad (5.54)$$

$$R = 0.91$$

Samples of Abu Roash `G` in TSW-21 well related to microport flow units, where R35 values less than 0.5 μm, and it is equivalent to the groups (A) except sample (25H1) that has R35 equal 1.17 μm hence related to mesoport flow units (group C).

Figure (5.47) displays R35-permeability relation of the studied samples of the upper part of the Bahariya Formation obtained from TSW-wells.

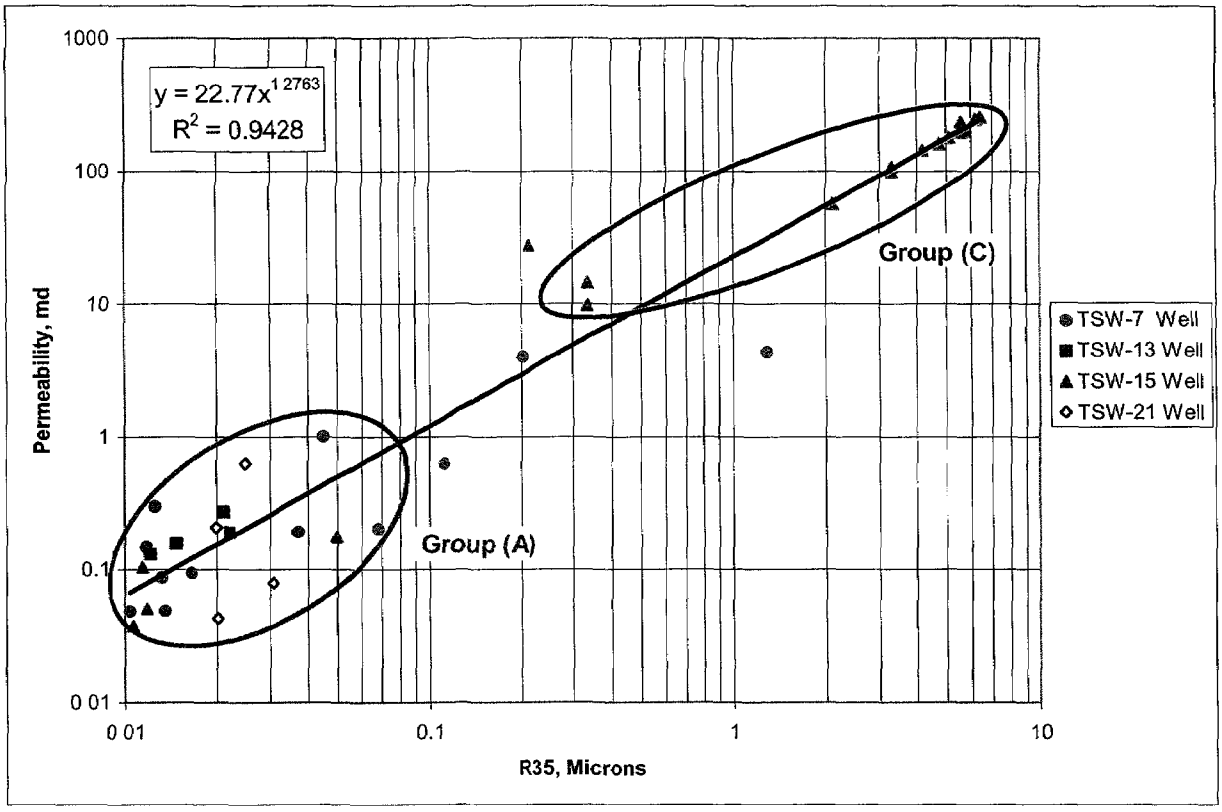

Fig. (5.47): R35 vs. permeability of U. Bahariya, TSW-7, 13, 15 and 21 wells.

The studied samples have a relation which is expressed by the following equation:

$$K = 22.77(R35)^{1.2763} \qquad (5.55)$$

$$R = 0.97$$

The outstanding value of correlation coefficient shows that the permeability could be predicted with a very high precision. According to the previous classification based on R35 values, the Upper part of the Bahariya Formation has two types of flow units as follows:

1-Microport flow units: where R35 values less than 0.5 μm (group A).

2-Macroport flow units: where R35 values ranging between 2 and 10 μm (group C, except 3 samples).

5.9 PVC's versus R35 relations

Figure (5.48) exhibits PVC2-R35 relation of the studied samples of the lower part of the Bahariya Formation obtained from BED1-11 well.

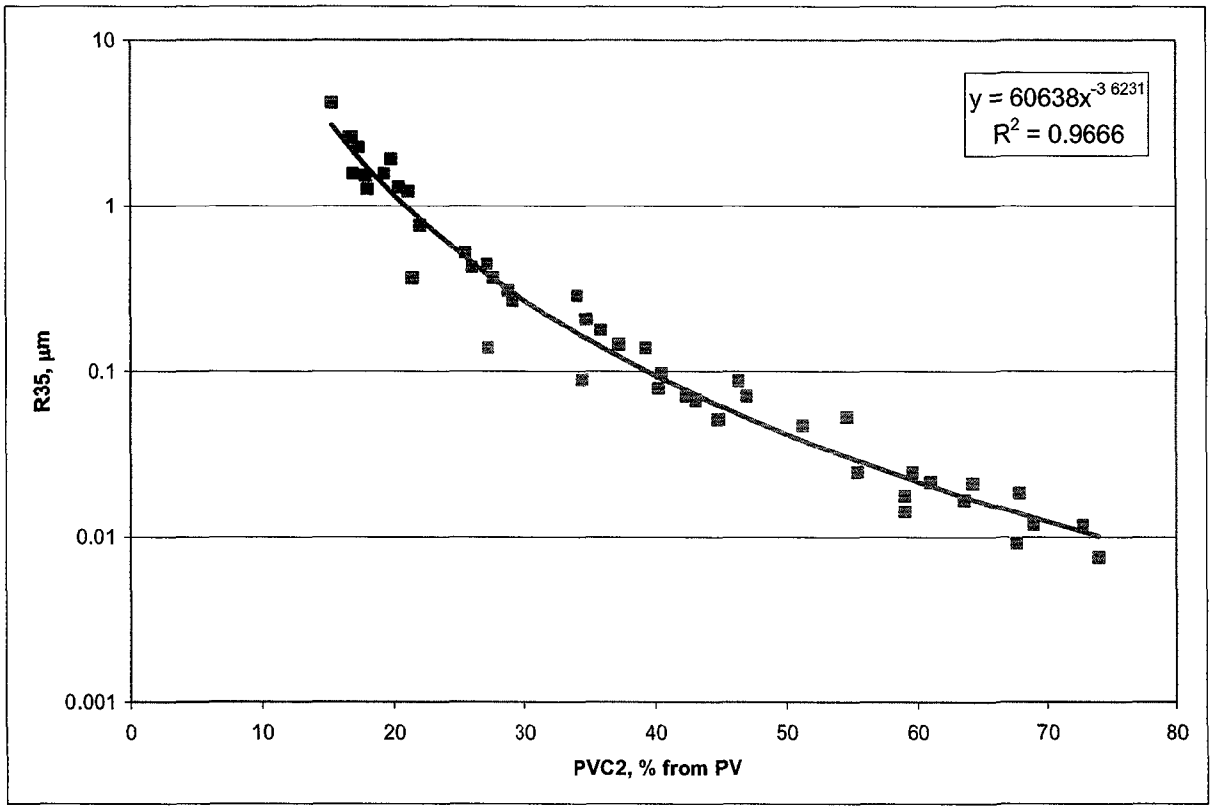

Fig. (5.48): PVC2 vs. R35 of L. Bahariya, BED1-11 well.

The studied samples have a very excellent relation which is expressed by the following equation:

$$R35 = 60638(PVC2)^{-3.6231} \qquad (5.56)$$

$$R = 0.98$$

Figure (5.49) displays PVC1-R35 relations of the studied samples from wells TSW-8 (Abu Roash `F`) and TSW-13.

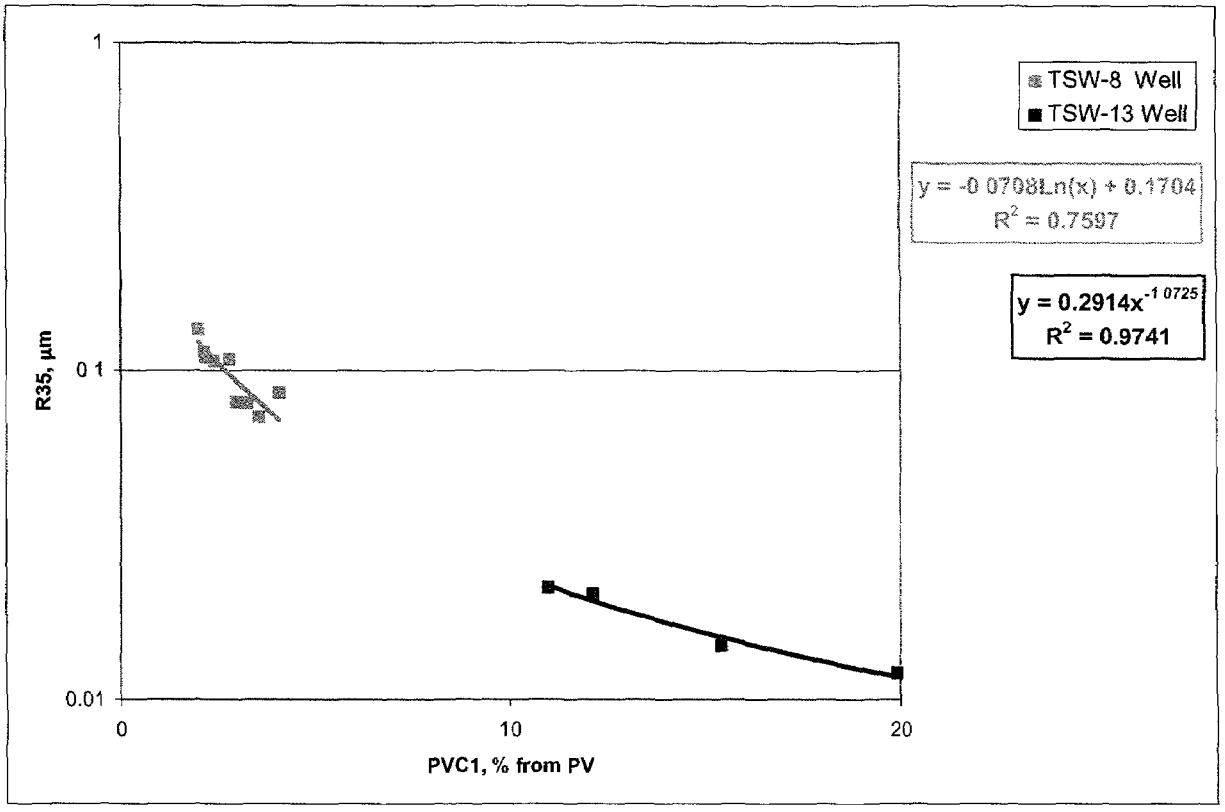

Fig. (5.49): PVC1 vs. R35 of wells TSW-8 and TSW-13.

In TSW-8 well, the studied samples have a weak relation which is expressed by the equation:

$$R35 = -0.0708\ Ln(PVC1)+0.1704 \qquad (5.57)$$

$$R = 0.87$$

But in TSW-13 well, the relation become more excellent and is expressed by the equation:

$$R35 = 0.2914(PVC1)^{-1.0725} \qquad (5.58)$$

$$R = 0.99$$

Figure (5.50) is a composite figure displays PVC2-R35 relations for wells TSW-7, TSW-13, TSW-15 and TSW-21.

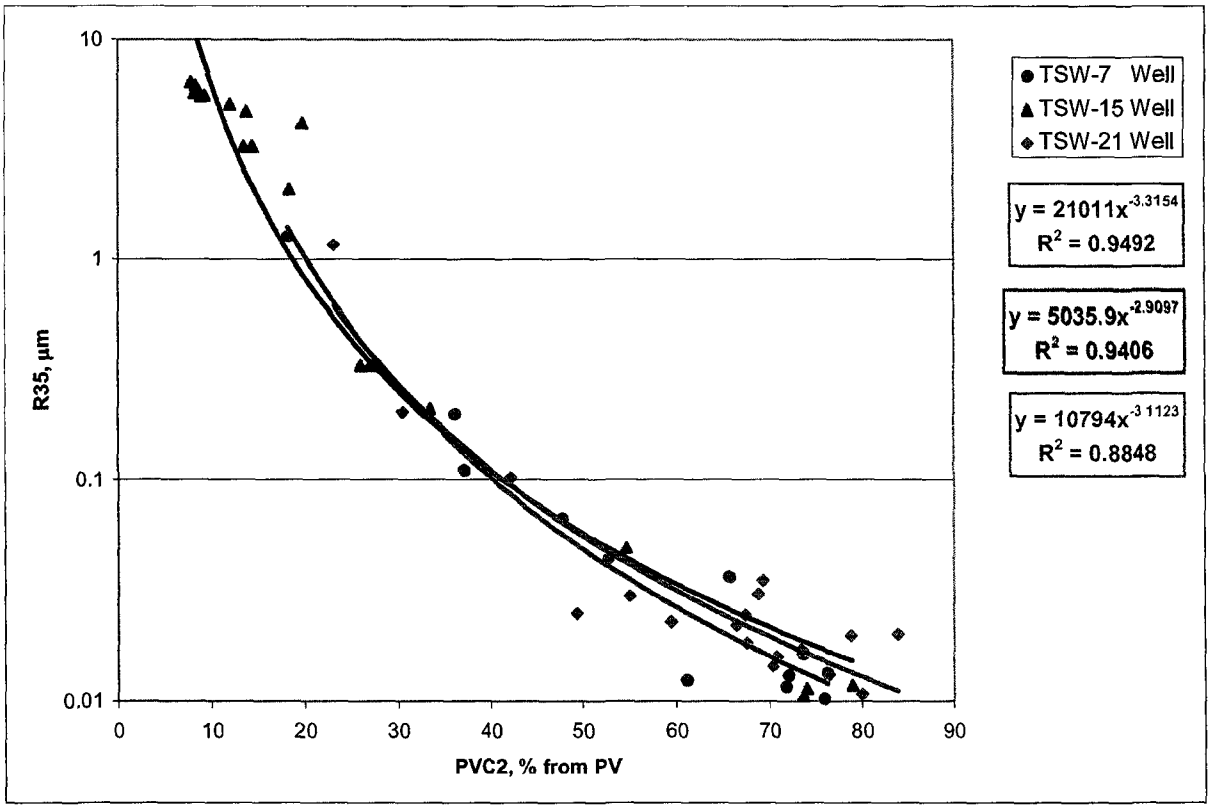

Fig. (5.50): PVC2 vs. R35 of TSW-7, 15 and 21 wells.

The studied samples in TSW-7 well have a very excellent relation which is expressed by the equation:

$$R35 = 21011(PVC2)^{-3.3154} \qquad (5.59)$$

$$R = 0.97$$

The same excellent relation was found in TSW-15 well, where the relation is expressed by the equation:

$$R35 = 5035.9(PVC2)^{-2.9097} \qquad (5.60)$$

$$R = 0.97$$

Also in TSW-21 well, where the relation is expressed by the equation:

$$R35 = 10794(PVC2)^{-3.1123} \qquad (5.61)$$

$$R = 0.94$$

Figure (5.51) displays PVC2-R35 relation for Abu Roash `G` samples in TSW-21 well.

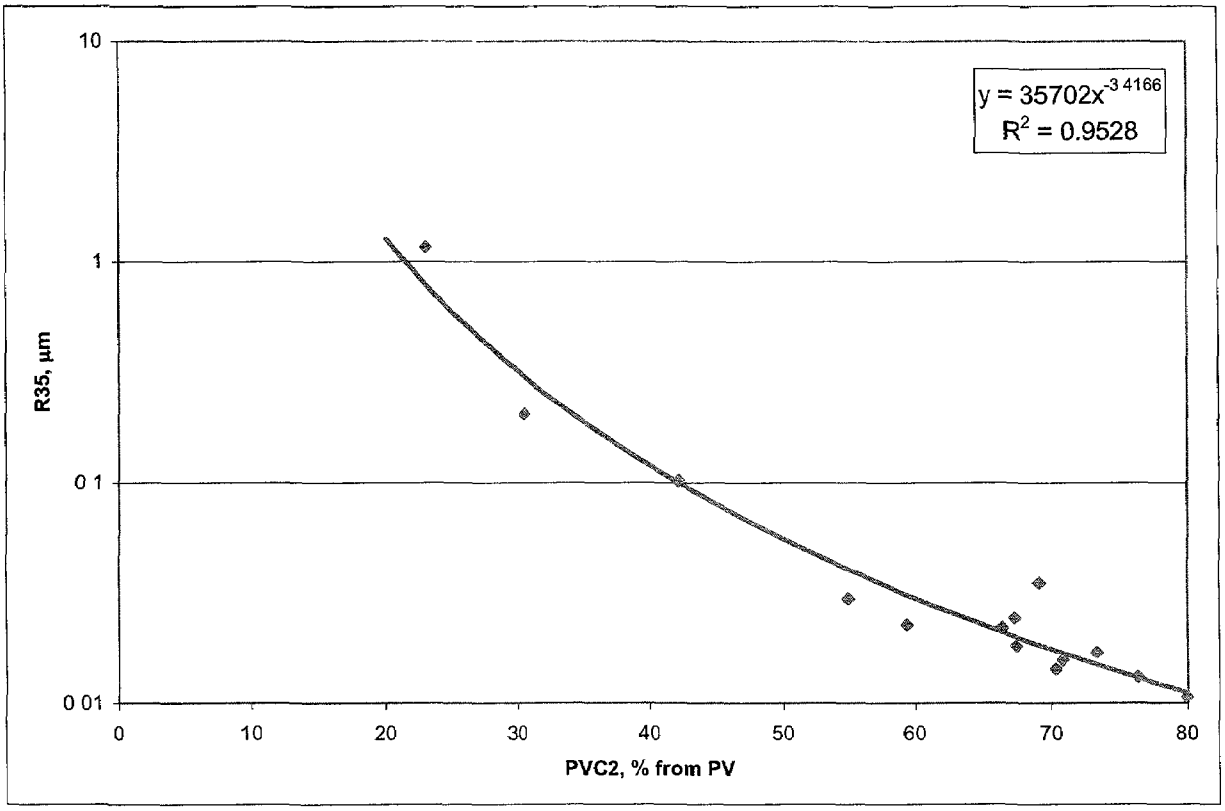

Fig. (5.51): PVC2 vs. R35 of Abu Roash `G`, TSW-21 well.

The studied samples have an excellent relation which is expressed by the equation:

$$R35 = 35702(PVC2)^{-3.4166} \qquad (5.62)$$

$$R = 0.98$$

The outstanding value of correlation coefficient revealed the very high possibility to predict R35 from PVC2 with a very high precision.

The same excellent relation was found in the studied samples of the upper part of the Bahariya Formation obtained from TSW-wells (Fig. 5.52).

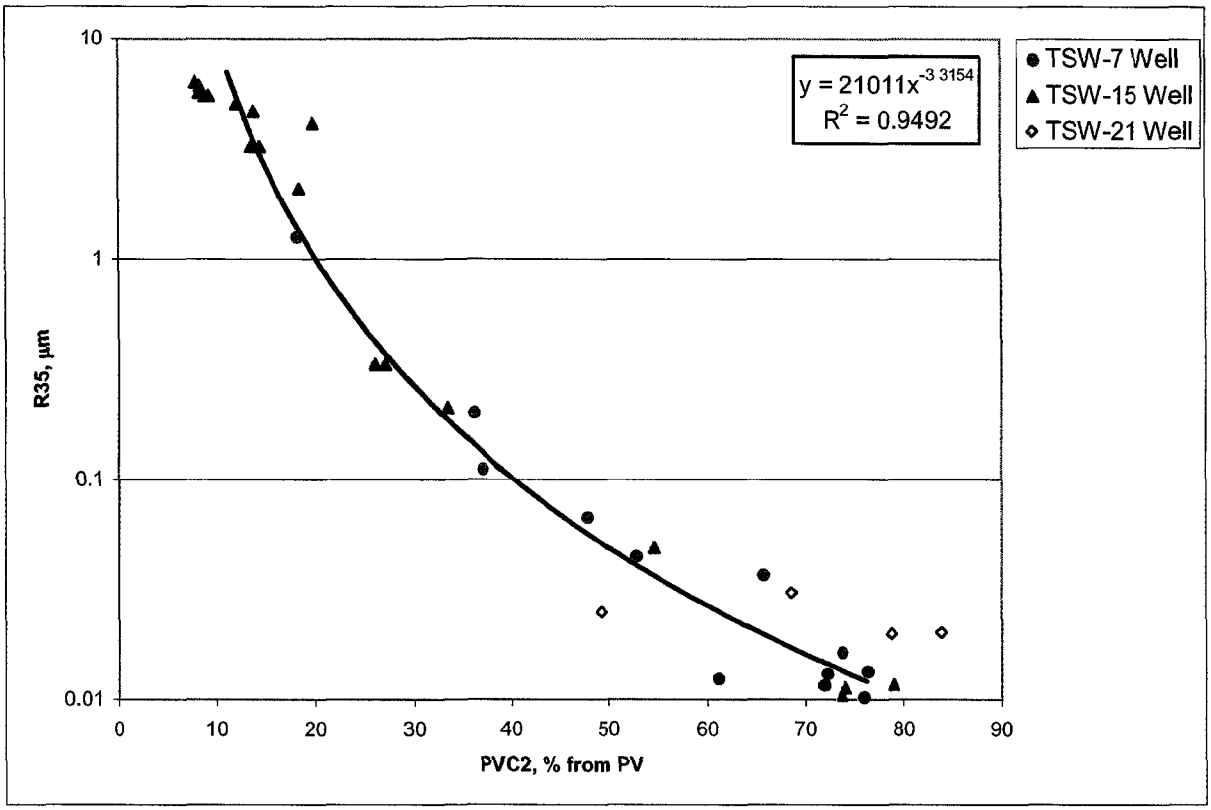

Fig. (5.52): PVC2 vs. R35 of U. Bahariya in all TSW wells.

The relation is expressed by the following equation:

$$K = 21011(PVC2)^{-3.3154} \qquad (5.63)$$

$$R = 0.97$$

5.10 Refined porosity concept

Concerning the reservoir pore spaces, all the pores are not contributing to the fluid flow and hence they act to disturb the relationship of porosity and permeability. So, in order to enhance the relationship, the pore throat size distribution was used to delineate that pore which doesn't contribute to the fluid or gas flow through the rock. According to El Sayed (1995):

$$\phi_{eff} = \phi_t (1-Sw_{irr}) \qquad (5.64)$$

Where:

ϕ_{eff} = effective porosity, %.

ϕ_t = total porosity, %.

Sw_{irr} = irreducible water saturation, %.

In the present study, effective porosity or (refined porosity) is defined as that part of rock pore spaces above certain pore throat cutoff. In order to high more light on the refined porosity concept, the petrophysical model introduced by El Sayed and Kiss (1997) was borrowed to explain the portion of the microporosity and then the refined one as shown in figure (5.53).

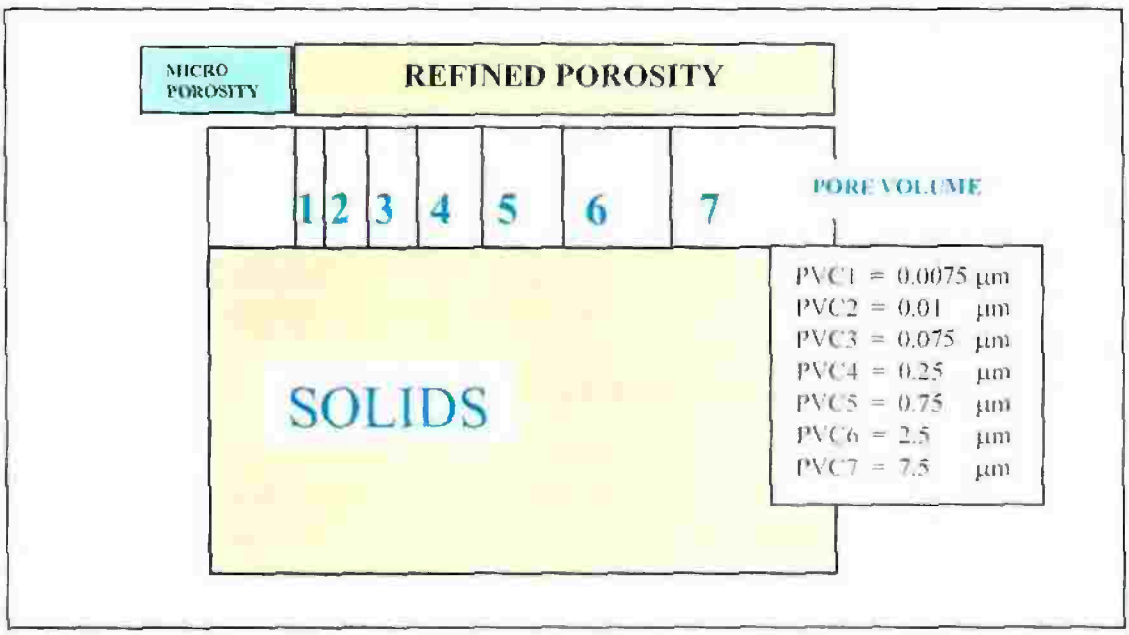

Fig. (5.53): Reservoir model (after El Sayed and Kiss, 1997)

The improving of porosity and permeability relationship is adding value to the refined porosity concept which could be used to enhance that relationship for any group of samples and to be used in reservoir production calculations and oil reserve estimation.

5.10.1 Calculation of refined porosity

The refined porosity is calculated as the following:

1-Select the pore-throat cutoff value. In the present study `0.0035` micron was selected as the pore-throat cutoff that equivalent to that portion of pore volume (Sw_{irr}) that uninvaded with mercury at 30,000 psi.

2-From the pore throat size distribution, determine the percentage of pore spaces that are controlled by the specific pore-throat.

3-Deduct that percentage from the measured pore volume and calculate the refined pore volume.

4-Calculate the refined porosity using the refined pore volume.

5.10.2 Refined and mercury porosity results

The calculated refined and mercury porosity for the lower part of the Bahariya Formation in BED1-11 well are listed in table (5.53), where the results of TSW-7, 8, 13, 15 and 21 wells are listed in table (5.54) through (5.58) respectively, on the other hand the results of Abu Roash `G` in TSW-21 well samples are listed in table (5.59). Also the results of the studied samples of the upper part of the Bahariya Formation obtained from wells TSW-7, 13, 15 and 21 are listed in table (5.60).

5.10.3 Refined versus mercury porosity relations

Figure (5.54) displays porosity-permeability relation of the studied samples of the lower part of the Bahariya Formation in BED1-11 well with a correlation coefficient (R=0.90) and the same relation after applying the refined porosity concept (Fig. 5.55), where the correlation coefficient was slightly improved to be (R=0.92). Also, figure (5.56) is a composite figure displays porosity-permeability relations of all TSW-wells with a certain correlation coefficient. Figure (5.57) exhibits the same relations after applying the refined porosity concept, the improvement in the relations in TSW-7 and TSW-21 wells is higher than that of TSW-8, 13 and 15 wells. Table (5.61) displays the correlation coefficients values before and after applying the refined porosity concept in TSW-7, 8, 13, 15 and 21 wells.

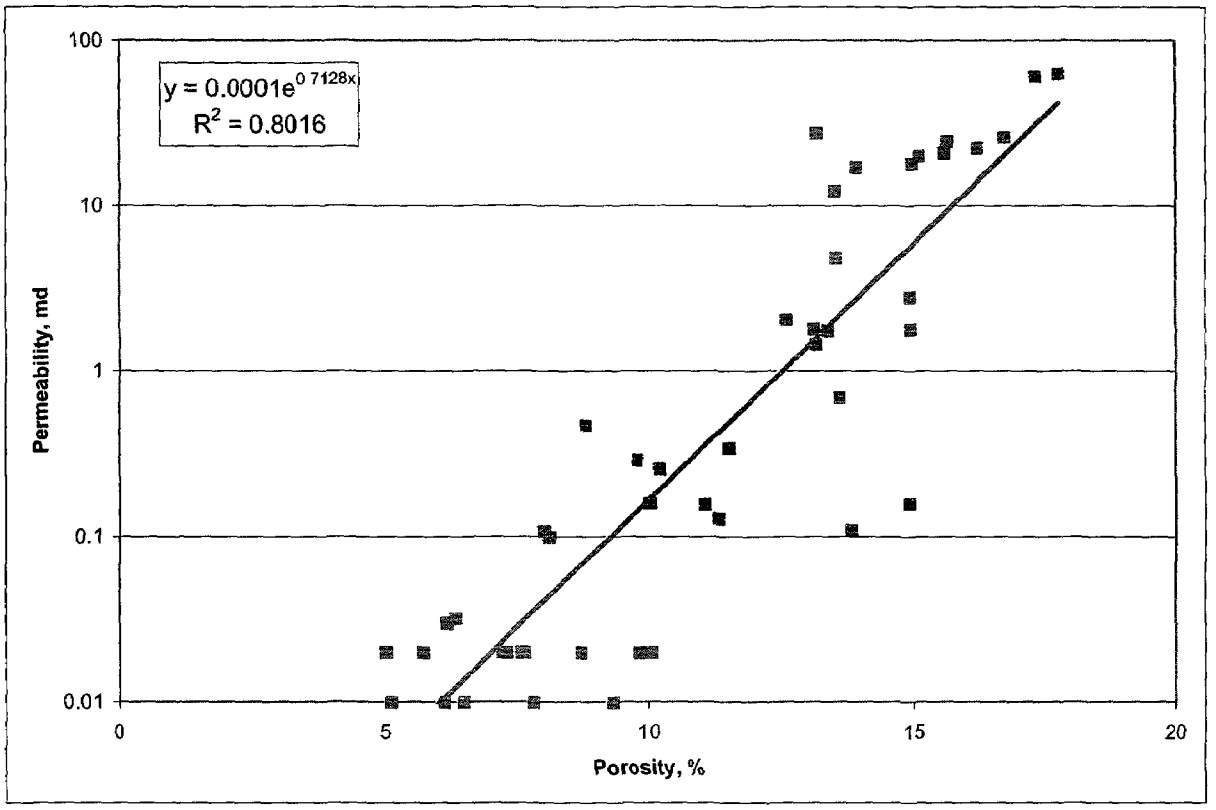

Fig. (5.54): Porosity vs. permeability of L. Bahariya, BED1-11 well.

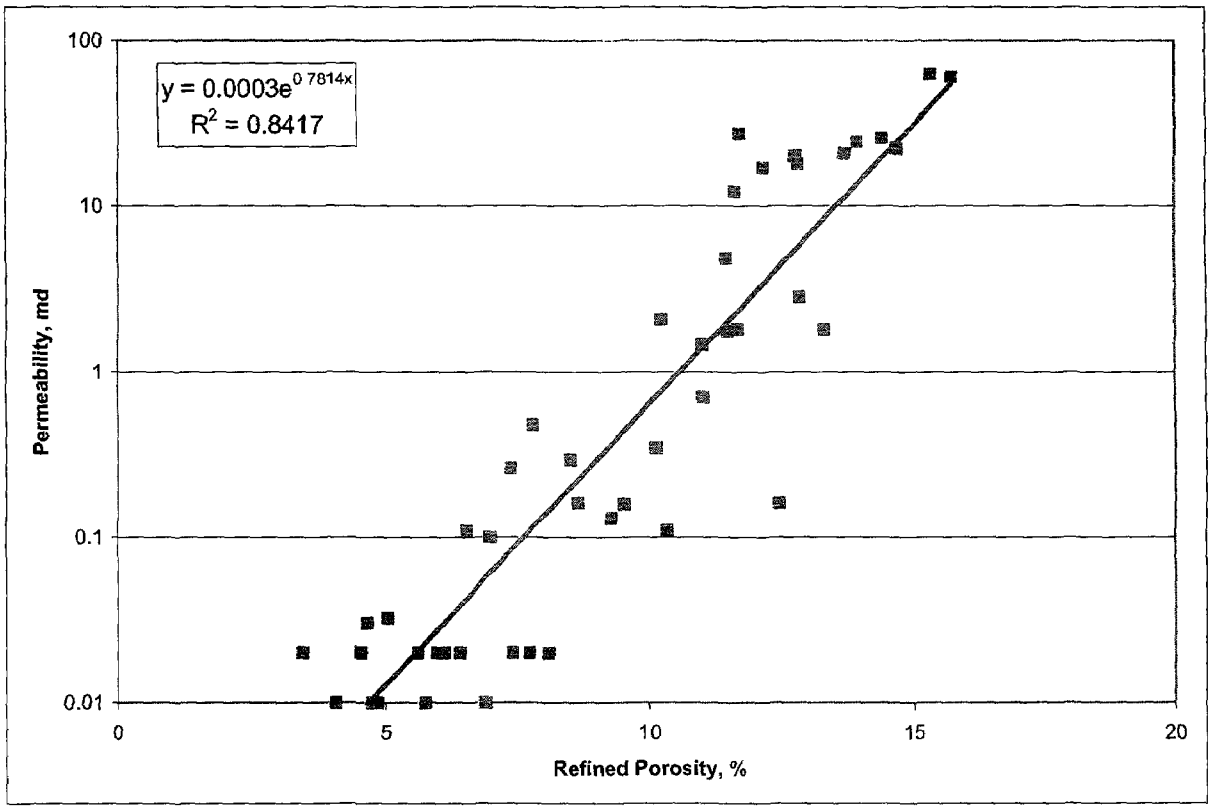

Fig. (5.55): Refined porosity vs. permeability of L. Bahariya, BED1-11 well.

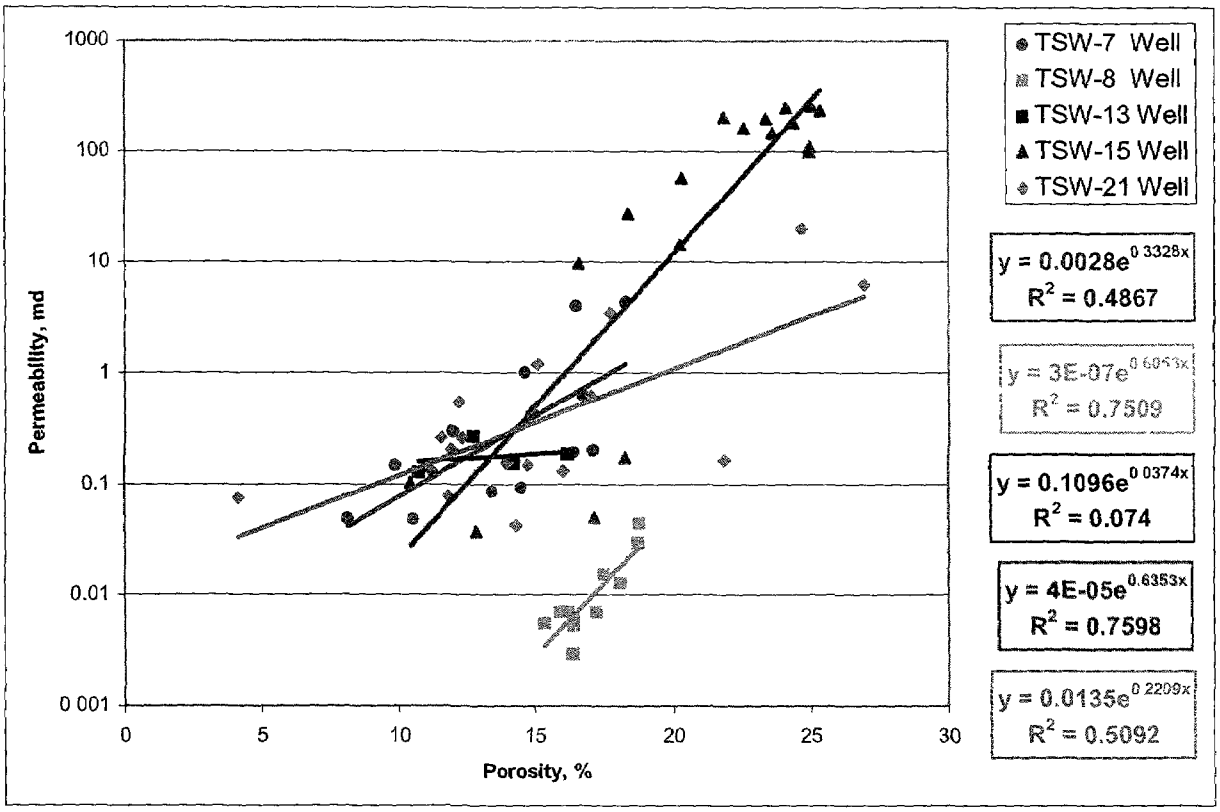

Fig. (5.56): Porosity vs. permeability of all TSW wells.

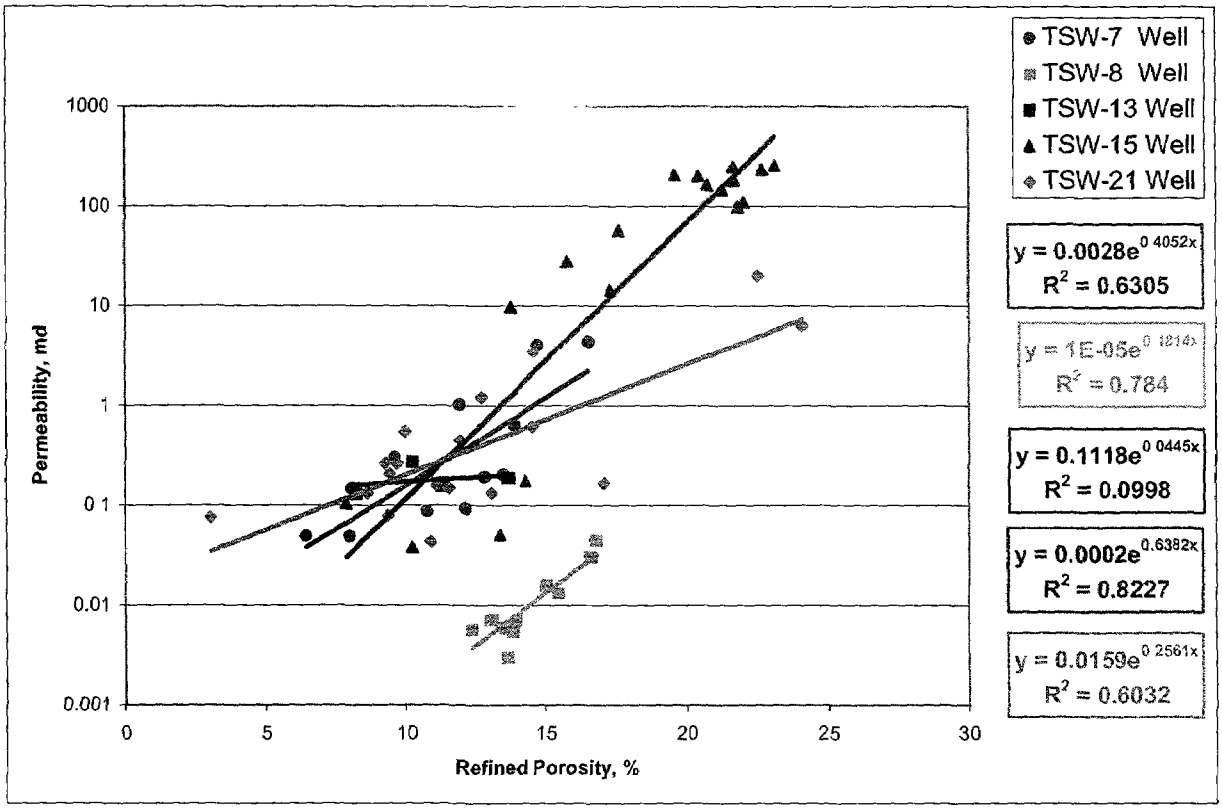

Fig. (5.57): Refined porosity vs. permeability of all TSW wells.

To check the validity of refined porosity values in the lower part of the Bahariya Formation in BED1-11 well, a relation was constructed between refined porosity and mercury porosity that was resulted from capillary pressure test (Fig. 5.58).

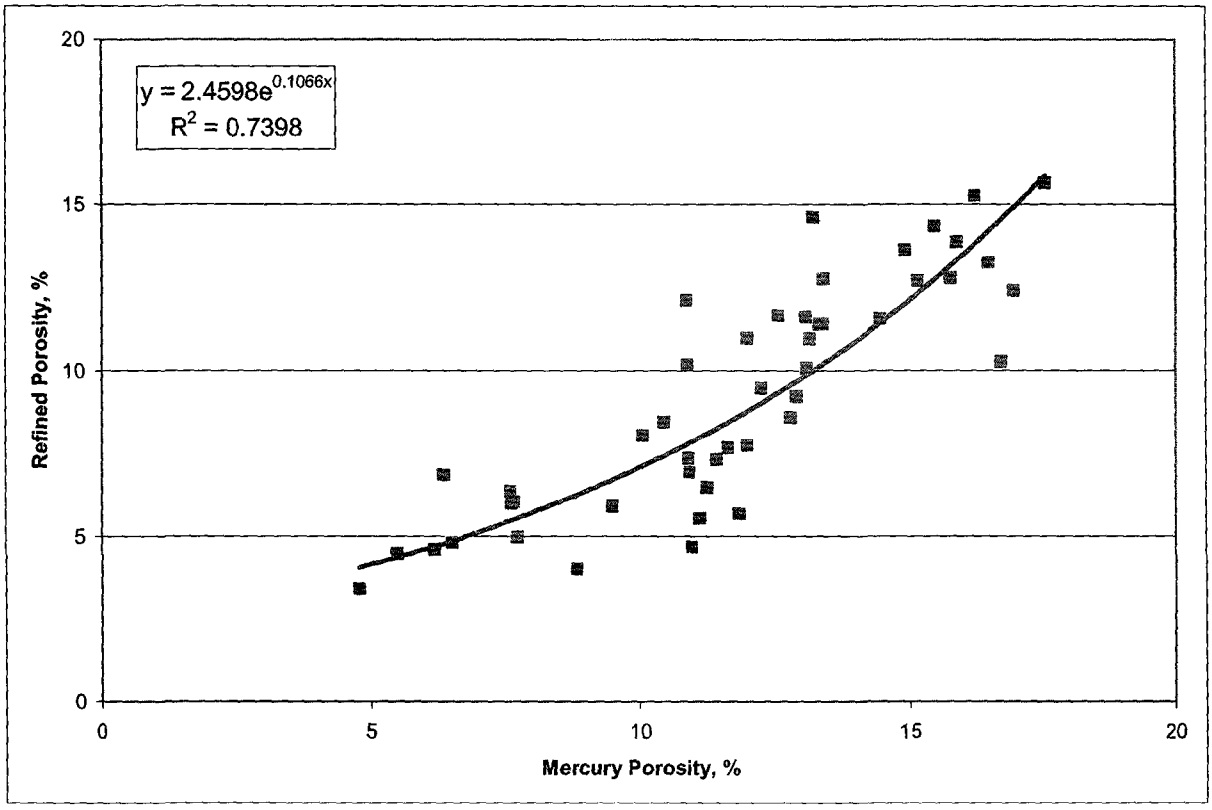

Fig. (5.58): Mercury porosity vs. refined porosity of L. Bahariya , BED1-11 well.

The studied samples have a good relation which is expressed by the following equation:

$$\Phi_R = 2.4598e^{0.1066\Phi hg} \qquad (5.65)$$

$$R = 0.86$$

To check the validity of refined porosity values in all TSW wells, a relation in each well was constructed between refined porosity and mercury porosity that resulted from capillary pressure test (Fig. 5.59).

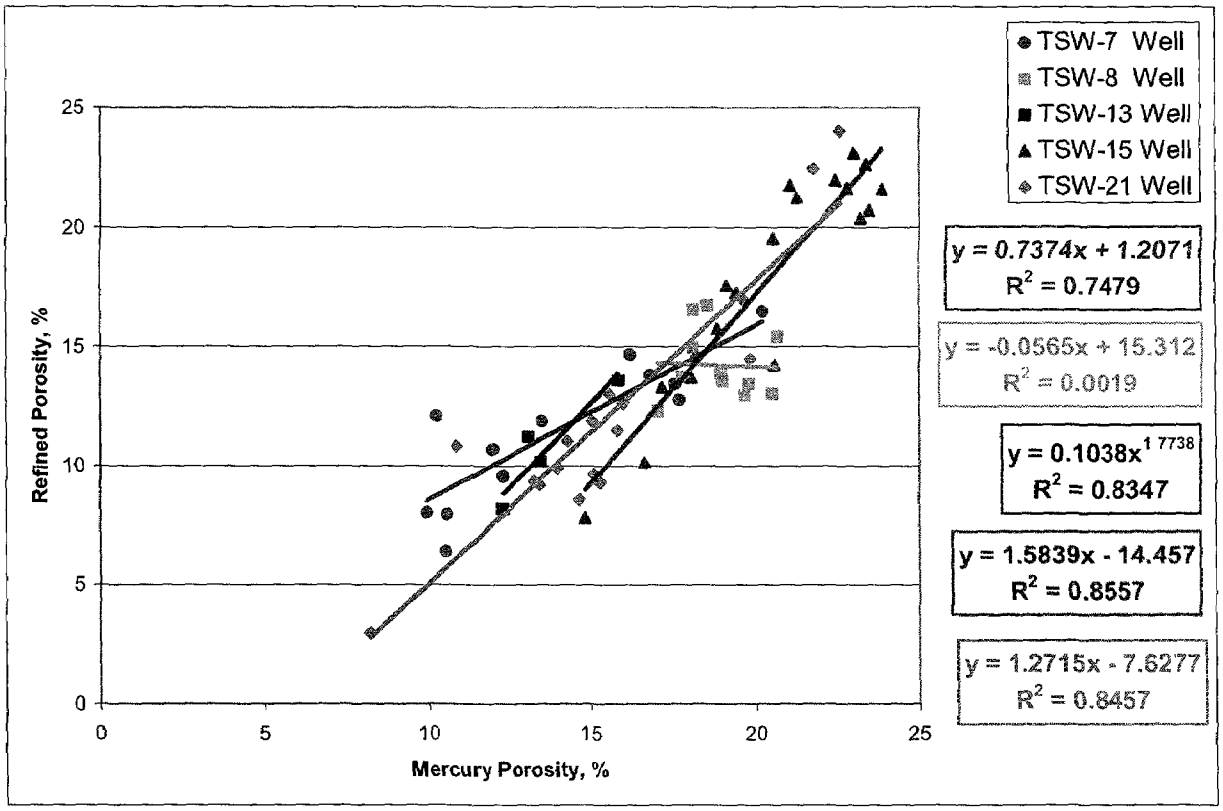

Fig. (5.59): Mercury porosity vs. refined porosity of TSW-7, 8, 13, 15 and 21 wells.

In TSW-7 well the relation is expressed by the following equation:

$$\Phi_R = 0.7374\ \Phi hg + 1.2071 \qquad (5.66)$$

$$R = 0.86$$

Where in TSW-8 well (Abu Roash `F`), nearly there is no relation.

$$\Phi_R = -0.0565\ \Phi hg + 15.312 \qquad (5.67)$$

$$R = 0.04$$

The excellent relations were found in TSW-13 well where:

$$\Phi_R = 0.1038\ \Phi hg^{1.7738} \qquad (5.68)$$

$$R = 0.91$$

In TSW-15 well the relation is expressed by the following equation:

$$\Phi_R = 1.5839\ \Phi hg - 14.457 \quad (5.69)$$

$$R = 0.93$$

Finally in TSW-21 well, where:

$$\Phi_R = 1.2715\ \Phi hg - 7.6277 \quad (5.70)$$

$$R = 0.92$$

Figure (5.60) displays the same relation of Abu Roash `G` Member in TSW-21 well before applying refined porosity with a correlation coefficient (R=0.73), after applying refined porosity concept (Fig. 5.61), the correlation coefficient was improved to be (R=0.79).

Figure (5.62) displays porosity-permeability relation of the upper part of the Bahariya Formation obtained from TSW-wells with a correlation coefficient (R=0.90), after applying refined porosity concept (Fig. 5.63), the correlation coefficient was slightly improved to be (R=0.93). For all the studied samples (except TSW-8 well), it can be concluded that porosity-permeability relation has been improved upon applying refined porosity concept.

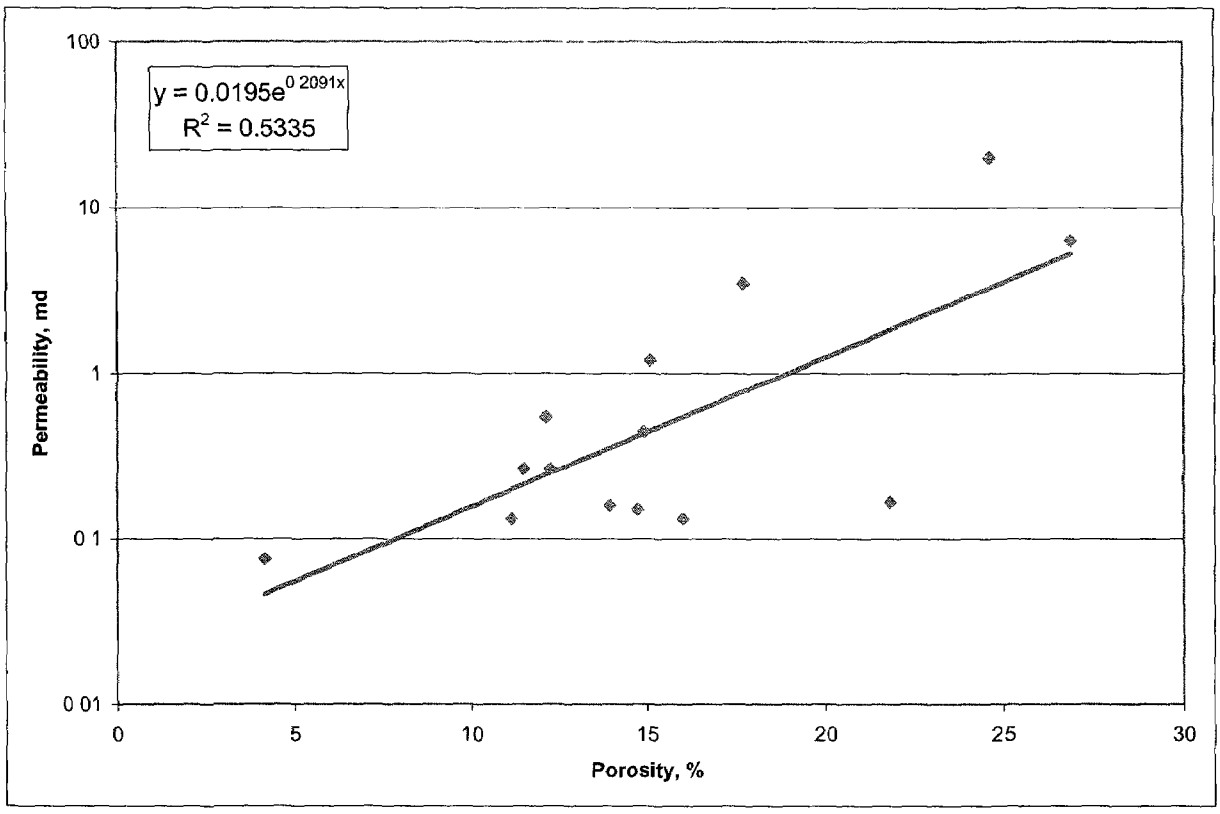

Fig. (5.60): Porosity vs. permeability of Abu Roash `G`, TSW-21 well

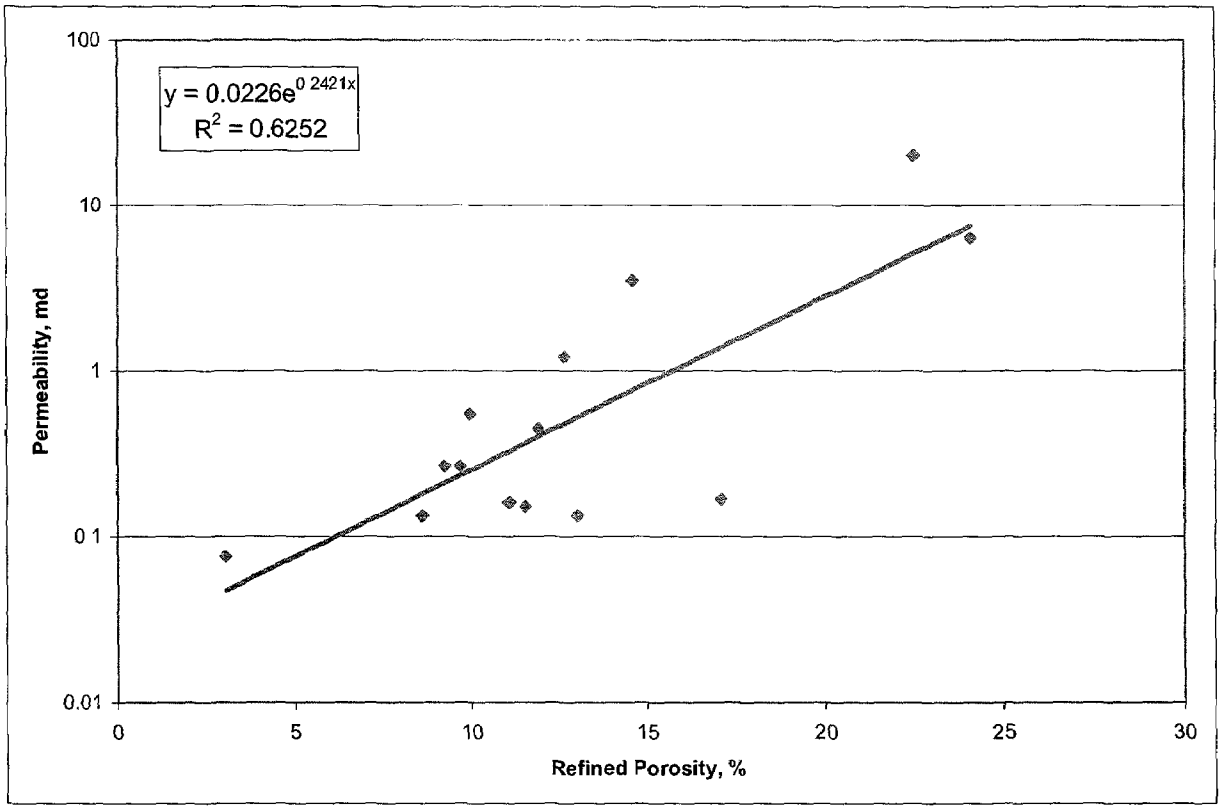

Fig. (5.61): Refined porosity vs. permeability of Abu Roash `G`, TSW-21 well

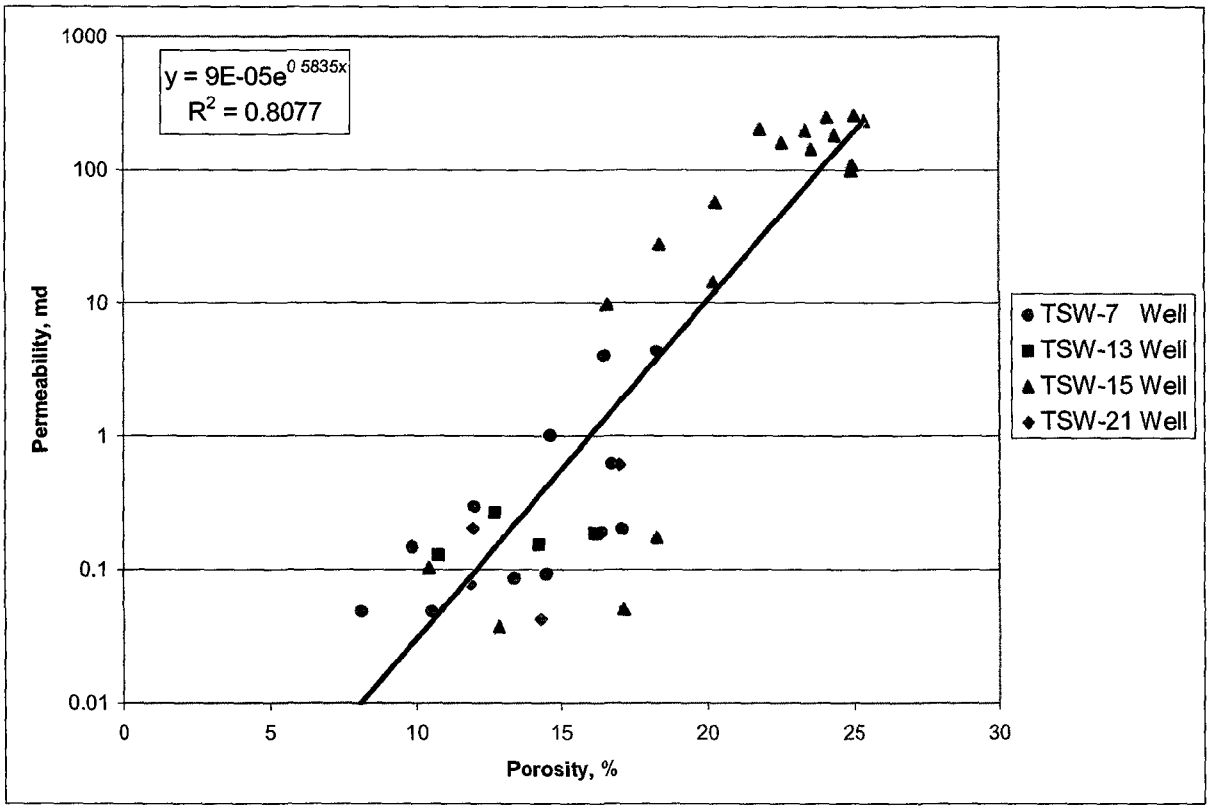

Fig. (5.62): Porosity vs. permeability of U. Bahariya, TSW-7, 13, 15 and 21 wells.

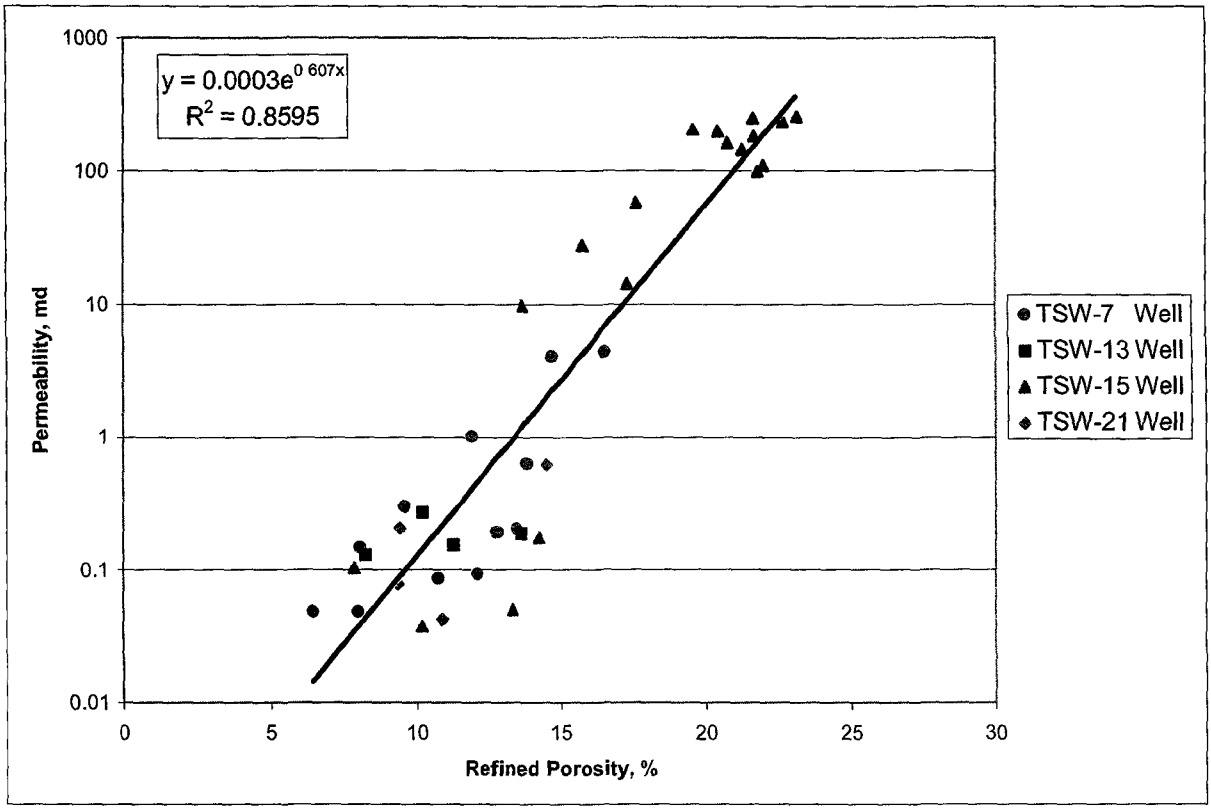

Fig. (5.63): Refined porosity vs. permeability of U. Bahariya, TSW-7, 13, 15 and 21 wells.

To check the validity of refined porosity values in Abu Roash `G` in TSW-21 well, a relation was constructed between refined porosity and mercury porosity that resulted from capillary pressure test (Fig. 5.64).

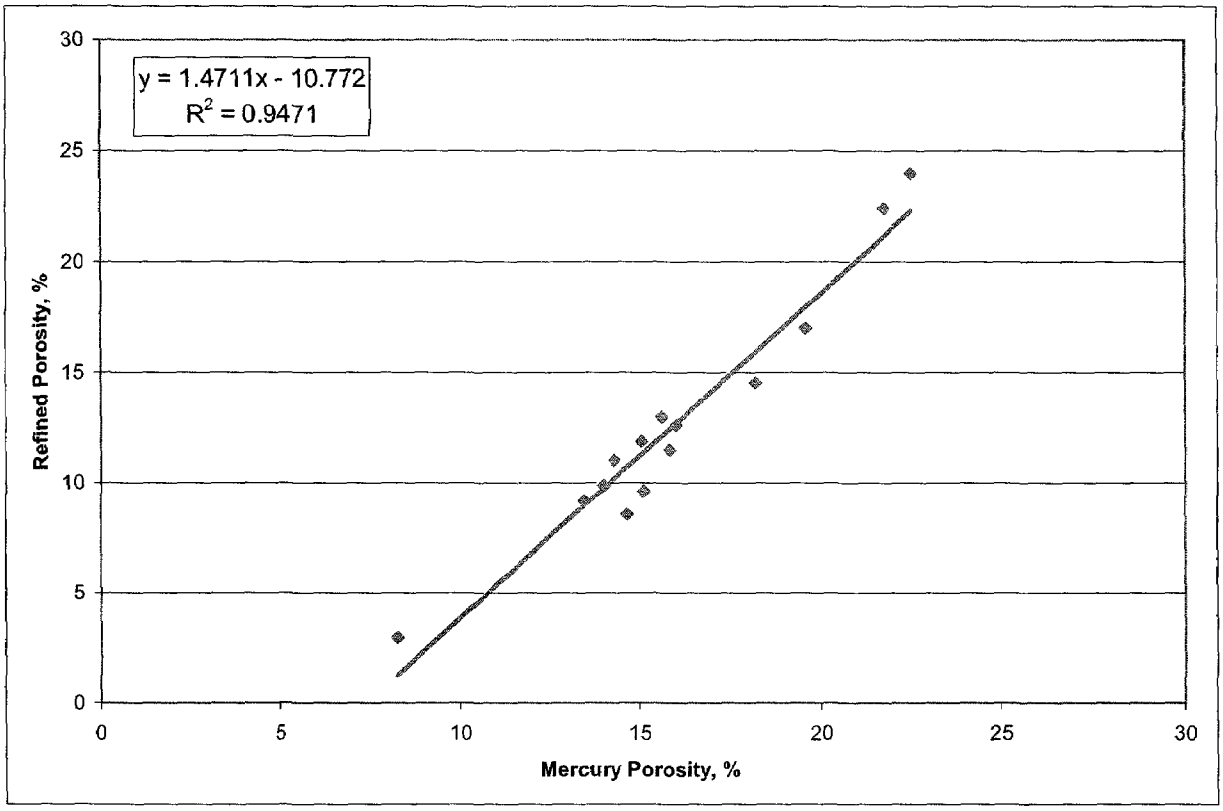

Fig. (5.64): Mercury porosity vs. refined porosity of Abu Roash `G`, TSW-21 well.

The studied samples have an outstanding relation which is expressed by the following equation:

$$\Phi_R = 1.4711\ \Phi hg - 10.772 \qquad (5.71)$$

$$R = 0.97$$

To check the validity of refined porosity values in the upper part of the Bahariya Formation, a relation was constructed between refined porosity and mercury porosity that resulted from capillary pressure test (Fig. 5.65).

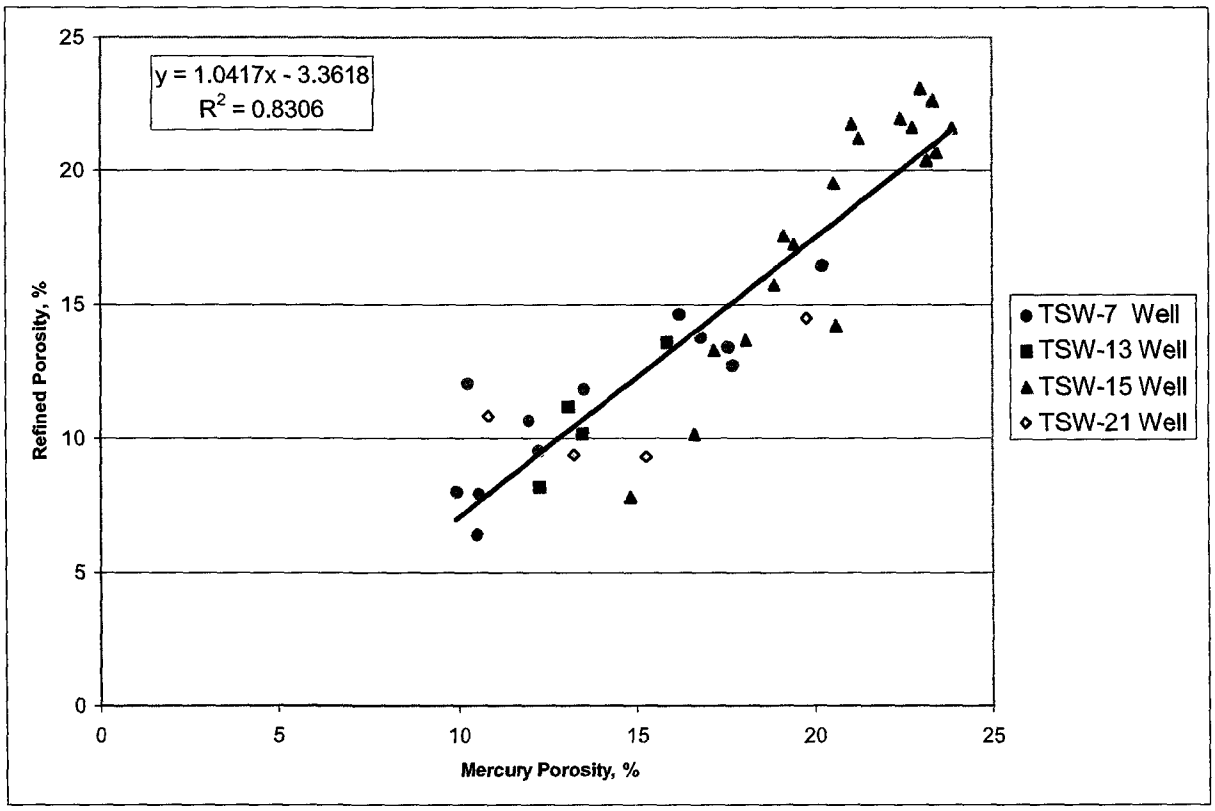

Fig. (5.65): Mercury porosity vs. refined porosity of U. Bahariya, TSW-7, 13, 15 and 21 wells.

The studied samples have an excellent relation which is expressed by the following equation:

$$\Phi_R = 1.0417\ \Phi hg - 3.3618 \qquad (5.72)$$

$$R = 0.91$$

5.11 Discussion of the results

In the present study, we have traced the groups that resulted from the porosity-permeability relations (anisotropy) for the Bahariya Formation (the upper and the lower parts) and Abu Roash Members (`G` and `F`), through the different capillary pressure derived parameters to show the distinctive characteristics for each group, we found out the following:

A-The lower part of the Bahariya Formation in BED1-11 well: capillary pressure derived parameters displayed the anisotropy present in the studied samples resultant from the facies change and represented by three groups, each group has its petrophysical parameters. Samples of group (A) always has the petrophysical properties that reflect their lithology (highly cemented, laminated sandstones), this group characterized by highest values of displacement pressure, water saturation, tight and narrow range of pore size distribution, lowest values of MHR and R35, On the other hand group (B) has moderate properties, figure (5.66) shows an example of this group but samples of group (C) have the best flow properties that reflects their lithology (clean sandstones with less cement and clays) so this group has the lowest values of displacement pressure, water saturation, wide range of pore size distribution, highest values of MHR and R35 .

B-The upper part of the Bahariya Formation compiled from TSW-wells: also capillary pressure derived parameters showed the anisotropy present here but the facies change resultant from the clay content, this represented by two groups. Samples of group (A) has the petrophysical properties that reflect their lithology (highly argillaceous to argillaceous, laminated sandstones), this group characterized by highest values of displacement pressure, water saturation, tight and narrow range of pore size distribution, lowest values of MHR and R35, on the other hand, the samples of the second group (group C) characterized by the absence of clay (nearly), so they have the best flow properties that reflects their lithology (clean sandstones, slightly argillaceous)

so this group displayed the lowest values of displacement pressure, water saturation, wide range of pore size distribution, highest values of MHR and R35. Figure (5.67) shows an example of this group, where we find pore spaces with a large pore throats hence high flow properties.

C-The results of petrophysical parameters (porosity, permeability and capillary pressure derived parameters show that in general, the upper part of the Bahariya Formation in TSW-field has better reservoir properties than that of the lower part of the Bahariya Formation in BED-1 field.

D-Although figure (5.8) displays three groups (A, B and C) for the studied samples of the upper part of the Bahariya Formation obtained from TSW-wells, but group (B) has been missed through the different relations of capillary pressure derived parameters, this is due to: two samples of group B (7H2 & 18H1) have been related to group (C) and the remaining samples of group B (3, 2H2, 31H1 & 31H2), related to group (A), hence capillary pressure derived parameters are more accurate for sample separation into different groups.

E-Abu Roash `G` in TSW-21 well: samples of this member as a whole characterized by tight flow properties due to the high clay content and the lamination in the sandstone samples, so it is considered as non-reservoir as a whole (group A), but some samples have the reservoir properties due to the less clay content (group C, that represented by two samples) so these samples have better flow parameters than group (A).

F-TSW-8 well (Abu Roash `F`): samples of this member represent the cap rock properties due to their lithology (marl). Figure (5.68) shows an example of this group, where we find isolated pore spaces with no connections to others, so the flow properties are very tight.

Table (5.62) displays a comparison of the different petrophysical parameters of the previously mentioned units.

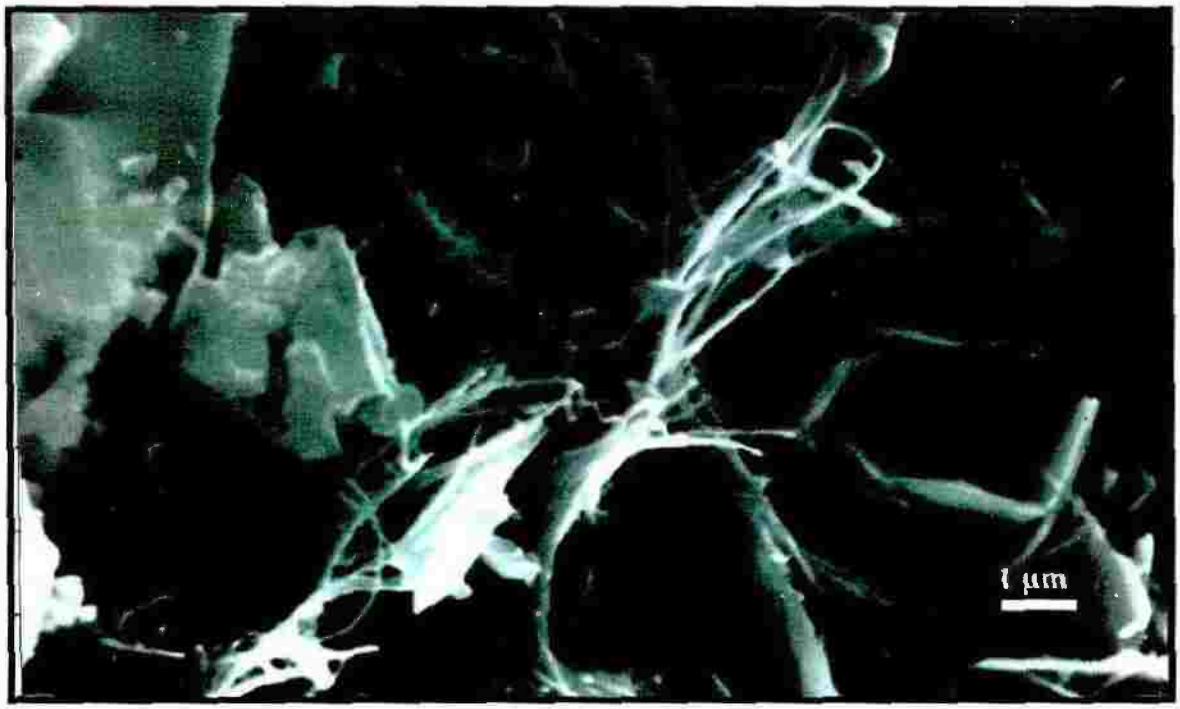

Fig. (5.66): SEM photomicrograph shows pore bridging hairy illite, sample 12, ϕ=14.9%, k=1.82 md, MHR=0.79µm, Swirr=10.9%. L. Bahariya, BED1-11 well.

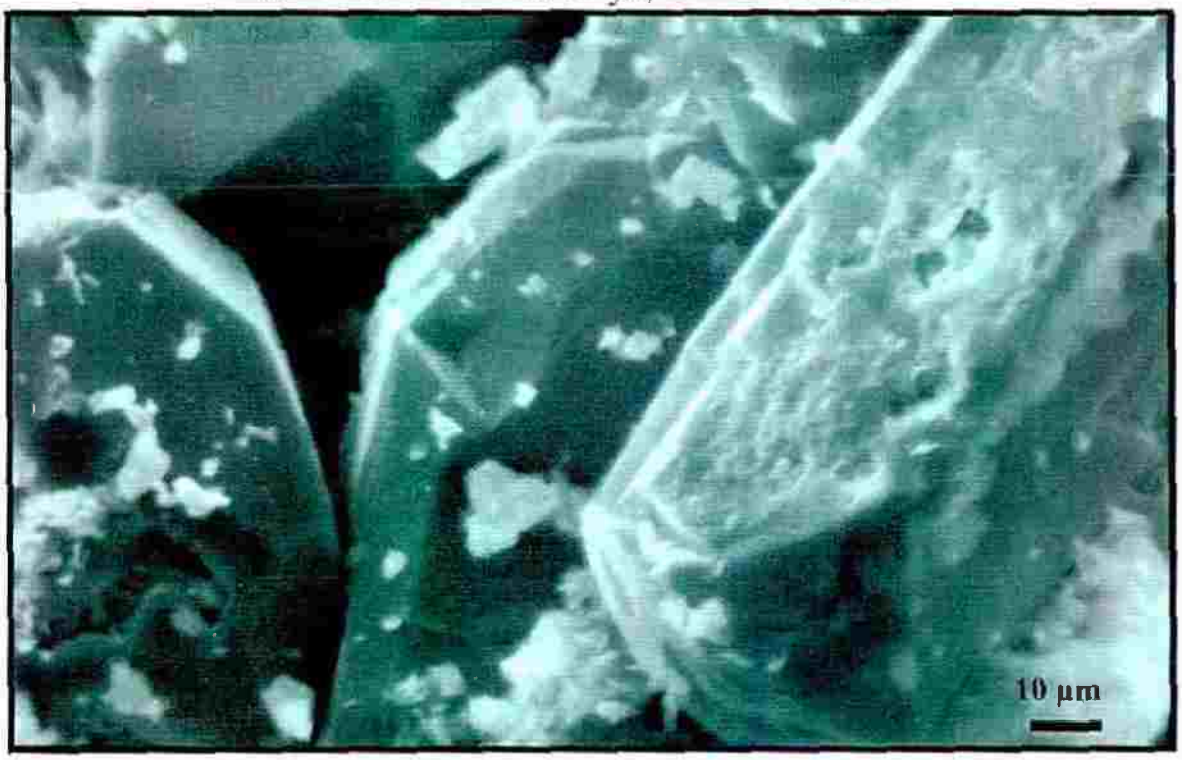

Fig. (5.67): SEM photomicrograph shows authigenic quartz overgrowth lining the intergranular pores, sample 11H1, ϕ=20.2%, k=14.5 md, MHR=2.15µm, Swirr=14.5%. U. Bahariya, TSW-15 well.

Fig. (5.68): SEM photomicrograph shows foraminiferal test in micrite cement, increasing the moldic porosity, sample 58, ϕ=18.7%, k=0.045 md, MHR=0.17µm, Swirr=10.4%. Abu Roash (F), TSW-8 well.

5.12 Some petrophysical parameters against depth

Figures (5.69) through (5.73), display respectively porosity, permeability, mean hydraulic radius, PVC's values and bulk density values against depth of the lower part of the Bahariya Formation in BED1-11 well, (TSW-8 & TSW-13 wells), (TSW-7, TSW-15 and TSW-21 wells), Abu Roash 'G' Member in TSW-21 well and the upper part of the Bahariya Formation compiled from TSW-wells.

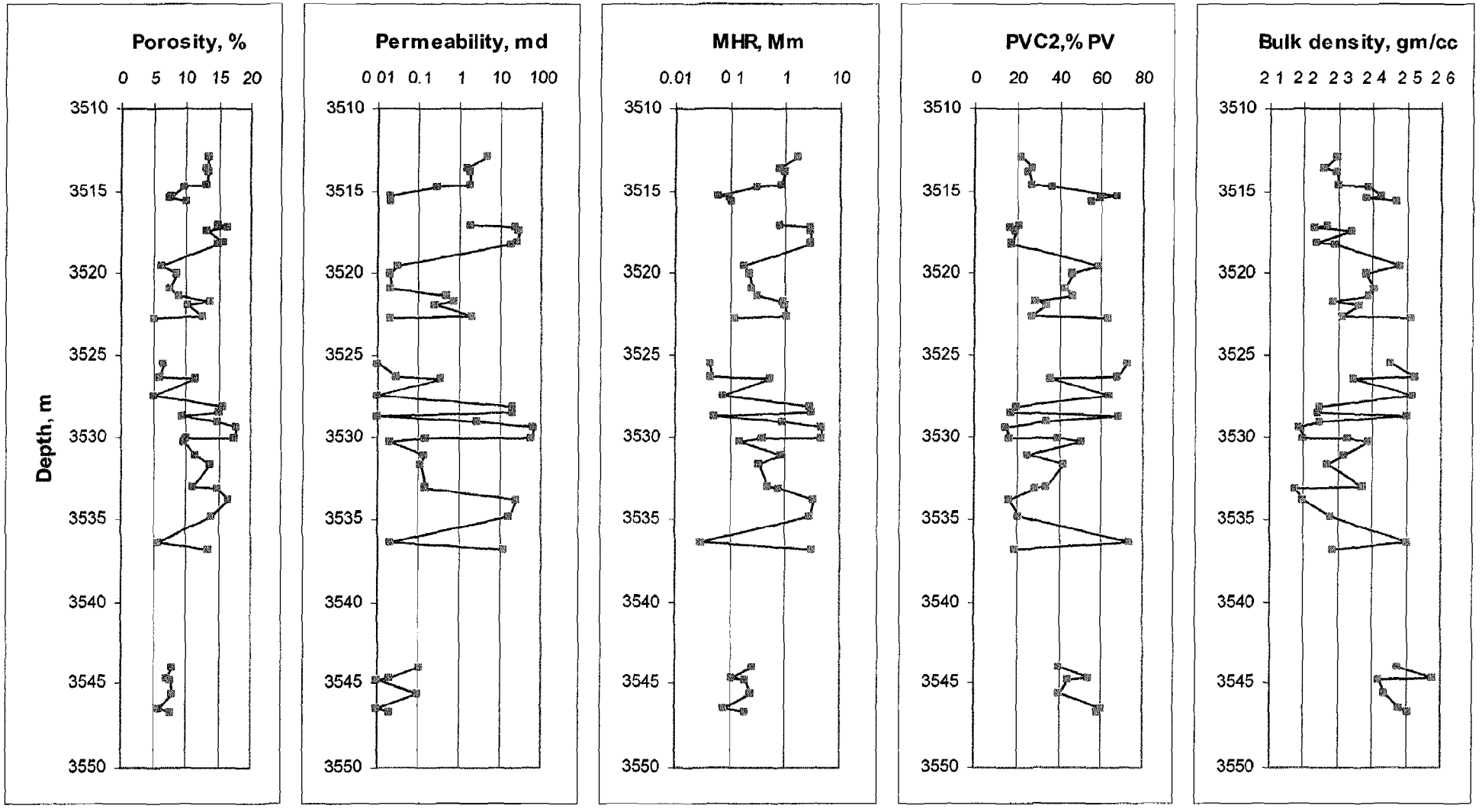

Fig. (5.69): Φ, K, MHR, PVC2 and bulk density of L. Bahariya, BED1-11 well.

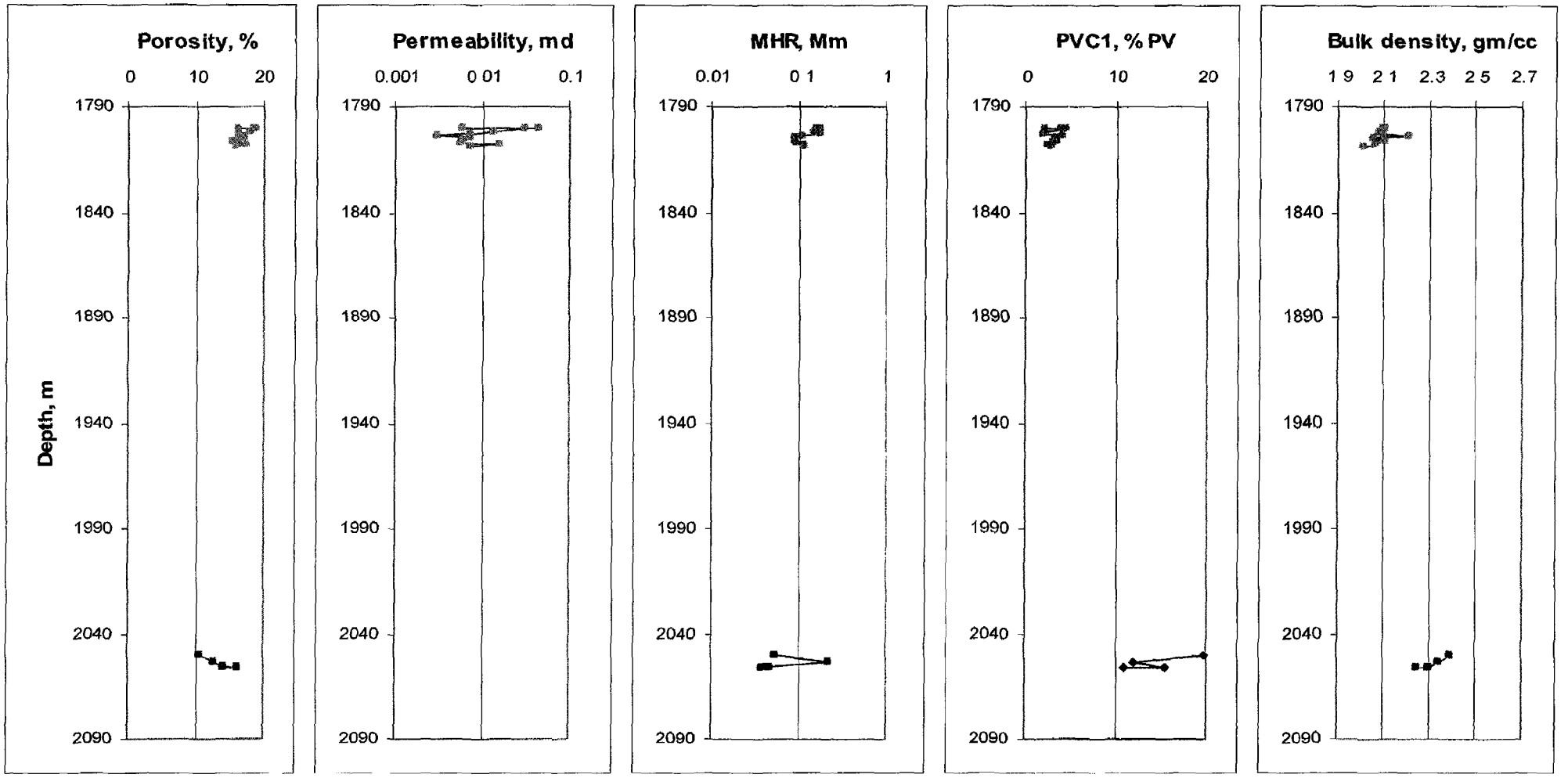

Fig. (5.70): Φ, K, MHR, PVC1 and bulk density of wells TSW-8 and TSW-13.

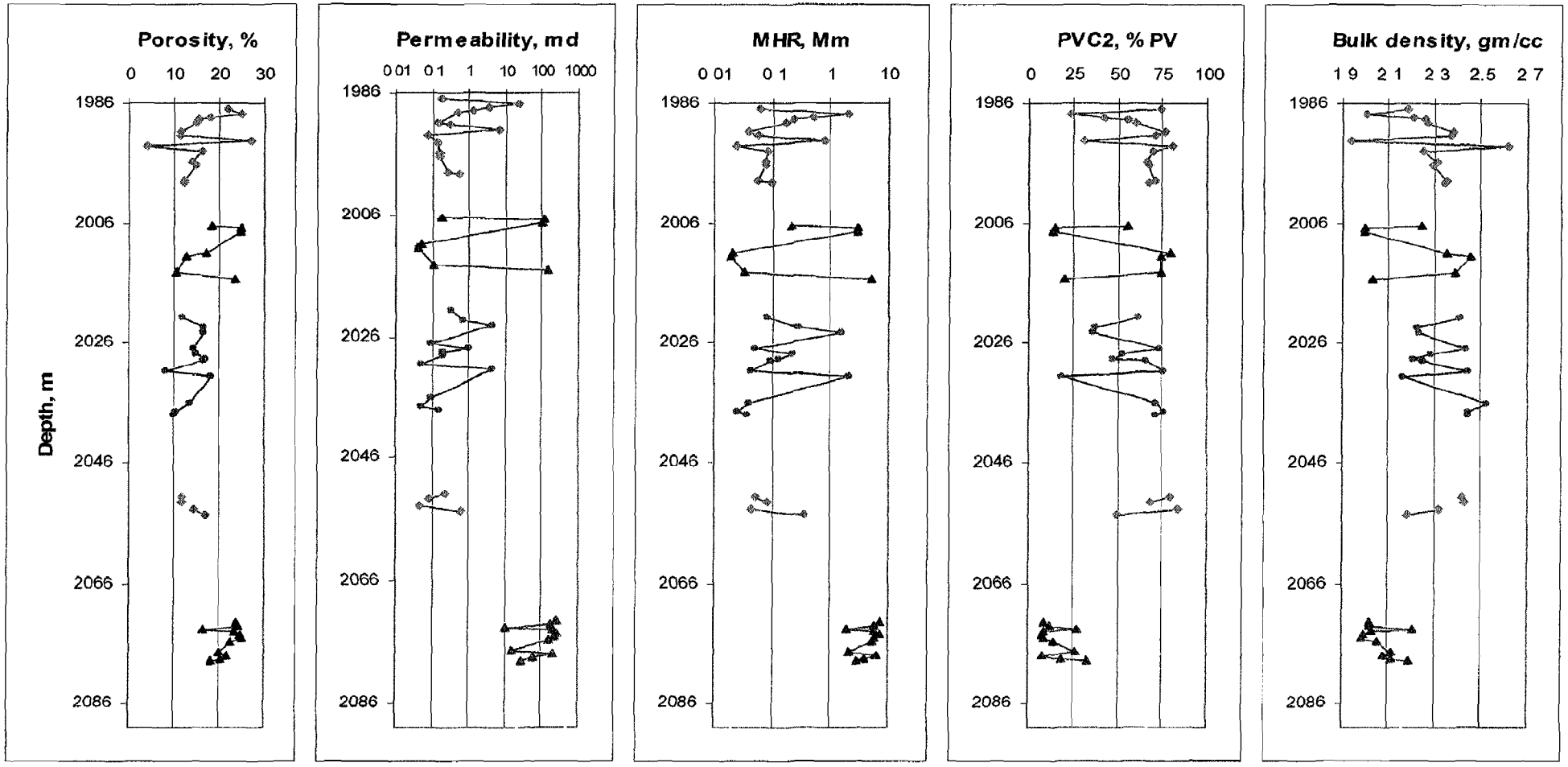

Fig. (5.71): Φ, K, MHR, PVC2 and bulk density of TSW-7, 15 and 21 wells.

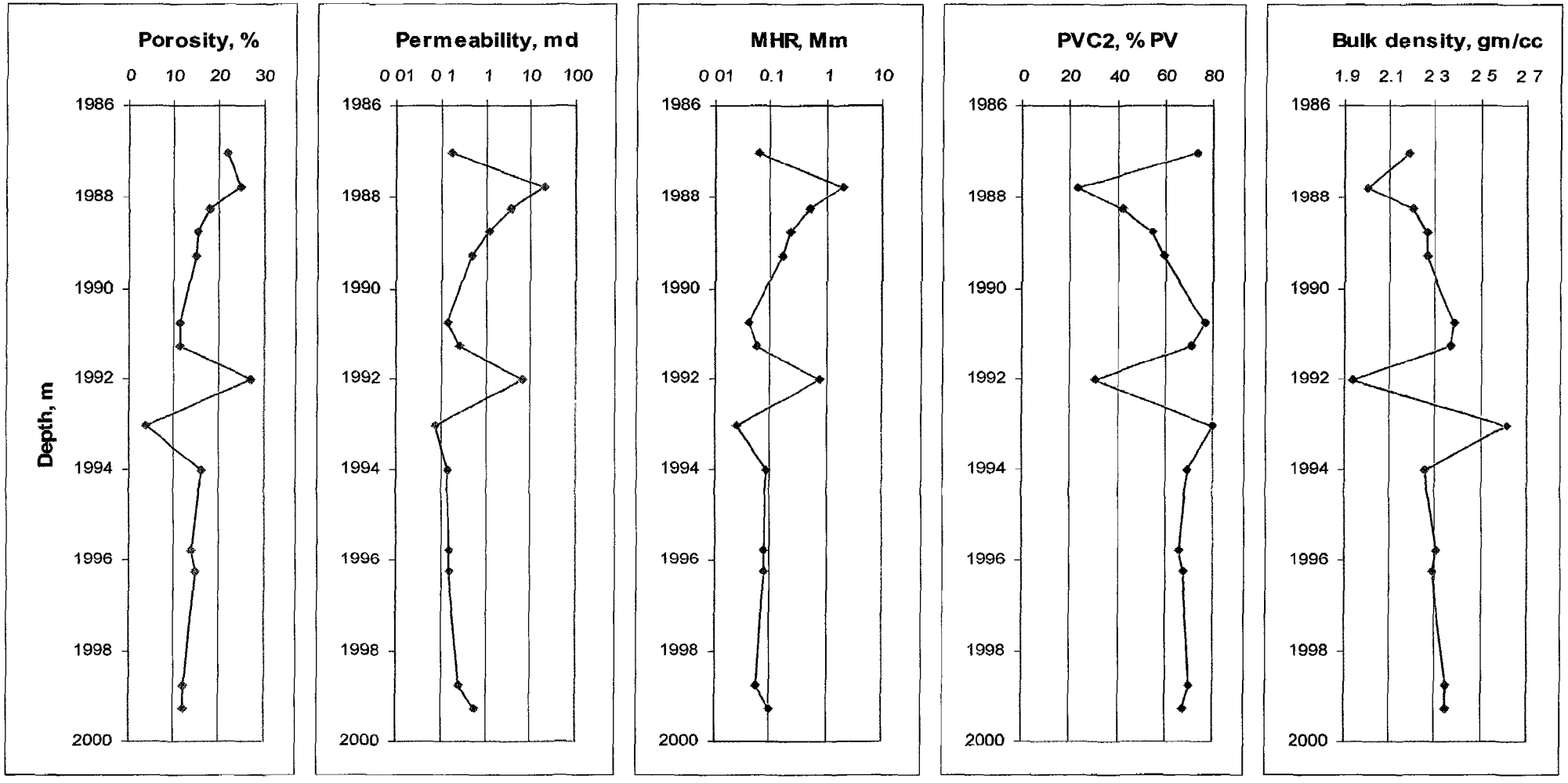

Fig. (5.72): Φ, K, MHR, PVC2 and bulk density of Abu Roash `G` Member, TSW-21 well.

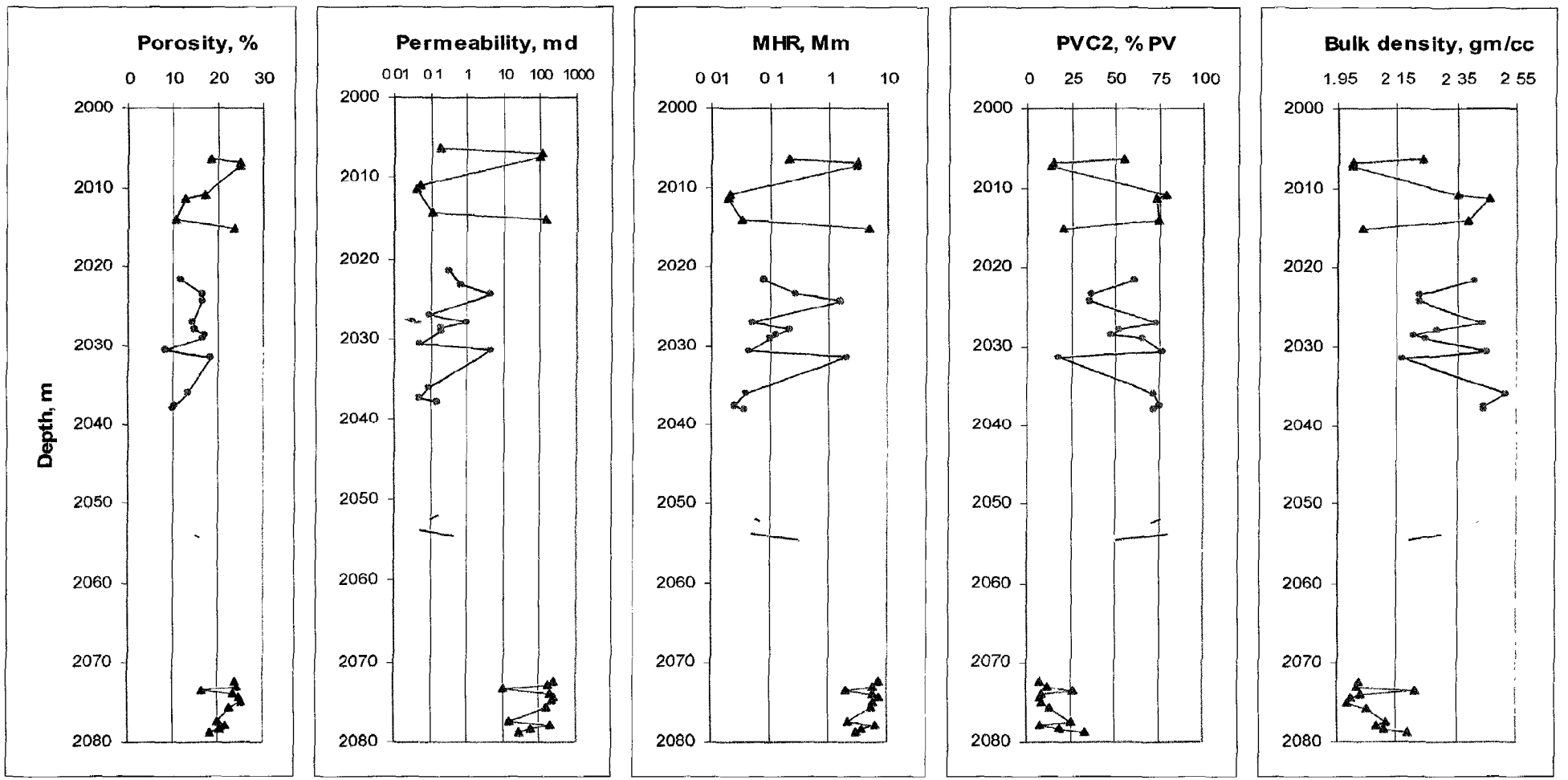

Fig. (5.73): Φ, K, MHR, PVC2 and bulk density of U. Bahariya, TSW-7, 15 and 21 wells.